NSK Technical Journal

Motion & Control

No.11 October 2001

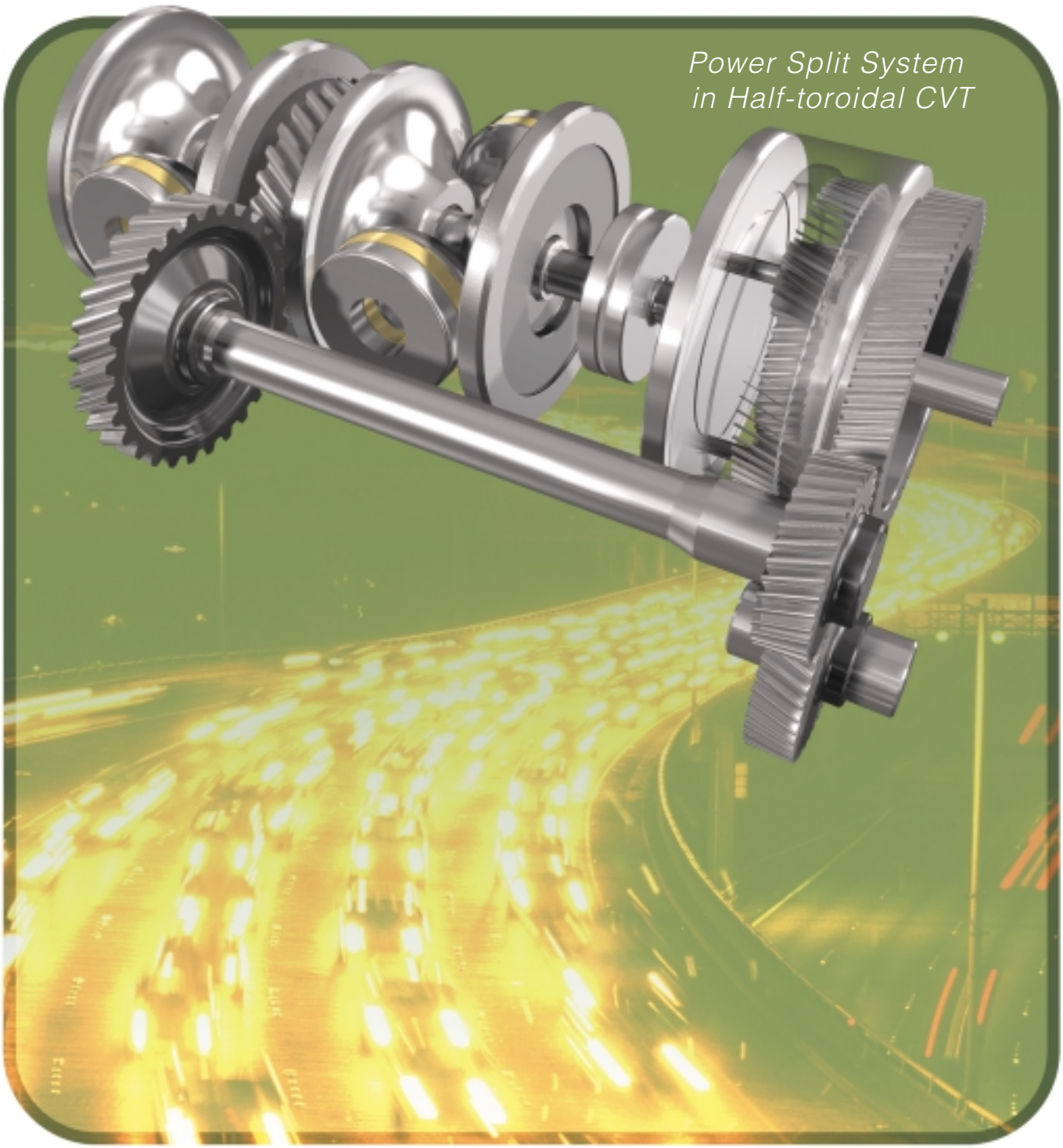

ISSN1342-3630

NSK

MOTION & CONTROL No.11
NSK Technical Journal
Printed and Published: October 2001
ISSN1342-3630
Publisher: NSK Ltd., Ohsaki, Shinagawa, Tokyo, JAPAN
Public Relations Department
TEL +81-3-3779-7051
FAX +81-3-3779-7431
Editor: Kyozaburo FURUMURA
Managing Editor: Yasuhiko MORITA
Design, Typesetting & Printing: Fuji Ad. Systems Corp.

Cover photos: Power Split System in Half-toroidal CVT

NSK Technical Journal

Motion & Control

No. 11
October 2001

NSK

Contents

Development of New Life Equation for Ball and Roller Bearings

Hiromichi Takemura
Bearing Technology Center
Youichi Matsumoto and Yasuo Murakami
Corporate Research and Development Center

ABSTRACT

The conventional rolling bearing life equation, which is based on the theory of Lundberg and Palmgren, does not reflect actual bearing life for all operating conditions. For instance, while the actual life of a bearing under clean lubrication is 20 times longer than the calculated life, actual life under contaminated lubrication is as low as one-tenth of the calculated life.

To solve this problem, the following Advanced Bearing Life Equation was developed with the a_{NSK} life modification factor:

$L_{able} = a_1 a_{NSK} L_{10}$

The new a_{NSK} factor is based on data from bearing life tests involving over 450 roller bearings and over 550 ball bearings under a variety of operating conditions. The new life equation with the a_{NSK} factor provides a more accurate figure for calculated life and actual life.

1. Introduction

It has been almost 40 years since the rolling bearing life equation (1) was publicized by Lundberg and Palmgren, and standardized by ISO[1].

$$1n\frac{1}{S} \propto \frac{\tau_0^c \cdot N^e \cdot V}{Z_0^h} \quad \cdots\cdots\cdots\cdots\cdots\cdots\cdots\cdots\cdots\cdots\cdots\cdots(1)$$

Bearing technology has rapidly advanced in recent years. The dimensional accuracy, and in particular, material cleanliness of bearings, have improved remarkably compared to those of long ago. Today, by combining the latest in other bearing-related technologies, to include filtering technologies, bearings used in relatively clean environments generally have a longer rolling fatigue life than those standardized in ISO[2] life equations.

For instance, bearings that were operated under a heavy load and ideally lubricated conditions achieved a life 20 times as long as their theoretical life[3]. When used under less load, their actual life tended to be longer. In fact, some test bearings have been satisfactorily operating for nearly 20 years to date. These phenomena, like the theoretical fatigue phenomenon seen in the form of S-N curves in rotating and bending fatigue tests, predict the existence of a limit to rolling fatigue[4]. In view of these circumstances, a new life equation (2) that takes fatigue load limit into account was proposed [5)-11)].

$$1n\frac{1}{S} \propto N^e \int_V \frac{(\tau - \tau_u)^c}{Z_0^h} dV \quad \cdots\cdots\cdots\cdots\cdots\cdots\cdots\cdots\cdots\cdots (2)$$

The new life equation being proposed in this paper has its roots in the vast amount of information in our database[12] of X-ray fatigue analyses. This database consists of experimental data gathered over the past 20 years by NSK's market services, for the sole purpose of determining the service life of various bearings on the market.

The new equation is based on a previous report[4] and assumes $(P\text{-}P_u)/C$ as a basic function of fatigue load limit. Parameters are defined as the contamination factor (a_c), for contamination by lubricant, and the viscosity ratio (κ), for viscosity. This paper describes the concept, theoretical construction, and development of the new theoretical life equation.

2. Basic Data for New Life Equation

2.1 Ball Bearing Tests

Table 1 shows the test conditions for more than 550 bearings under 40 different conditions. 10 types of deep groove ball bearings, double row angular contact ball bearings, and special ball bearings were tested. The test bearings had an outer diameter of 35 mm to 80 mm and an inner diameter of 10 mm to 35 mm. The test load (P/C) was in the range of 0.10 and 0.71. Some bearings were lubricated with oil and others with grease. Clean lubricant tests and contaminated lubricant tests were performed separately. Test temperatures were between 50°C and 218°C, and bearing running speeds ranged from 1 000 min^{-1} to 22 000 min^{-1}. In addition, tests for the low lambda ratio lubrication region (λ= minimum oil film thickness/bearing race surface roughness) were conducted utilizing low-viscosity lubricating oil[13]. The test bearings were made of through-hardening steel SUJ2 (SAE 52100) having a surface hardness of Hv750.

For the contaminated lubricant tests, various foreign particles were added to the lubricants before starting testing (Size: 10 μm ~ 150 μm; hardness: Hv350 ~ Hv870; amount: 100 ppm ~ 3 000 ppm). As shown in Fig. 1, flaking

Table 1 Ball bearing test conditions

Test No.	Type of bearings	P.C.D. (mm)	Load (P/C)	Running speed (min^{-1})	Test temp. (°C)	Lubricant	Viscosity ratio, κ	Lubricated condition
1~3	6202	25.5	0.39	3000~8000	120~218	Grease	0.1~0.39	Clean
4~7	6203	29.0	0.34~0.44	3000~8000	120~218	Grease	0.1~0.42	Clean Contaminated
8~22	6206	46.5	0.15~0.71	1400~4900	50~130	VG10~HT320 oil	0.4~2.89	Clean Contaminated
23~26	6206 (Special)	46.5	0.31	3000~6000	125	AFT oil	0.6	Contaminated
27	6303	31.5	0.18	22000	110	Grease	1.5	Clean
28	6304	35.5	0.19	15000	113	Grease	1.4	Clean
29~31	HR6304	35.5	0.25	2400	70	VG90 oil	1.6	Contaminated
32, 33	B-29 (Special)	60.5	0.58	2513	100	AFT oil	0.6	Contaminated
34~38	6207 (Wide)	53.5	0.31~0.76	1000	60~90	Grease	0.6~1.45	Clean
39, 40	Double-row angular contact ball bearings	43.5	0.10~0.16	8000~9200	80	Grease	0.6	Clean

developed from a small dent in the raceway, and the L_{10} life was shorter by a few tenths of the conventional theoretical life[14), 15)].

For the clean lubricant tests, mostly subsurface-originated flaking occurred. Under the rolling surface, etching was less likely to occur, and structural change appearing like a white butterfly wing (referred to as butterfly wings) was observed as shown in Fig. 2. This butterfly wing was visible mostly around non-metal inclusions that were present in areas where the shear stress was highest (0.1 μm to 0.2 μm under the rolling surface). This type of flaking is caused by a concentration of stress around the inclusions and the subsequent propagation of fine cracks due to the cyclic contact stress[16)].

In tests under a high load (P/C = 0.71), the L_{10} life was 20 times longer than conventional theoretical life. In conditions where the contact surface pressure was in excess of 3.5 GPa, a white etching constituent (WEC) was observed. The bearings tested under a low load (P/C = 0.15) continue to operate to this very day even though their life has reached 53 times longer than their conventional theoretical life. This result suggests the

Fig. 1 Propagation of flaking from a small dent in ball bearing tests

Fig. 2 Butterfly under the raceway in a rolling bearing (parallel section)

Fig. 3 WEC (White Etching Constituent) structural change in deep groove ball bearing inner rings (parallel section)

existence of a fatigue load limit for rolling bearings[4].

In the tests under grease lubrication, many of the test bearings failed due to seizure. In the low-λ tests (λ= 1.5), the bearings showed an L_{10} life 10 times longer than the calculated life, in disagreement with the conventional theory.

2.2 Roller Bearing Tests

Table 2 shows the conditions under which roller bearings were tested. 37 groups of roller bearings totaling over 450 bearings were tested. The 17 types of tapered roller, special roller and ball, and thrust roller bearings listed in the table were tested. The bearings ranged in outer diameter from 40 mm to 1190 mm and in inner diameter from 17.5 mm to 630 mm. The test load in P/C ranged from 0.16 to 0.71. The tests were performed under three different lubrication conditions: clean, contaminated, and unfiltered. Some tests were focused on determining the effects of grease and oil lubrication and some tests were performed in a low-λ region at low speed (1.14 rpm). Test temperatures ranged from 40°C to 218°C and rotating speed from 1.14 rpm to 4000 rpm. The test bearings were made of SAE 52100 through-hardening steel with a hardness of about Hv750 and SAE 5120 case-hardening steel with a surface hardness of Hv750.

In all of the tests, the L_{10} life was determined when the bearing failed or reached an unacceptable level of vibration.

In the bearings tested with a lubricant to which various foreign particles (debris size: 10 μm~150 μm, hardness:

Table 2 Roller bearing test conditions

Test No.	Type of bearings	P.C.D. (mm)	Load (P/C)	Running speed (min^{-1})	Test temp. (°C)	Lubricant	Viscosity ratio (κ)	Lubricated condition
1~9	LM11749/710	28.6	0.35~0.46	1500~3400	120~218	VG10~VG68 oil	0.6~4.00	Clean Contaminated
10~19	L44649/610	38.6	0.16~0.71	3000	51~62	VG10~VG68 oil	0.59~4.00	Clean Contaminated
20~22	Roller & ball bearings	15.9~18.0	0.19~0.20	1000	50~130	Grease	0.46~0.48	Clean
23, 24	P34-1 (Special)	49.1	0.30	4000	125	Grease	0.9	Clean
25	R34Z-21 (Special)	45.9	0.28	3500	110	75W-90 oil	1.54	Contaminated
26	R45-15 (Special)	53.2	0.24	3500	113	SX90 oil	1.53	Contaminated
27	DPB42 (Special)	54.5	0.30	3500	60	80W-90 oil	1.68	Contaminated
28	HM88649/610	53.2	0.28	3500	70	SX90 oil	1.66	Contaminated
29	HR30304	36.4	0.34	4000	100	80W-90 oil	1.36	Contaminated
30	32205	36.4	0.26	3500	80	80W-90 oil	0.99	Contaminated
31	30306C	50.9	0.32	3000	85	SX80 oil	2.35	Contaminated
32	440KVE	515.7	0.36	570	85	Grease	3.18	Unfiltered
33	23040	258.9	0.29	10.12	85	Grease	0.1	Unfiltered
34	22211	78.7	0.16	3000	40	VG10 oil	1.08	Unfiltered
35	22211EA	78.7	0.16	3000	40	VG10 oil	0.63	Unfiltered
36	294/630ME	879.9	0.20	1.14	60	VG460 oil	0.11	Unfiltered
37	NN3019	121.0	0.32	4000	85	Grease	4.00	Clean

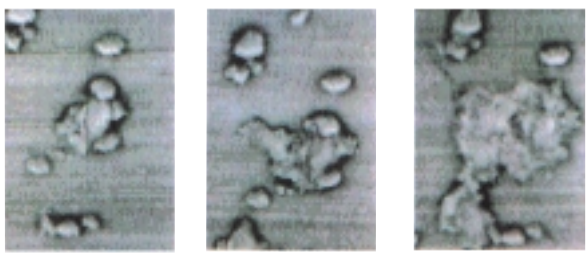

Fig. 4 Propagation of flaking from a small dent in roller bearing tests

Hv350 to Hv870, content: under 500ppm) were initially added, flaking developed from dents in the raceway surfaces caused by the foreign debris. In the bearings tested under circulating lubrication, dents were formed in the raceway surfaces and surface-originating flaking occurred. Similarly, in the bearings tested under lubrication without filtering (no foreign particles were deliberately added), dents were produced in the raceway surfaces by foreign particles approximately 100 μm in size that were generated during the test. The dents eventually gave rise to flaking (Fig. 4).

The bearings tested under clean lubrication and high load (P/C = 0.71) exhibited an L_{10} life approximately 5 times longer than the conventional calculated life because of the good lubrication conditions and the fact that edge load was not generated.

In the low-λ test where the test bearings were operated at a low speed of 1.14 rpm, the bearings exhibited slight wear of their raceway surfaces and showed an L_{10} life approximately 0.6 times lower than the conventional calculated life. In the tests with low-viscosity VG 10 lubricant, surface-originated flaking occurred because of poor oil film formation.

3. Construction of New Life Equation

3.1 Analysis of Life Test Data

In the clean environment, test results tended to depart from the L_{10} theoretical line with each decrease in the contact surface pressure (Bearing load: P/C), as shown in Fig. 5[3]. This suggests the existence of a fatigue load limit and the tendency of the load index, p, to exceed 3. Under the contaminated lubrication, bearing life was shortened and departed from the L_{10} theoretical line with each decrease in the contact surface pressure (Bearing load: P/C), as shown in Fig. 6.

Therefore, the new life equation utilizes the axis of abscissa to represent a function of $(P\text{-}P_u)/C$. This function is influenced by lubrication parameters according to the life test results in a low load region in clean environments. For bearing life in a contaminated environment, the axis of abscissa for the new life equation is defined as $(P\text{-}P_u)/C \bullet 1/a_c$. This is assuming that the effects resulting from the various types and kinds and shapes of foreign particles are closely related to bearing load and lubrication. These effects can be treated as a function in the form of a load parameter. The following equation, based on this concept, is for calculating surface-originated flaking.

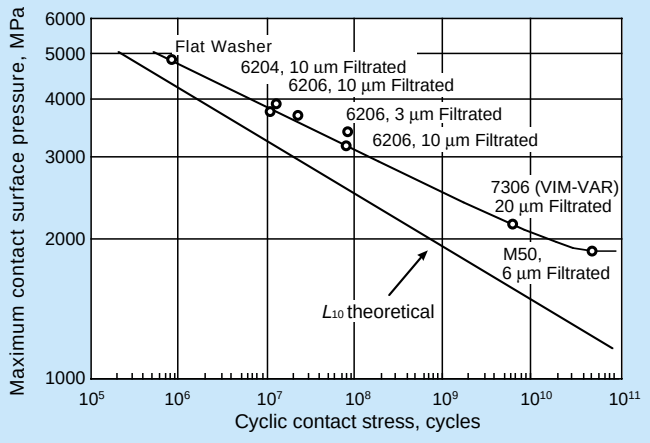

Fig. 5 Test results of life under clean environment

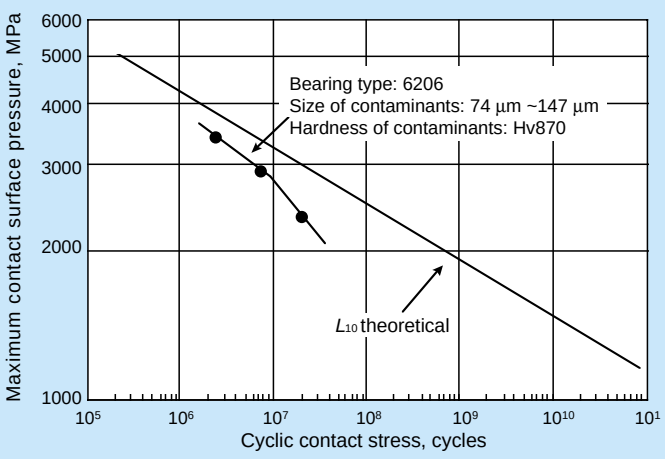

Fig. 6 Test results of life under contaminated lubrication

Table 3 Concept of factor a_c

Cleanliness	Very clean	Clean	Normal	Contaminated	Heavily contaminated
a_C factor	1	0.8	0.5	0.4~0.1	0.05
Application standard	~10 μm filtered	10~30 μm filtered	30~100 μm filtered	100 μm ~filtered or not filtered (oil bath, circulating lubrication, etc.)	· Not filtered · Presence of many fine particles
Application examples	· Sealed grease-lubricated bearings for electrical appliances and information technology equipment	· Sealed grease-lubricated bearings for electric motors, railway axleboxes and machine tools	· Open-type grease-lubricated bearings	· Automotive transmissions · Automotive wheel hubs · Reduction gears · Construction machinery	

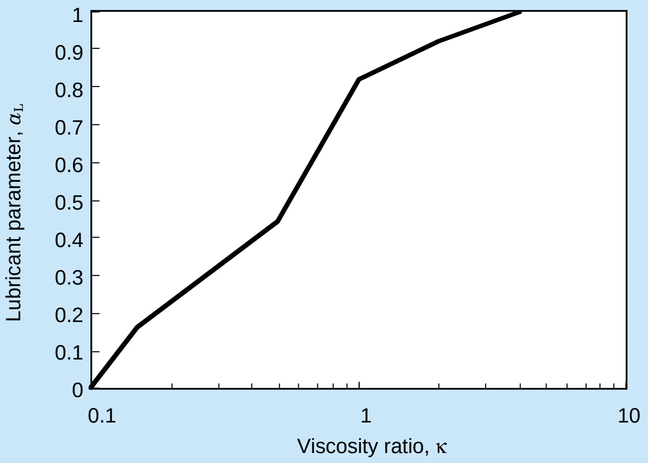

Fig. 7 Lubricant parameter a_L as a function of viscosity ratio (κ)

$$1\mathrm{n}\frac{1}{S}\propto N^{e}\frac{(\tau-\tau_{u})^{c}}{Z_{0}^{h}}V\times\left(\frac{1}{f(a_{C,}a_{L})}-1\right)\cdots\cdots\cdots\cdots\cdots(3)$$

where, V is the amount of stress, and a_c is the contamination factor (see Table 3). The effect of a lubricant is decided by its viscosity ratio (κ). The viscosity ratio is easily obtained by calculating the running speed and the pitch circle diameter of the bearing. Fig. 7 shows the relation between κ and the lubricant parameter (a_L), while taking into consideration the a_3 curve[17] and the lambda ratio theory[4), 13)].

The new life equation, which combines Equation (2) for subsurface-originated flaking and Equation (3) for surface-originated flaking newly introduced, proposes Equations (4) and (5).

$$1\mathrm{n}\frac{1}{S}\propto N^{e}\frac{(\tau-\tau_{u})^{c}}{Z_{0}^{h}}V\times\left(\frac{1}{f(a_{C,}a_{L})}\right)\cdots\cdots\cdots\cdots\cdots\cdots(4)$$

$$L_{able}=a_{1}\,a_{NSK}L_{10}$$ ÅcÅcÅcÅcÅcÅcÅcÅcÅcÅcÅc(5)ÅcÅ

where, the life modification factor a_{NSK} is a function of a_L and $(P\text{-}P_u)/C\bullet 1/a_c$ as shown in Equation (6).

$$a_{NSK}\propto F\left(a_{L},\left(\frac{P-P_{u}}{C\cdot a_{c}}\right)\right)\cdots\cdots\cdots\cdots\cdots\cdots\cdots\cdots\cdots\cdots(6)$$

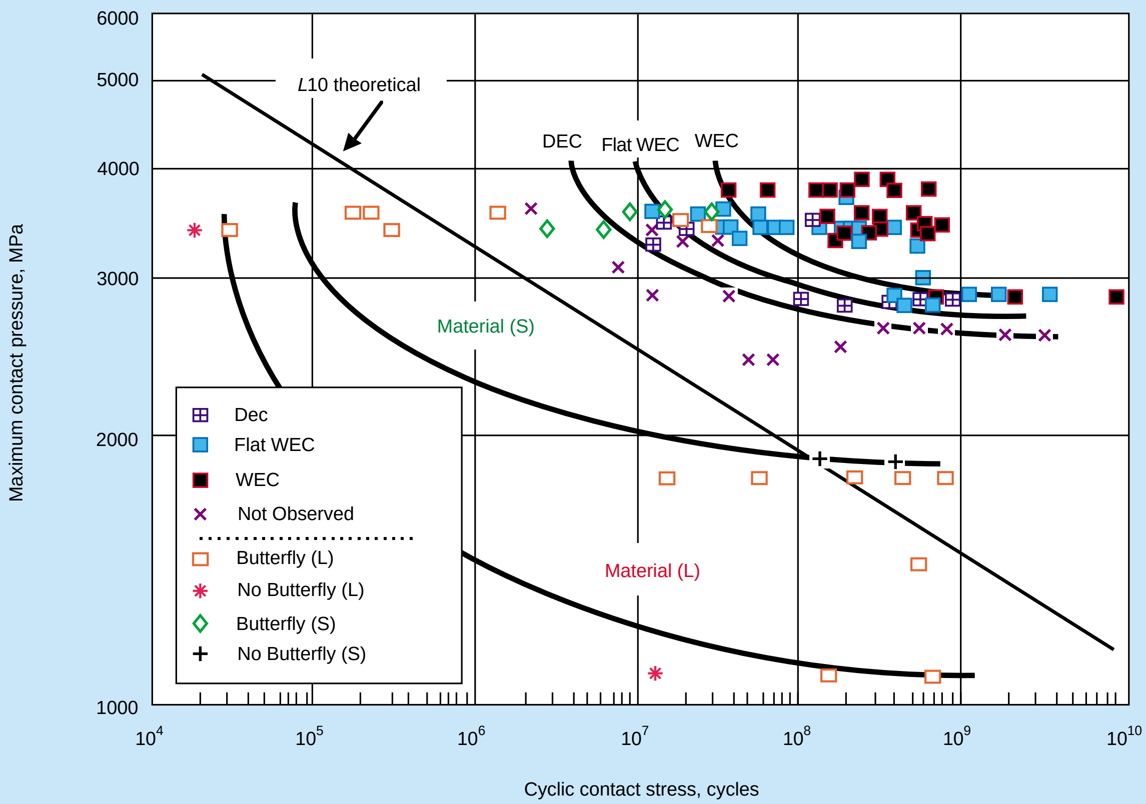

Fig. 8 Correlation between contact pressure, number of load cycles, and development of structural change

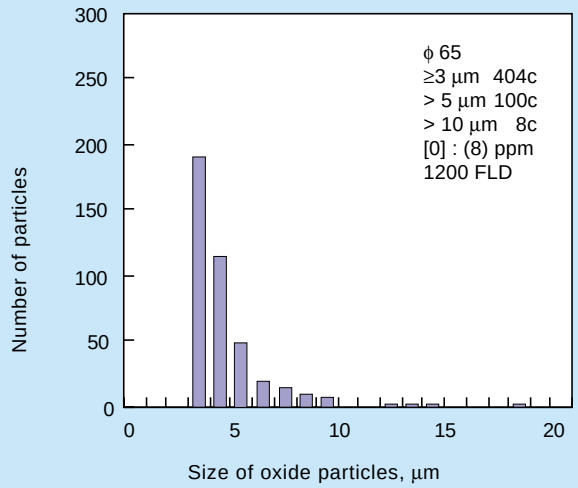

Fig. 9 Cleanliness of material L

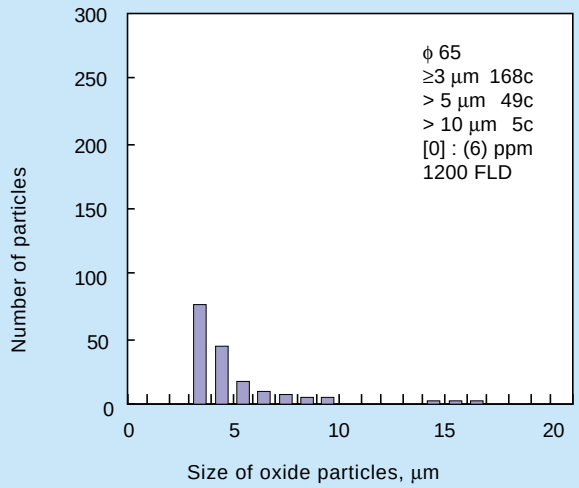

Fig. 10 Cleanliness of material S

3.2 Determination of Fatigue Load Limit P_u

To determine the fatigue load limit P_u, we studied the limits of butterfly wing occurrence. Fig. 8 shows the relation between contact surface pressure and structural change in ball bearings. Assume that L denotes the life test results for bearings made of low-purity material from an overseas source (see Fig. 9, Cleanliness of material L). S denotes the life test results of bearings made of NSK standard material, which have a relatively high purity (see Fig. 10, Cleanliness of material S). The results of an image analysis show different limits between L and S. Thus, in terms of the contact surface pressure limit and the occurrence of the butterfly wings, which is considered to be the main cause of subsurface-originated flaking around non-metallic inclusions, P_{max} = 1.3 GPa was obtained for the material L of low-purity, and P_{max} = 1.8 GPa for the NSK standard material.

However, the bearing fatigue limit of 10^7 cycles, as seen in the rotating bending fatigue test results of bearings made of bearing steel is reported to be $\sigma \fallingdotseq 800$ MPa[18]. It is also reported that the fatigue limit is lower when bearings made of materials with lower purity are tested. This fatigue limit of 800 MPa, when converted to shear stress, is given as τ = 400 MPa ~ 500 MPa and, when converted to contact surface pressure, is estimated at $P_{max} \fallingdotseq 1.3$ GPa. Therefore, based on the results of the butterfly theory, the rotational and flexural tests, in addition to a margin of safety, we defined the fatigue limit contact surface pressure as P_{max} = 1.5 GPa. The equivalent dynamic bearing load under this contact stress is the fatigue load limit, P_u. This fatigue load limit is valid for not only ball bearings, but also for roller bearings. Our tests verified that cylindrical roller bearings had no flaking even after being operated for 80 times their theoretical life at a contact surface pressure of P_{max} = 1.7 GPa.

3.3 Calculation of Contamination Factor, a_c

Table 3 gives values for the a_C contamination factor according to the degree of lubricant cleanliness. In testing of ball bearings and roller bearings under oil or grease lubrication and clean filtered lubrication, we obtained bearing lives several times as long as the conventional calculated lives. If foreign particles with a hardness of Hv350 or greater enter a bearing, indentations are generated in the contact surfaces and fatigue damage progresses over time which results in flaking. Operating conditions are divided into five classes in the new NSK life theory. The a_C contamination factors in the table below are used in life calculations to reflect the likelihood of such indentations being generated in a particular application.

In the test of ball bearings and roller bearings under contaminated lubrication, the bearing life dropped to 1/3 to 1/20 of the conventional calculated life. The life of bearings tested under unfiltered lubrication was 1/10 to 1 times the conventional calculated life, somewhat longer than the bearings tested under contaminated lubrication. Based on these findings, we determined the a_C contamination factor values that are listed in Table 3.

3.4 Concept of Material Factor

With a focus on improving bearing life against subsurface-originated flaking, NSK developed extremely purified bearing steel, SUJ2EP, that contains less non-metallic particles[19]. Bearings manufactured from this steel have performed well in our tests and in the market.

To improve bearing life against surface-originated flaking, NSK also developed Super-TF and Hi-TF bearings using improved TF technology[30]. These bearings have also performed well in our tests and in the market.

The NSK new life theory compensates for the contamination factor, a_C, by taking into consideration the life extending effects of bearing material and heat

treatment improvements.

3.5 Calculation of Life Modification Factor, a_{NSK}

In our previously proposed equation[4], the three adjustment factors such as a_2·a_3, a_4 and a_5 are supposed to be independent from each other. However, they actually influence each other. We therefore needed to improve the previous equation.

The new life equation is the product of the conventional life equation (ISO 281:1990) multiplied by the correction factor a_{NSK} as follows:

$$L_{able} = a_1 \, a_{NSK} L_{10} \quad \cdots\cdots\cdots(5)$$

In calculations by this new life equation, the fatigue load limit P_u, which is a conversion from the bearing equivalent load under an ideal maximum contact pressure of 1.5 GPa, is introduced; the contamination factor a_c shown in Table 3 is used; and the load parameter $(P\text{-}P_u)/C \bullet 1/a_c$ is set up on the axis of abscissa. In addition, the viscosity ratio κ is used as a lubrication parameter (a_L) to reflect the idea that better lubrication (higher κ) results in longer life. Consequently, the a_{NSK} correction factor in this new life equation is in the form of a function. Based on the aforementioned test results showing that under clean lubrication, ball bearings with better raceway surface roughness have longer life than roller bearings, this new life equation applies separately to ball bearings and roller bearings.

Fig. 11 shows the new life curves of ball bearings, and Fig. 12 shows those of roller bearings. Based on the experimental results, all these curves were plotted with $(P\text{-}P_u)/C \bullet 1/a_c$ on the axis of abscissa and with the viscosity ratio κ. In the process of establishing a_{NSK} as a function of κ, curves were assumed in view of the correlation among the data, and arrangements were made so that a_{NSK} may increase with κ. Furthermore, in the ball bearing tests shown in Fig. 6, although a test with κ = 4 was not performed, extrapolation based on the roller bearing tests was used to establish the function. The high κ (> 4) means that lubrication is good and the oil film parameter Λ is high (> 3).

The standard permissible range for the a_{NSK} factor was set at 0.1 to 50. For ideal lubrication conditions, the a_{NSK} factor can be set at 50. For bearings operated under heavily contaminated lubrication (a_c = 0.05), we defined the new life correction factor as the minimum, a_{NSK} = 0.1.

For such low loads acting on bearings as $(P\text{-}P_u)/C \bullet 1/a_c < 0.05$ on the axis of abscissa, we treated them as $(P\text{-}P_u)/C \bullet 1/a_c = 0.05$. As the lubrication parameter, we used the viscosity ratio κ, which is easy to calculate. We used κ = 4 for viscosity ratios larger than 4, and κ = 0.1 for those smaller than 0.1.

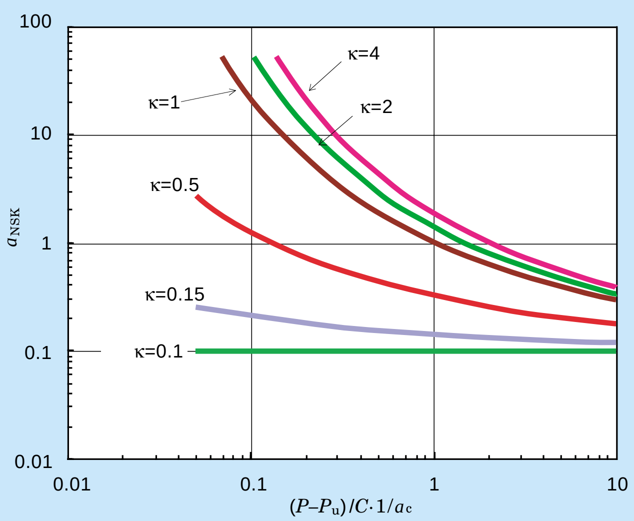

Fig. 11 New life equation curves for ball bearings

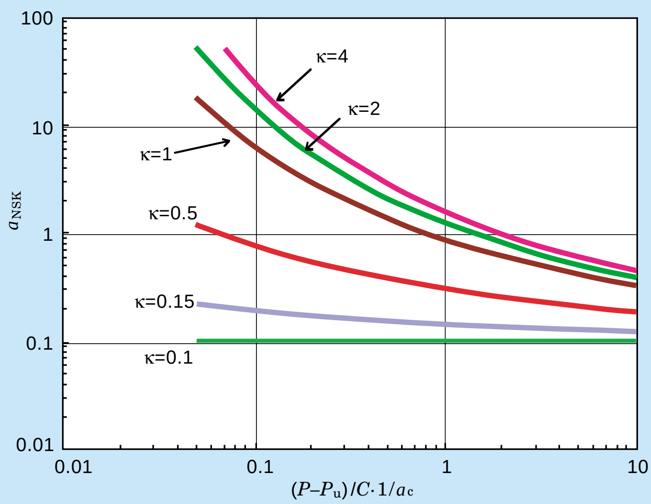

Fig. 12 New life equation curves for roller bearings

Table 4 Example of calculation with the new NSK life equation

Bearing type	Outer ring outer diameter (mm)	Inner ring inner diameter (mm)	Dynamic equivalent load P (N)	Fatigue load limit Pu (N)
6206	62	30	9700	490
Basic dynamic load rating C (N)	Contamination factor a_c	Running speed (min^{-1})	Temperature (°C)	Viscosity ratio κ
19500	0.5	4900	130	2.9

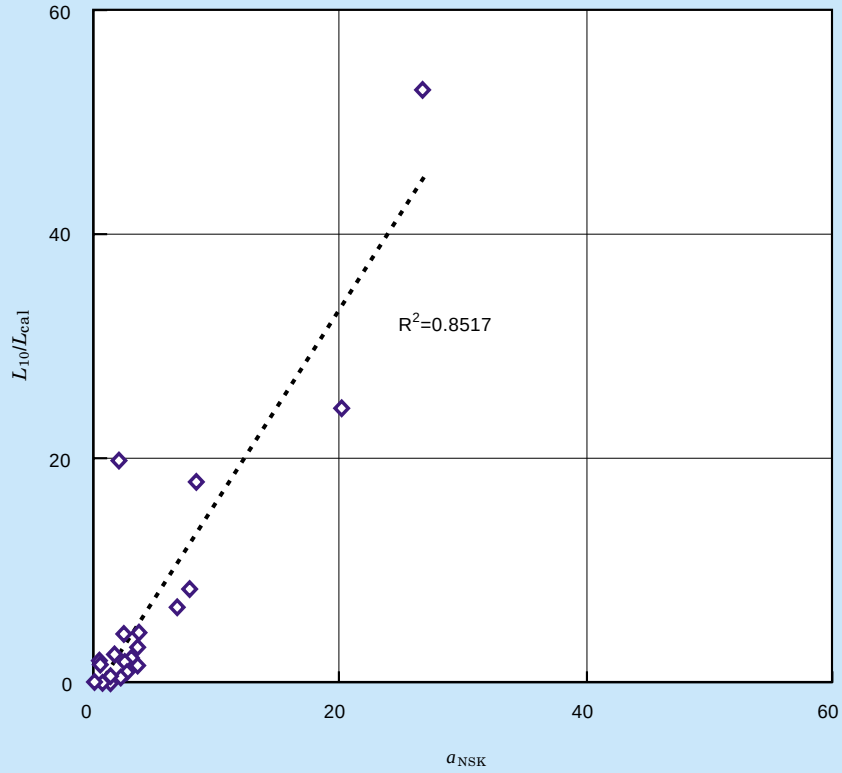

Fig. 13 Comparison of endurance test data and ball bearing life calculated with new equation

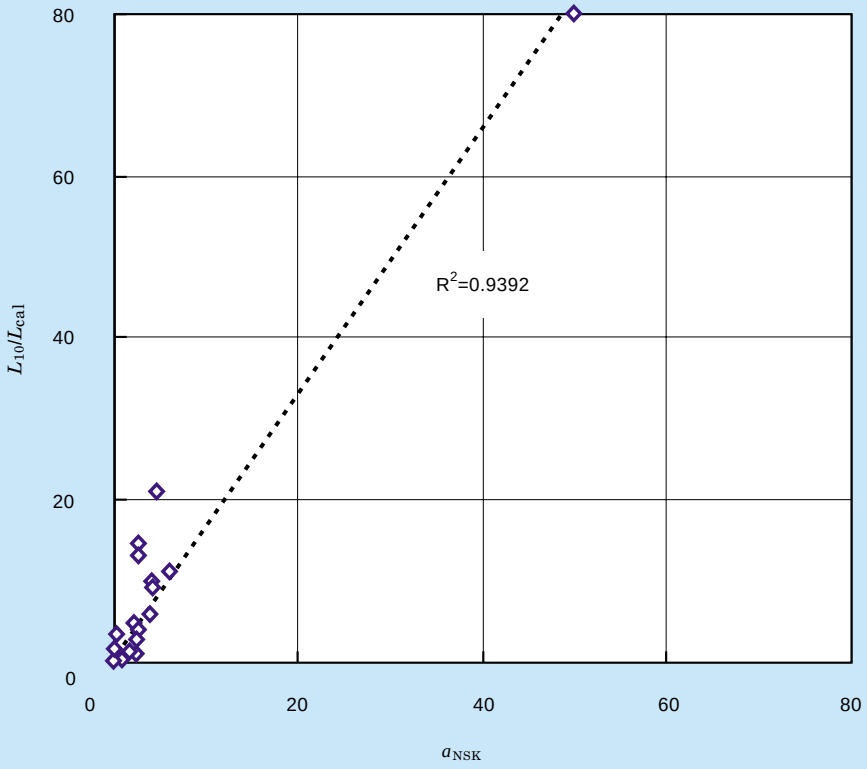

Fig. 14 Comparison of endurance test data and roller bearing life calculated with new equation

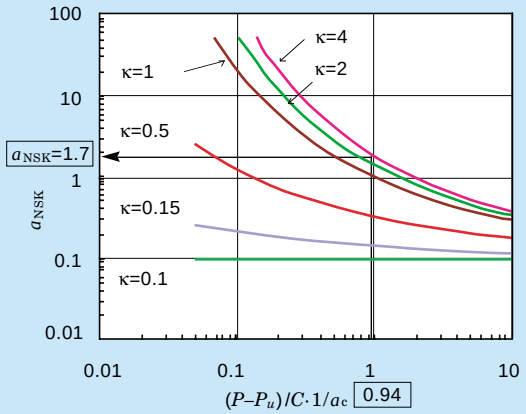

Fig. 15 Example of calculation using new life equation graph (for ball bearings)

3.6 Comparison Between New Equation Outcomes and Life Test Results

Fig. 13 compares endurance test data and ball bearing life calculated with the new equation. Fig. 14 compares endurance test data and roller bearing life calculated with the new equation. As is apparent, good agreement exists between life calculated with the new equation and the endurance test results.

3.7 Example of the New NSK Life Equation

Table 4 shows a calculation example using the new life equation for bearing 6206, a single-row deep groove ball bearing with an outer diameter of 62 mm and an inner diameter of 30 mm. The bearing was operated under normal lubrication conditions with Syntheses HT 320 oil at an inner ring rotation speed of 4900 rpm and a temperature of 130°C.

Fig. 15 is a graph of the new life equation for ball bearings. Calculating $(P\text{-}P_u)/C \cdot 1/a_c$ on the axis of abscissa, we obtained $(P\text{-}P_u)/C \cdot 1/a_c = 0.94$. Then, we went up on the graph to a point where the value of the lubrication parameter κ was 4.00, and read the value of a_{NSK} along the axis of ordinate. We obtained $a_{NSK} = 1.7$ and substituted this value in the new life equation to obtain (L able) = 47 hrs. This result is indicated in Fig. 15.

4. Conclusion

The new bearing life equation, based on the life tests of a total of more than a thousand ball bearings and roller bearings, allows prediction with a higher accuracy of bearing service life in various operating conditions in the market. Calculation results from this new equation, defined by the life modification factor (a_{NSK}), agreement with actual life test results[21].

a_{NSK} is a function of the load parameter $\{(P\text{-}P_u)/C\}$, the contamination factor (a_c) and the viscosity ratio (κ). In this load parameter, P is the dynamic equivalent load on a rolling bearing, and P_u is the bearing load below which the bearing does not fail after more than 10^{11} revolutions. The fatigue load limit is defined, based on the butterfly theory[3], as a bearing load equivalent to a contact surface pressure of 1.5 GPa. However, the fatigue load limit can be adjusted to reflect the effects of edge loading, rolling element skidding and other factors.

The life modification factor (a_{NSK}) applies to ball bearings and roller bearings, with some distinctions between both types. The new bearing life equation more accurately predicts bearing life under various running conditions.

References

1) G. Lundberg and A. Palmgren: Dynamic Capacity of Rolling Bearings, Ingeniorsvetenskapsakademiens Handlingar, No. 196 (1947)
2) ISO 281:1990
3) K. Furumura, Y. Murakami, T. Abe: ASTM, STP 1195 (1993), p.199-210
4) H. Takata, K. Furumura, Y. Murakami: ASME/STLE Tribology Conference (1995-10), p.11-16
5) T.A. Harris and J.I. McCool: ASME/STLE Tribology Conference (1995-10), p.1-13
6) SKF: General Catalogue, #4000E (1989)
7) FAG: Waelzlager Standardprogram, #WL41510/2DB (1989)
8) E. Ioannides and T.A. Harris: Transactions of ASME, Journal of Tribology, 107 (1985), p.367-378
9) T.A. Harris and J.I. McCool: ASME/STLE Tribology Conference (1995-10), p.1-13
10) Zwerlein O., Schlicht, H.: ASTM 771, J.J.C. Hoo, ed. American Society for Testing and Materials (1982), p.358-379
11) James R. Carely: SAE Technical Paper No. 9217212 (1992)
12) N. Mitamura, Y. Murakami, Krieger: SAE Technical Paper 972712 (1997), p.10
13) H. Takemura, N. Mitamura, Y. Murakami: 31st International Symposium on Automotive Technology and Automation, 98NM071 (1998), p.71-78
14) R. Michael, T. Shiratani, Y. Murakami, K. Abe: SAE Technical Paper 940728 (1994)
15) Y. Murakami, H. Takemura, A. Fujii, K. Furumura:

NSK Technical Journal No. 655 (1993), p.17-24*
16) H. Takemura, Y. Murakami: Fatigue Design 1995 International Symposium (sponsored by VTT, co-sponsored by ESIS, ASTM and EIS), p.345-356
17) Beiblatt 1993, DIN ISO 281
18) Y. Murakami, T. Toriyama, K. Tsubota, K. Furumura: Bearing Steel: into the 21st Century, ASTM STP 1327, J.J.C. Hoo and W.B. Green, Eds., ASTM (1998), p.105, 87
19) K. Furumura, Y. Murakami, K. Abe: NSK Technical Journal No. 656 (1993), p.15-21*
20) Y. Murakami, N. Mitamura, K. Furumura: NSK Technical Journal No. 652 (1992), p.9-16*
21) H. Takemura, Y. Matsumoto, Y. Murakami: SAE Technical Paper 2000-01-2601 (2000), p.7
*in Japanese

Hiromichi Takemura

Youichi Matsumoto

Yasuo Murakami

Development of the Half-Toroidal CVT POWERTOROS Unit (3)

Development of the Power-Split System

Shinji Miyata and Hisashi Machida
Corporate Reseach and Development Center

ABSTRACT

This paper describes a power-split system, which uses a toroidal variator and a planetary gear set. We have tested and analyzed a power-split system using a single-cavity Continuously Variable Transmission (CVT) and have confirmed a power transmission efficiency of 96 percent. Therefore, we believe that the power-split system will be developed vigorously.

1. Introduction

Growing concern about environmental problems in recent years has been boosting the demand for vehicles with greater fuel economy and lower exhaust emissions. CVTs have been attracting attention as a means to meet such demands. The rapid development and progress[1] of the toroidal CVT, in particular, has resulted in the development of a traction-drive type CVT that is capable of high torque transmission. NSK started research and development of the half-toroidal CVT in 1978. We tested several prototypes, which resulted in the completion of a half-toroidal CVT: the POWERTOROS unit[2]. In November 1999, POWERTOROS units were installed in Nissan Cedric and Gloria Sedans, thus achieving a world first by successfully bringing the traction-drive type half-toroidal CVT to the market. The half-toroidal CVT, thus made practically available, is so constructed that it can supersede a reduction gear in an automatic transmission (A/T). Fuel economy has been improved by approximately 10 percent in comparison to conventional automatic transmissions[3] by efficient transmission of power, which is 90 to 92 percent for this half-toroidal CVT[4]. To meet the demand for more efficient CVTs, a power-split system[5], which utilizes a differential gear unit by combining a half-toroidal CVT and a planetary gear, is being brought about as the second generation of the half-toroidal CVT. Theoretically, we estimate that this system will have a transmission efficiency of 96 percent at maximum speed. Although a power-split system has been around for a long time, it had not become a reality due to the lack of a suitable toroidal CVT.

This paper reports on the results of our analysis in pursuit of the theoretical efficiency of a power-split system incorporating a half-toroidal CVT. In addition, our measurement of the power and efficiency of the power-split system and comparison of the theory and the measurements are also covered.

2. Comparison Between Power-Split System and Geared Neutral System

Many studies have been conducted on the mechanism of

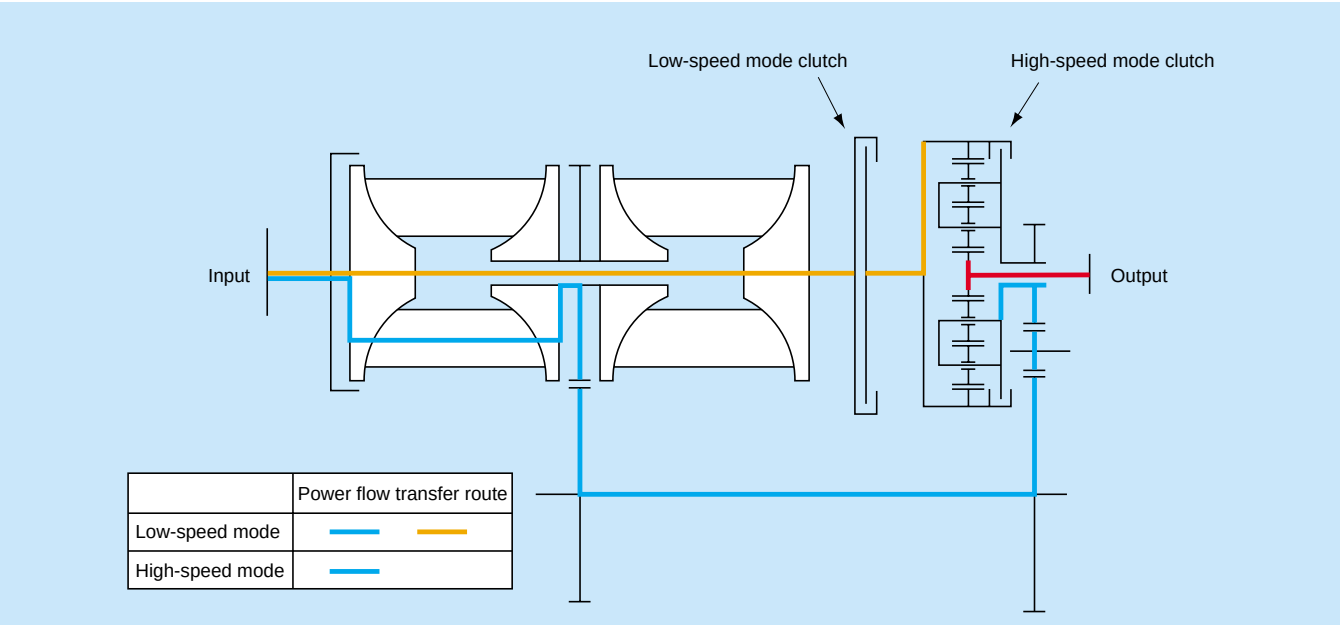

Fig. 1 Layout of geared neutral system

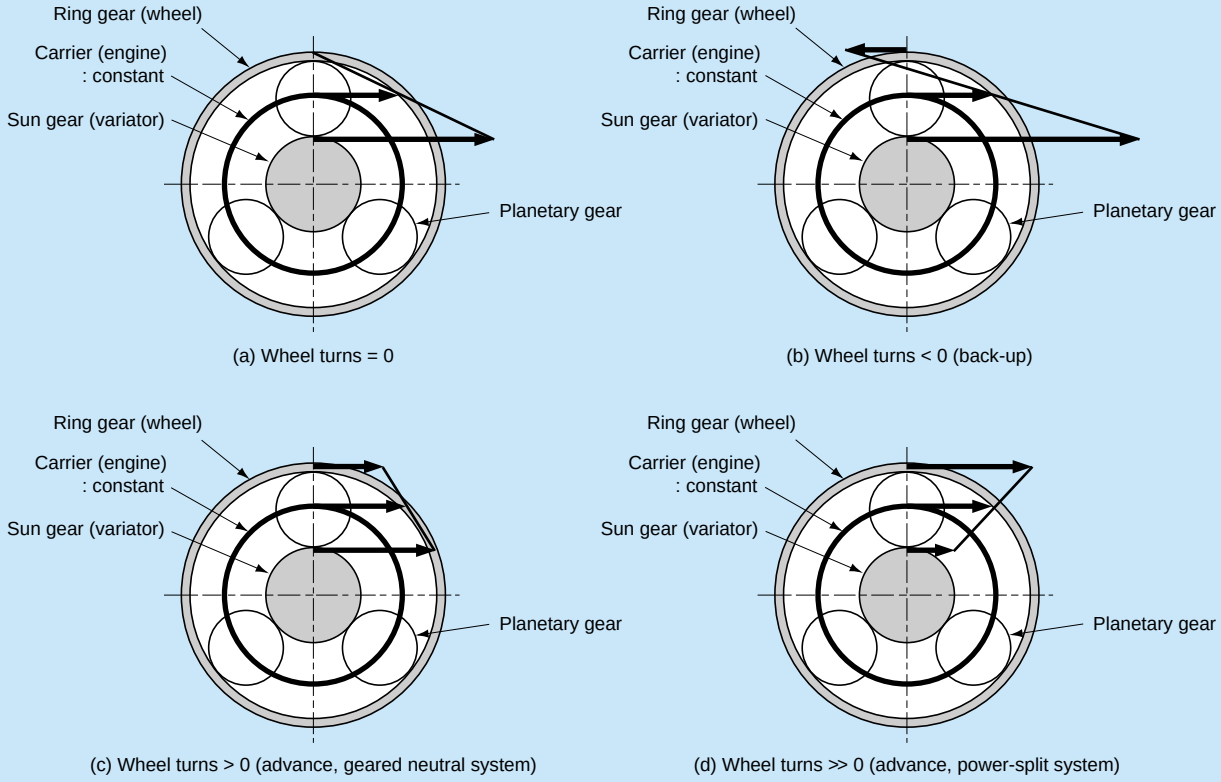

Fig. 2 Mechanism of geared neutral system and power-split system

utilizing gears differentially by combining a half-toroidal variator (hereinafter referred to as a variator) and a planetary gear system. Among many combinations available, the combination of a power-split system and a geared neutral system is considered to be most practical. The following subsections discuss these two systems.

2.1 Geared neutral system

Particularly noted among the numerous research and developments made on geared neutral systems to date is the study of Fellows[6]. As illustrated in Fig. 1, this system comprises two modes[7]: a low-speed mode for starting forward, running at low speeds, or for moving backwards, and a high-speed mode for use in high-speed running. In the low-speed mode, the low-speed clutch is engaged to obtain output drive force from the ring gear as a differential component of the sun gear and the carrier. In low-speed mode, output rotation speed is increased as the sun gear is rotated at a lower speed, or rather, as the variator is shifted for lower speed. In high-speed mode, where the clutch for high-speed mode is engaged, higher output rotation speed is obtained as the variator is shifted for higher speed.

In low-speed mode, the geared neutral system can change output rotation to neutral as shown in Fig. 2 (a), or to forward, or to backward, as shown in Figures 2 (b) and 2 (c). This is accomplished by utilizing the differential mechanism of the planetary gear as the variator gear ratio is shifted. When the variator gear ratio is engaged from the neutral position toward speed-up, the vehicle backs-up; and when it is shifted from the neutral position toward speed-down, the vehicle advances. Thus, the geared neutral system is an infinitely variable transmission that requires no clutch for starting.

In low-speed mode of the geared neutral system, power circulates within the system. Whereas high power may also pass through the variator, sufficient care needs to be taken to ensure power transmission efficiency and endurance[8].

2.2 Power-split system

Okoshi was possibly the first to devise a power-split system in 1987. But the system devised by Okoshi consisted of a dual planetary gear arrangement, resulting in a complex construction. From there, we devised a layout of a single planetary gear system of simpler construction (Fig. 3).

Our system consists of a low-speed mode, a high-speed mode, and a back-up mode. In low-speed mode, a low-speed clutch (K1) engages while the variator shifts toward speed-up providing high-speed output rotation. In high-speed mode, a high-speed clutch (K2) engages providing output rotation from the sun gear as a differential component of the carrier and the ring gear. In high-speed mode, higher-speed rotation is obtained as the variator is shifted into lower speed (Fig. 2 (d)). Fig. 4 offers comparison of the power-split system and the geared neutral system for overall reduction ratios of the variator

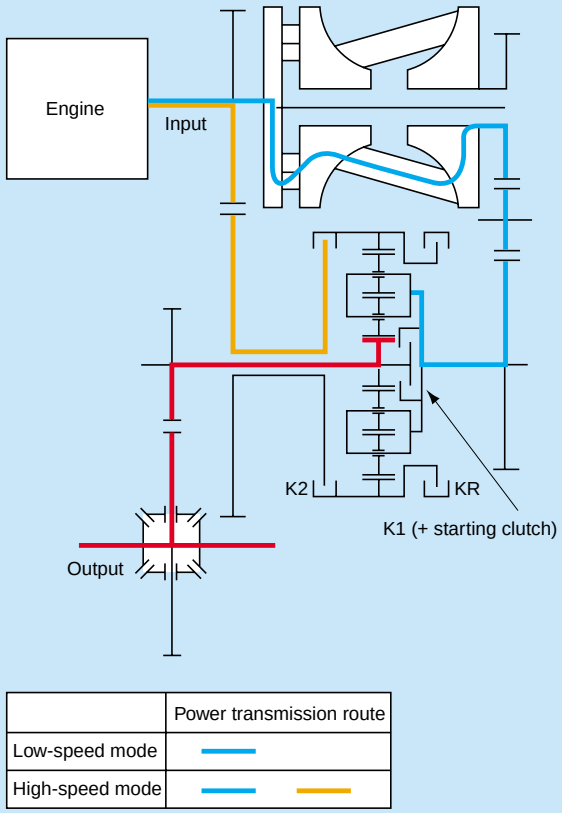

Fig. 3 Layout of power-split system for FF vehicle

and the CVT system. The power-split system requires a starting clutch. In high-speed mode of the power-split system, power circulates within the system but the power passing through the variator is small. Fig. 5 shows how power flows through the variator and the ring gear, assuming that no power is lost in the variator and the gear. The power flowing through the variator in high-speed mode of the power-split system is given by:

$$P_{\mathrm{vin}} = -\frac{\rho+1}{i_{\mathrm{v}} \cdot i_1 \cdot i_2 - \rho - 1} \cdot P_{\mathrm{E}} \quad \cdots\cdots (1)$$

where,

P_{vin}: power on variator input disk
P_{E}: engine power
ρ: number of sun gear teeth/number of ring gear teeth of planetary gear
i_{v}: variator reduction ratio
i_{j}: gear reduction ratio (j = 1, 2)
i_0: $= 1/\rho$

Using Morozumi's equation[9] for the transmission efficiency, η_{o}, of planetary gear, the theoretical efficiency of the power transmission from the engine shaft to the sun gear is expressed as:

$$\eta_{\mathrm{total}} = \frac{\eta_0 (i_0 i_1 i_2 i_{\mathrm{v}} + 1 - i_0)}{i_0 i_1 i_2 i_{\mathrm{v}} + \eta_{\mathrm{v}} \eta_1 \eta_2 (\eta_0 - i_0)} \quad \cdots\cdots (2)$$

where,

η_{total}: theoretical transmission efficiency of the power-split system
η_{o}: transmission efficiency of the planetary gear
η_{v}: theoretical transmission efficiency of the variator
η_{j}: transmission efficiency of the gear pair (j = 1, 2)

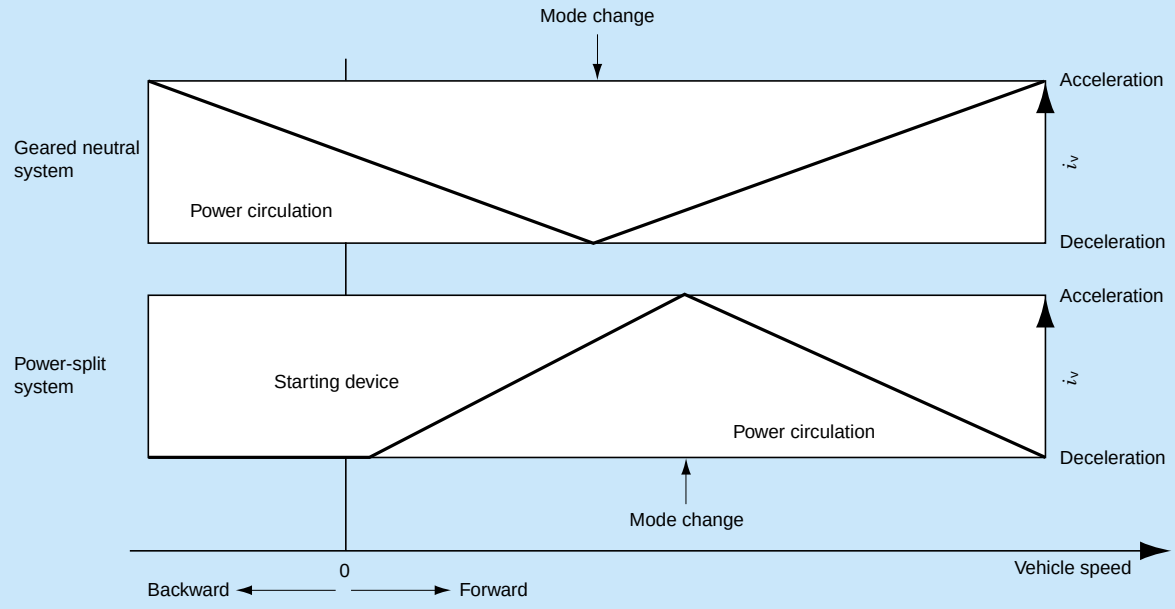

Fig. 4 Difference between a geared neutral system and a power-split system

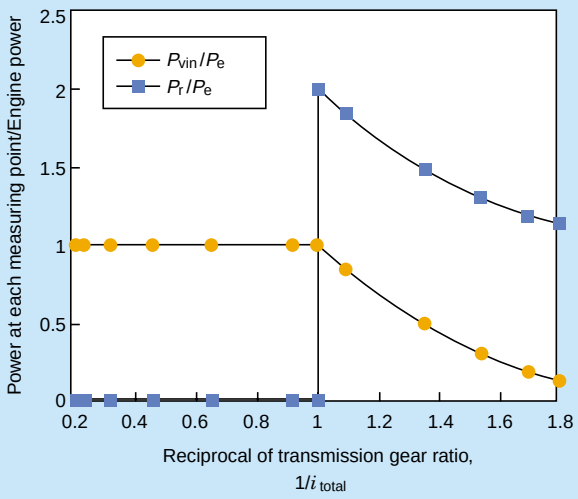

Fig. 5 Theoretical power flow of a power-split system

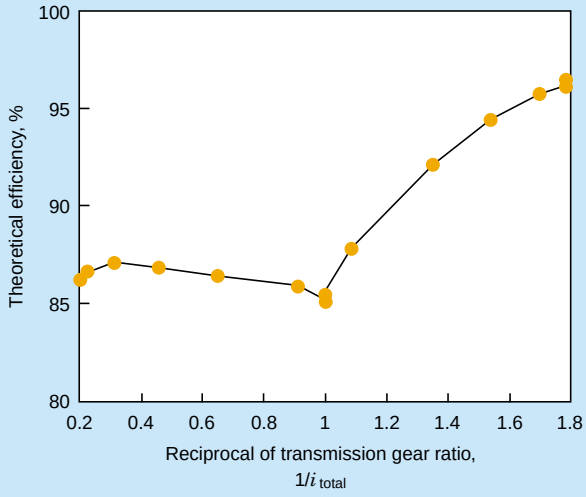

Fig. 6 Theoretical efficiency of a power-split system with single-cavity CVT

Here, the equation of Machida et al.[10] is used for the transmission efficiency of the variator, η_v, and η_j are used to represent the transmission efficiency of the gear pair. Fig. 6 shows the theoretical power transmission efficiencies of the power-split system, having a variator whose specification is listed in Table 1, and operated under conditions listed in Table 2.

Although the power-split system requires a starting clutch, it does provide a wide range of reduction ratios, and is highly efficient at transmitting power due to power flowing through the variator being small as shown in Fig. 5.

Table 1 Variator specification

Maximum input torque	(N•m)	150
Transmission ratio range		8.6
Variator ratio range		4.8
Disk outer diameter	(mm)	156
Cavity diameter	D (mm)	132
Disk radius	R_o (mm)	40
Half contact angle	θ (deg)	62.5

Table 2 Condition data

Input running speed	(rpm)	2 000
Input torque	(N•m)	150
Oil temperature	(˚C)	80

Table 3 Combinations of planetary gear sets

Case	①	②	③	④	⑤	⑥
Sun gear	Variator	Variator	Engine	Engine	Wheel	Wheel
Carrier	Engine	Wheel	Variator	Wheel	Engine	Variator
Ring gear	Wheel	Engine	Wheel	Variator	Variator	Engine
N_W/N_E	$\frac{1-\rho}{\beta}+\frac{\rho}{\alpha\cdot i_v}$	$\frac{1}{1-\rho}\left[\frac{1}{\beta}-\frac{\rho}{\alpha\cdot i_v}\right]$	$\frac{\rho}{\beta}+\frac{1-\rho}{\alpha\cdot i_v}$	$\frac{1}{1-\rho}\left[-\frac{\rho}{\beta}+\frac{1}{\alpha\cdot i_v}\right]$	$-\frac{1-\rho}{\rho\beta}+\frac{1}{\rho\alpha\cdot i_v}$	$\frac{1}{\rho}\left[\frac{1}{\beta}-\frac{1-\rho}{\alpha\cdot i_v}\right]$
Geared neutral system availability	○	○	△	△	○	○
Power-split system availability	○	○	N/A	N/A	○	○

○: available △: available depending on conditions N/A: not applicable

3. Conditions Vital for a Power Circulating CVT System

Fig. 7 illustrates a model of a power circulating CVT system having a single planetary gear. The three elements of a planetary gear (sun gear, carrier, and ring gear) can be combined with the three shafts (variator output shaft, variator bypassing shaft, and power-split system output shaft) into six different configurations as listed in Table 3.

The number of revolutions of each of the three elements of a planetary gear is given by:

$$N_R - N_C = \rho\,(N_S - N_C) \quad \ldots\ldots (3)$$

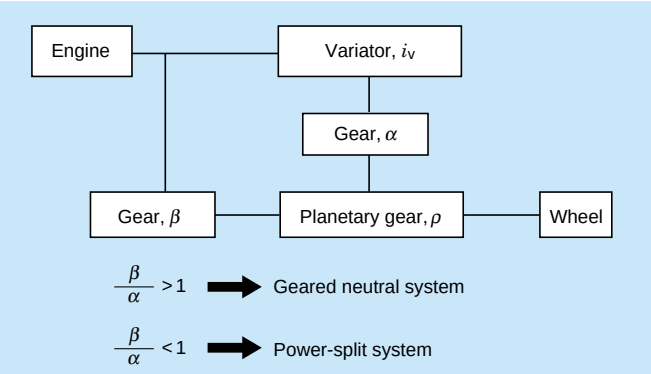

Fig. 7 Model of planetary gear set and variator

We then calculated the output/input rotation rate, N_W/N_E, for each of the six combinations. N_W denotes the number of output revolutions, and N_E the number of input revolutions of the power-split system.

As a result, the relation between the output and input rotation speed can be expressed by a general equation as follows:

$$\frac{N_W}{N_E} = f_1(\alpha,\beta,\rho) + \frac{f_2(\alpha,\beta,\rho)}{i_v} \quad \cdots\cdots\cdots\cdots\cdots\cdots (4)$$

Since $|N_W/N_E|$ must become larger as the variator is shifted for lower speed in the high-speed mode of the power-split system, one of the conditions (5) below must also be satisfied in Equation (4):

$$\begin{matrix} f_1>0, & f_2>0, & \alpha<0, & \beta>0 \\ f_1<0, & f_2<0, & \alpha>0, & \beta<0 \end{matrix} \quad \cdots\cdots\cdots\cdots\cdots\cdots\cdots\cdots (5)$$

Therefore, we can determine that the power-split system does not apply to cases ③ and ④. For the same reason, the geared neutral system can be readily applied to cases ③ and ④ in the low-speed mode. As for the other cases of ①, ②, ⑤ and ⑥, continuously variable transmission systems having a low-speed and high-speed mode can be developed using a one planetary gear set.

4. Experimental Verification of the Power-Split System

We measured experimentally the power and the power transmission efficiency of the power-split system having a single-cavity CVT. Fig. 8 illustrates a sectional view of the single-cavity CVT used as a variator in the experiment. Fig. 9 shows transmission efficiency curves of the variator. The maximum transmission efficiency of this variator, with the same specifications as those listed in Table 1, is approximately 85 percent.

Fig. 10 shows a configuration of the power-split system. A 300 kW DC dynamometer was used for the driving force absorber. To determine the power flowing through the power-split system, the torque and the number of shaft revolutions were measured and calculated at three locations: (1) a system output point, (2) between the variator output shaft and the planetary gear, and (3) on the bypass shaft. Switching between low-speed and high-speed modes was accomplished by engaging and disengaging the coupling.

Fig. 11 shows the results of a power-split system speed change test performed at a constant running speed of the input shaft under no load. The output shaft running speed continuously changed in proportion to variator gear ratio changes. In Fig. 11, the measurements agree with the theoretical lines. Fig. 12 shows the power measured at the three locations mentioned earlier. Power flow transferred at approximately 1.7 times the input power to the power-split system, and passed through the bypass shaft (③) immediately after mode change. In high-speed mode,

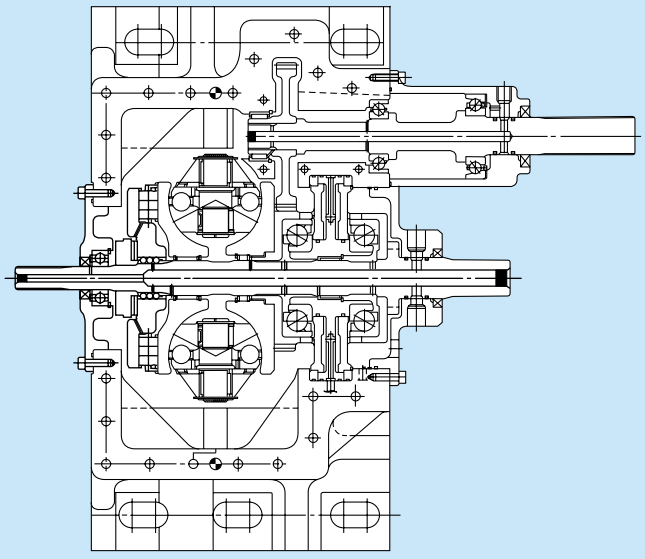
Fig. 8 Single-cavity CVT

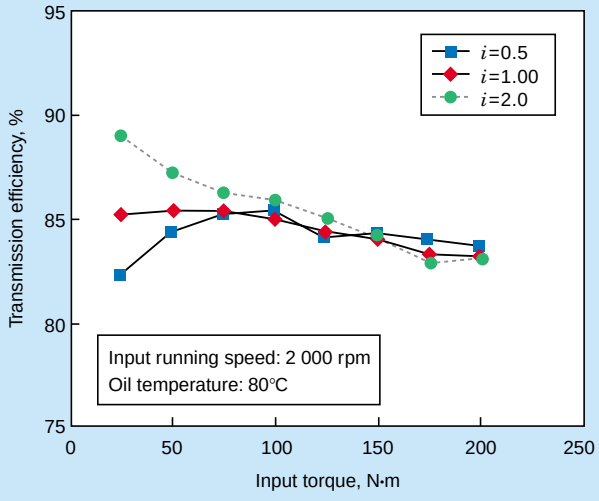

Fig. 9 Efficiency of the single-cavity test box

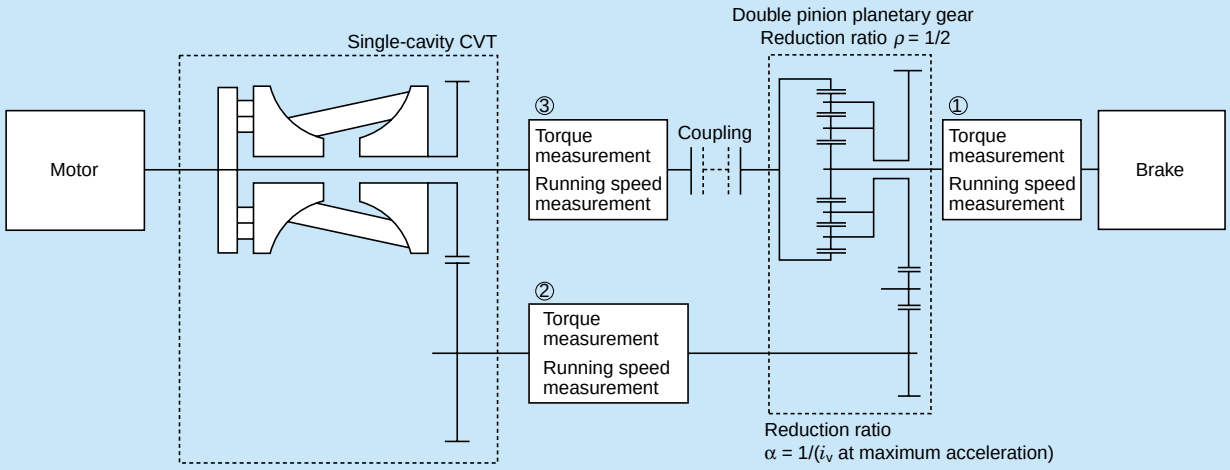

Fig. 10 Power-split system with single-cavity CVT

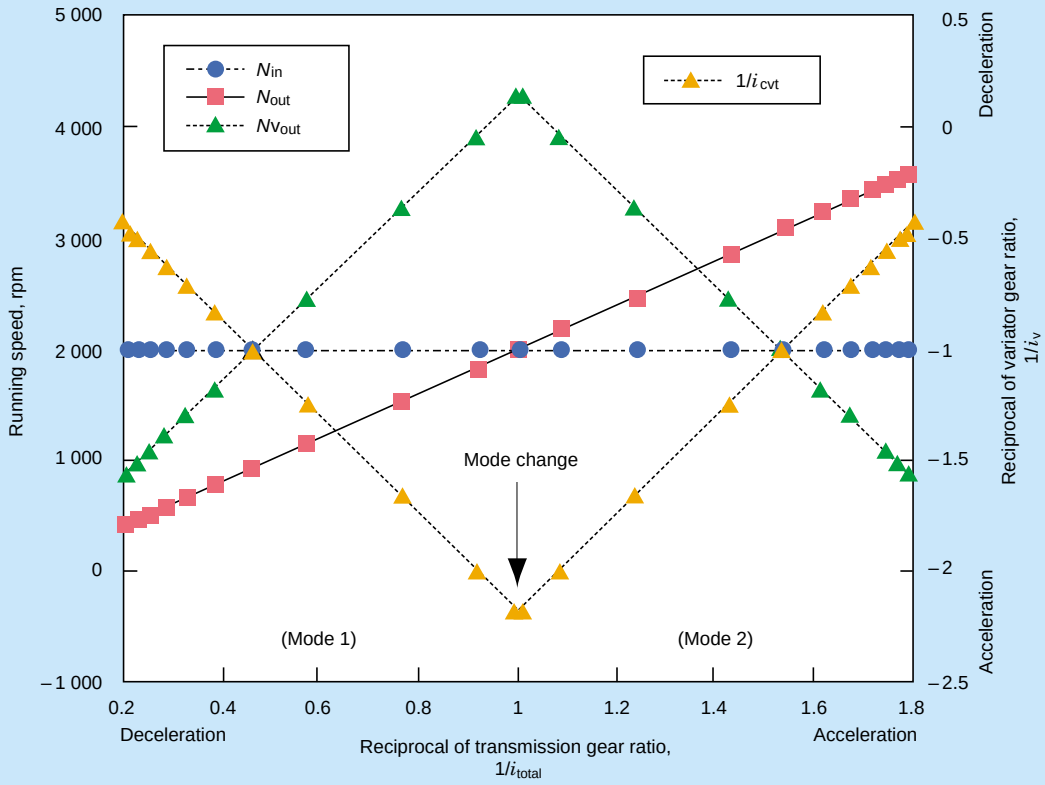

Fig. 11 Test result of ratio changing without load

power flowing through the variator reduced with gear ratio changes. Finally, only 10 percent of the power-split system input power transferred through the variator once the vehicle reaches maximum speed. Additionally, power flow transferred through the variator from the output disk side toward the input disk side in high-speed mode. This was exactly as we had anticipated based on our theory.

Measurements of transmission efficiency of the power-split system are shown in Fig. 13, in which the axis of abscissa represents the reduction ratio of the power-split system and vehicle speeds when the engines were running at 1 600 rpm and 5 400 rpm. The overall transmission efficiency of the system is between 80 and 85 percent for low-speed mode, and reached a maximum of 96 percent

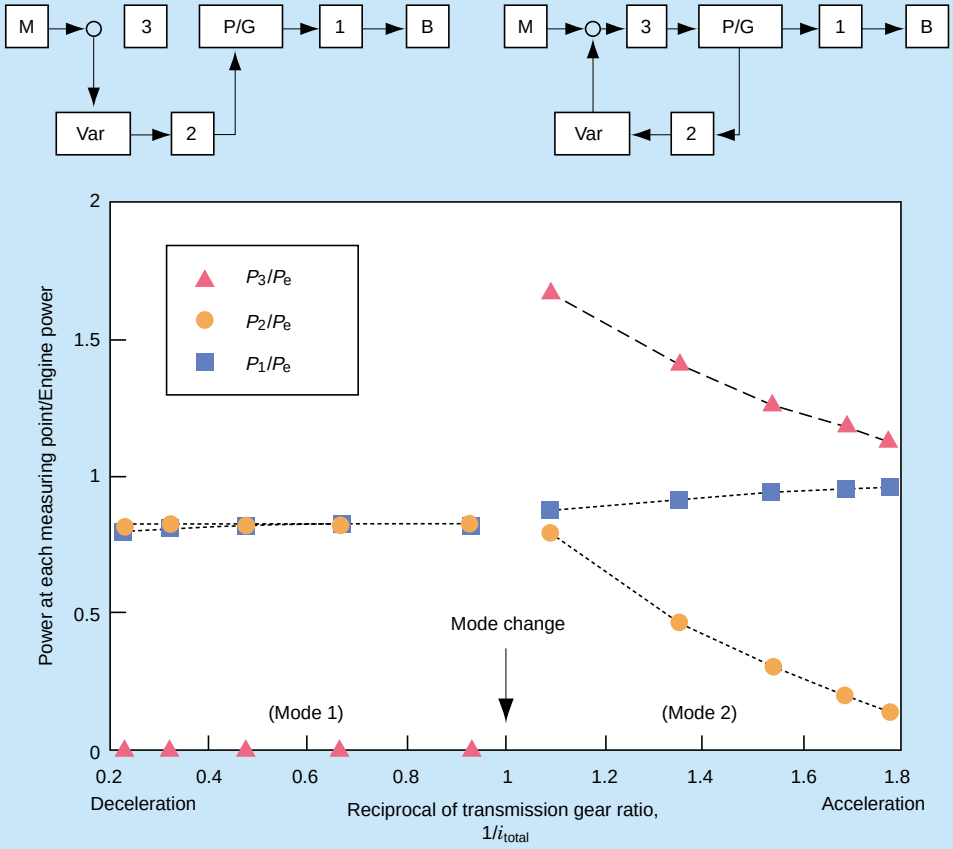

Fig. 12 Test result of power flow of power-split system

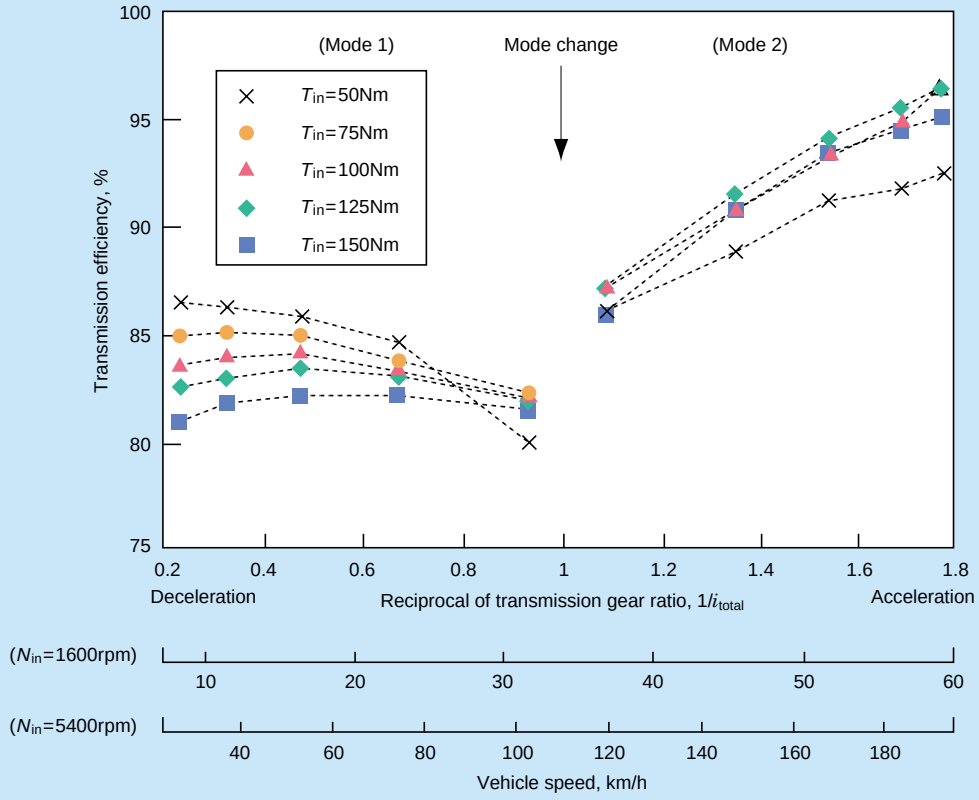

Fig. 13 Efficiency of power-split system

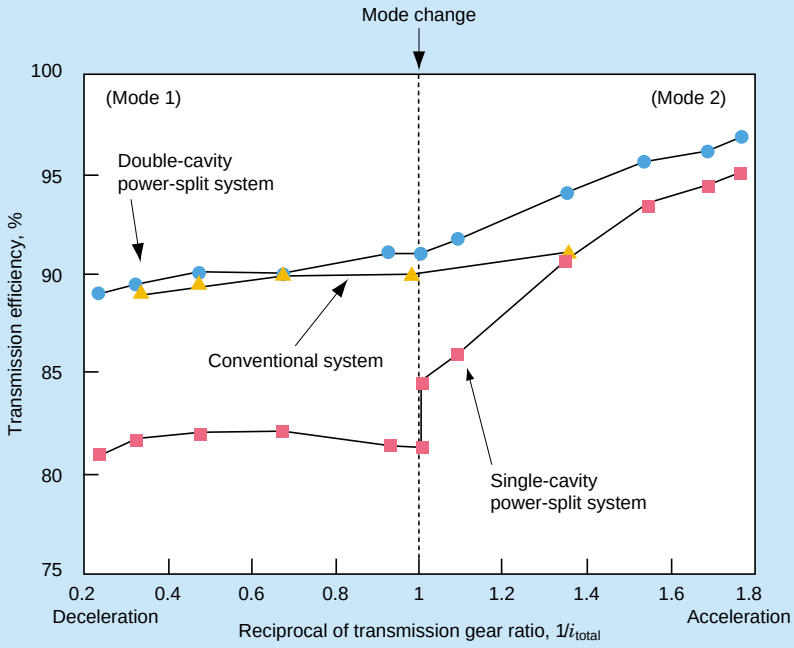

Fig. 14 Efficiency of power-split system with double-cavity CVT

during high-speed mode. This transmission efficiency includes the power loss from the gears, seals, and bearings used in the power-split system. It does not, however, include power loss from the hydraulic pumps for control and lubrication. Thus, the experimental results, like the analytical results, verify the high power transmission efficiency of the power-split system having a half-toroidal CVT. Our results also assure the possibility of designing a transmission with a power-split system.

5. Application of Double-Cavity CVT to Power-Split System

We have described a power-split system comprising of a single-cavity CVT for small FF vehicles, which is small in size and consists of fewer parts. However, this system can also be incorporated with a double-cavity CVT in place of a single-cavity CVT. A power-split system with a double-cavity CVT has a wide reduction ratio range and its theoretical transmission efficiency is approximately 90 percent in low-speed mode. In high-speed mode, its maximum theoretical transmission efficiency is 97 percent as shown in Fig. 14.

References

1) H. Machida et al., JSAE Paper 963402 (1996)
2) NSK Technical Journal, 669 (2000), 9-20*
3) T. Takeuchi, Kouseinou CVT no kaihatsu to sono hyouka, ISS Seminar (2000)*
4) NSK Technical Journal, 670 (2000), 2-10*
5) H. Okoshi, Japanese Patent, JP 2929592B*
6) Thomas G. Fellows et al., SAE Paper 910408 (1991)
7) Japanese Patent, JP H 11-63146A*
8) A. Kubo, The Japan Society of Mechanical Engineers Journal 101,950 (1998), 62
9) M. Morozumi, Yuusei haguruma to sadou haguruma no sekkei keisanhou, (1984), 178, Sankei Shuppan-sha*
10) H. Machida et al., SAE Paper 950675 (1995)
*in Japanese

Shinji Miyata

Hisashi Machida

Automobile Transmission Performance and Bearing Type

Takao Obara
Bearing Technology Center

ABSTRACT

Automobile transmissions are required to have a high load-carrying capacity and efficiency, while maintaining compactness and low noise. The level of these requirements increases every year. As a result, requirements for transmission bearings have become much more demanding. Although new developments in bearing technology are important for meeting the ever-increasing level of requirements, experience teaches us that it is still important to have a clear understanding of how bearings influence transmission performance.

1. Introduction

Automobile transmissions must meet various requirements to include the ability to change gears smoothly, have a high load-carrying capacity, remain compact, keep weight at a minimum, and be highly efficient and quiet. These requirements have become increasingly stringent year after year. As a result, requirements for transmission bearings must also meet higher standards.

In order to meet such requirements, bearing technology is naturally important, but a clear understanding of how bearings influence transmission performance is also important.

This paper explains the relation between transmission performance and types of bearings, which is fundamental to the development of bearing applications for automobile transmissions.

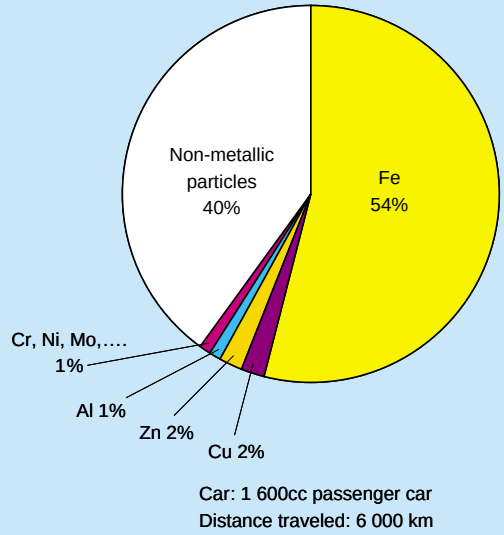

Fig. 1 Particles contained in used manual transmission oil

2. Characteristics of Transmissions

Generally speaking, automobile transmissions allow drivers to choose running speeds by using either an automatic transmission or a gearbox. Drivers can select a gear ratio that results in engine output torque being converted into vehicle speed.

There are various types of automobile transmissions, which are classified according to driving systems. General-purpose, two-wheel drive vehicles are classified into transmissions for FR vehicles (hereinafter called T/M) and transaxles for FF vehicles (hereinafter called T/A). They

Table 1 Power transfer elements and lubricating oil for various types of transmissions

Transmission type	Power transfer elements	Lubricating oil
Manual T/M Manual T/A	Helical gear Spur gear	Gear oil
Automatic T/M	Planetary gear	ATF
Automatic T/A	Planetary gear Helical gear	ATF
Half-toroidal CVT	Roller and disc Helical gear	Traction oil
Steel belt CVT	Belt and pulley Helical gear Planetary gear (for moving back)	ATF CVT fluid
Dry hybrid V-belt CVT	Belt and pulley Helical gear	Gear oil (Pulley assy not lubricated)

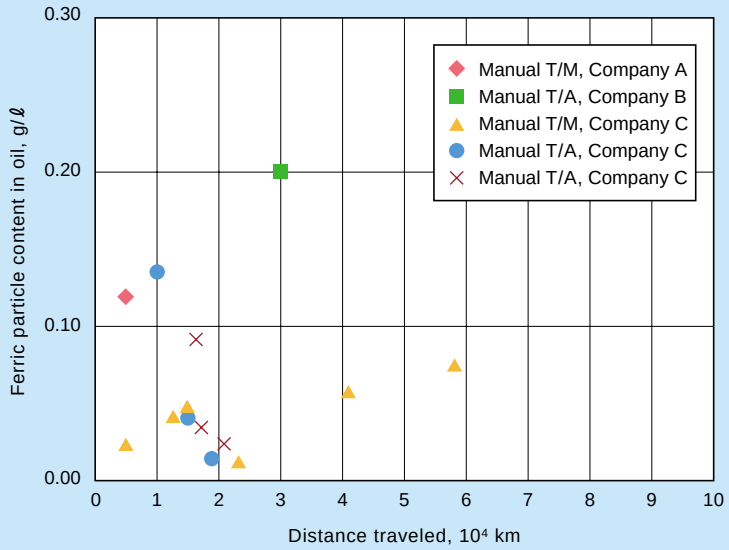

Fig. 2 Amounts of ferrous contamination in transmission oil

can be also classified by change-speed gearbox into manual transmissions, automatic transmissions, and CVTs. Table 1 lists power transfer elements and lubricating oils for specific types of transmissions for two-wheel drive vehicles.

For most of these transmissions, gears in an aluminum case transfer power and are lubricated with oil.

3. High Load-Carrying Capacity, Smaller, and Lighter Transmissions & Types of Bearings

Rolling bearings that enable transmissions with a higher load-carrying capacity, compactness, and improved weight are needed. Simultaneously, rolling bearings with longer life and a smaller size are also needed. The following bearing combinations are the most common in shaft support systems:

(1) 1 ball bearing + 1 ball bearing
(2) 1 cylindrical roller bearing + 1 cylindrical roller bearing (for relatively low axial load)
(3) 1 ball bearing + 1 cylindrical roller bearing
(4) 1 tapered roller bearing + 1 tapered roller bearing

Whereas tapered roller bearings have the largest axial load carrying capacity, the last bearing combination is the most advantageous in meeting the goal of having a transmission that is more lightweight, has a higher load-carrying capacity, and is more compact.

For applications where tapered roller bearings cannot serve long enough or where other types of bearings are needed to fulfill a longer life, a basic approach is to use larger rolling elements (balls or rollers) to achieve a higher basic load rating. This approach alone, however, is insufficient. Considering that actual bearing life in transmissions is shorter than the rating fatigue life, NSK analyzed oils from several transmissions (Figs. 1 and 2). We also analyzed the fatigue pattern of bearings from transmissions of actual vehicles using NSK's unique fatigue analysis technology. As a result, we determined that fatigue of transmission bearings originates not in internal fatigue, which is a pattern of material fatigue affecting rating fatigue life, but rather from surface fatigue that is caused by the foreign inclusion.

We then developed a technology to ensure long bearing life in the presence of foreign inclusions. We have thus successfully introduced Sealed-Clean bearings[1)] and TF Series bearings[2)] into the market. These bearings are the result of the above-mentioned analysis. The optimization of various specifications has contributed to the development of transmissions that are more lightweight, have a higher load-carrying capacity, and are more compact.

4. Transmission Efficiency Improvement & Type of Bearings

The main factors of transmission torque loss include:

(1) Oil resistance
(2) Mating loss of gears
(3) Frictional loss of sliding and rolling parts

The dynamic frictional torque of rolling bearings is approximately less than one-fourth of that of slide bearings while under conventional operating conditions. As for low-torque rolling bearings, tapered roller bearings require less torque compared to other types. This is due to

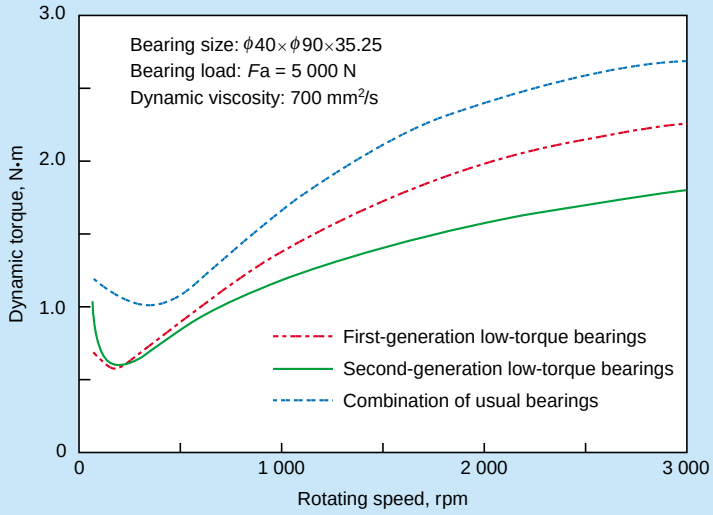

Fig. 3 Performance of low-torque bearing combinations compared with normal bearing combinations

the fact that sliding friction takes place between the inner ring large rib and the roller ends of tapered roller bearings.

NSK's first-generation low-torque tapered roller bearings achieved frictional torque at a level of approximately 20 percent lower than that of general tapered roller bearings (Fig. 3). This is a result of:

- Improved inner ring large rib surface roughness
- Improved roller end surface roughness
- Improved roller end shape
- Optimized outer ring, inner ring, and roller rolling contact surface crowning

The development of NSK's first-generation low-torque tapered roller bearings was focused on the reduction of frictional torque in single bearings. Our second-generation low-torque tapered roller bearings have been developed with emphasis placed on the optimization of their internal specifications (including roller diameter, number of rollers, roller length, and contact angle). This is in consideration of life, rigidity, and frictional torque when two of them are combined, reflecting their actual operating conditions. As a result, the second generation further reduced the low torque of the first generation by about 20 percent (Fig. 3).

These first-generation and second-generation low-torque tapered roller bearings have been contributing to the improvement of automobile transmission system efficiency.

5. Sounds and Vibrations of Transmissions & Types of Bearings

The sounds and vibrations of an automobile transmission can be classified into a booming sound during running, a gear noise, and a rolling bearing sound and vibration (Fig. 4).

Since rolling bearings are designed to carry load and rotary motion using rolling elements, they intrinsically have sound and vibration characteristics that may affect the sound and vibration properties of transmission systems as well. There are some types of noises produced by rolling bearings, and they have a specific frequency.

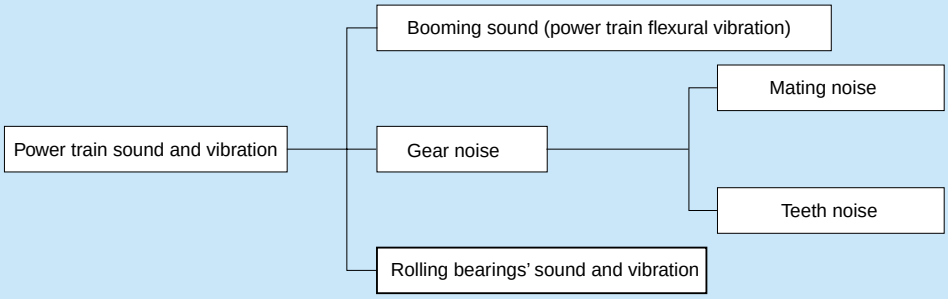

Fig. 4 Sound and vibration generated in automobile power train systems

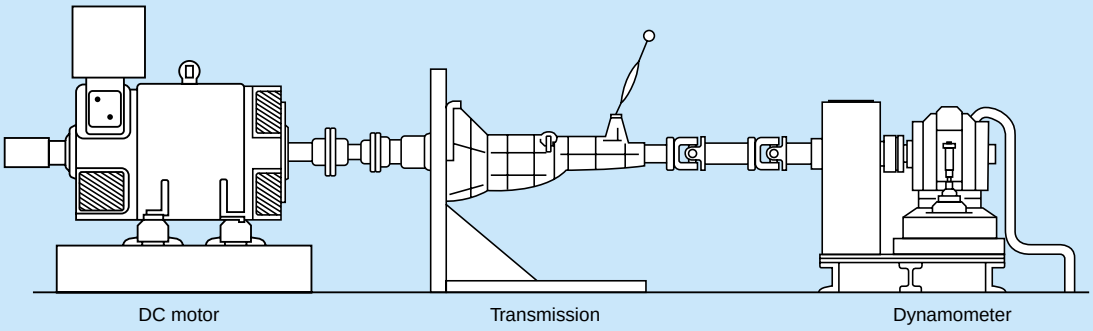

Fig. 5 Test equipment using full-size transmission

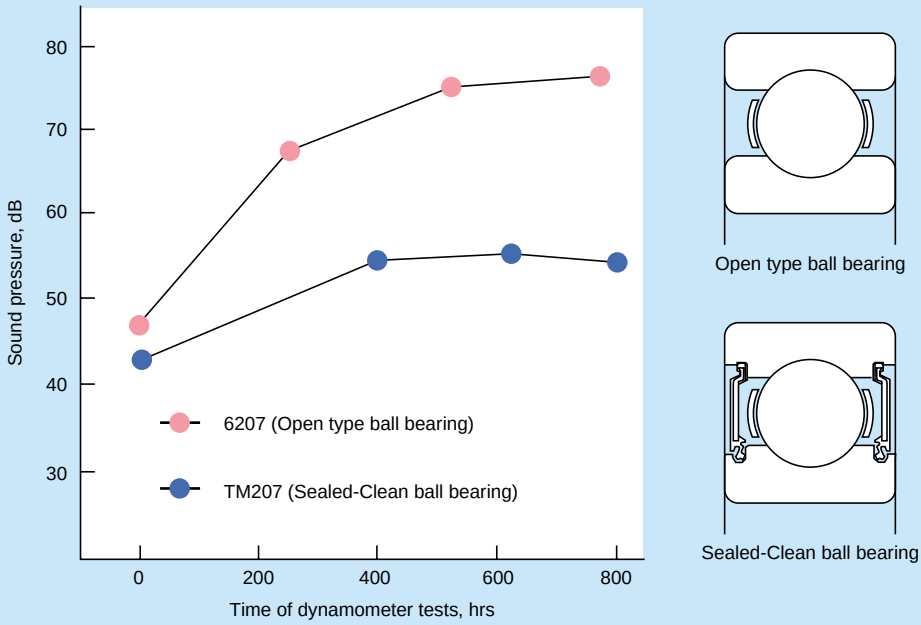

Fig. 6 Sound pressure of bearings after full-size transmission tests

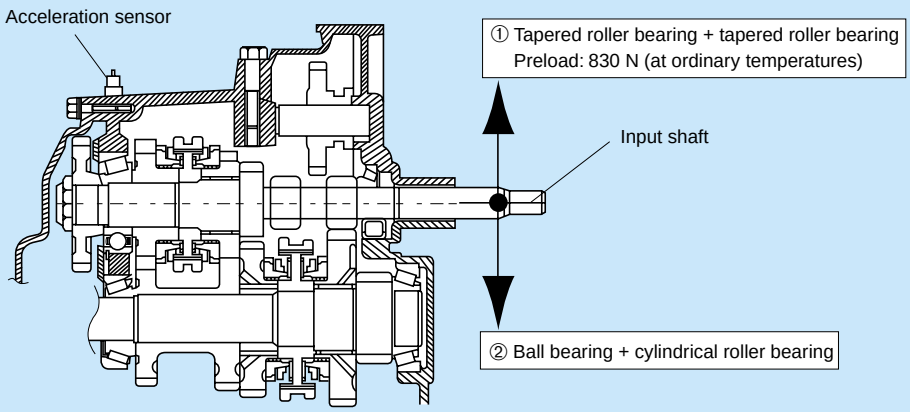

Fig. 7 Cross-section of transaxle

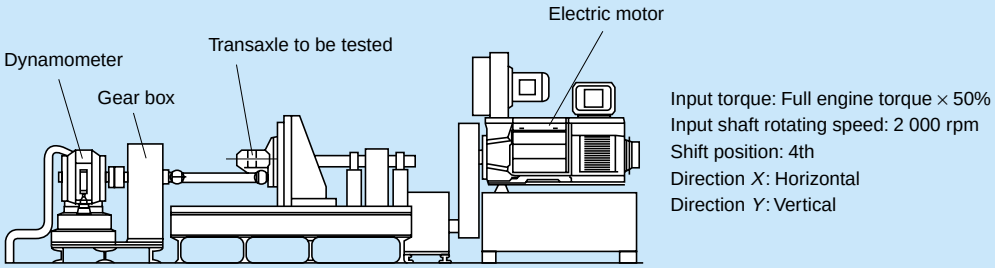

Fig. 8 Test equipment using full-size transaxle

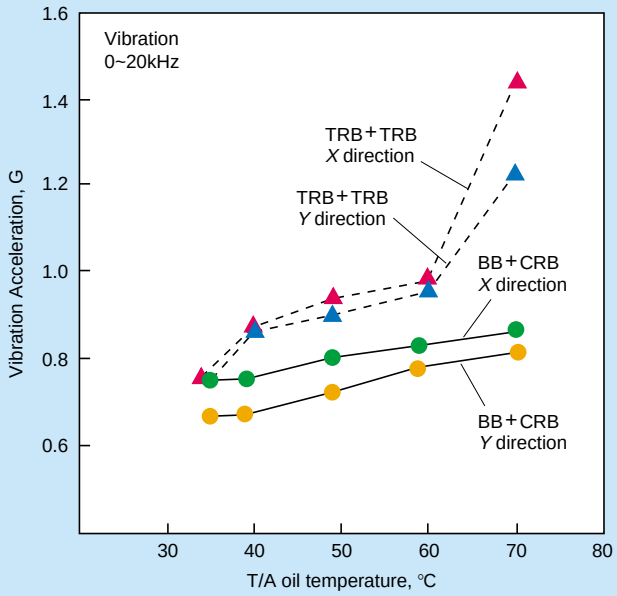

Fig. 9 Transaxle test results

Frequency analysis is, therefore, often used to diagnose the causes of noises[3].

Contaminated lubricating oil of bearings in transmissions can be the cause of bearing noise. NSK technology for improving bearing life in the presence of foreign inclusions described in Section 3 is also effective against age deterioration of bearings due to sound pressure originating from foreign inclusions. Fig. 6 presents an example of sound pressure test results of Sealed-Clean ball bearings and open-type ball bearings, as tested in a full-size transmission (Fig. 5).

As a factor of gear misalignment, bearing rigidity is considered to have effects on the sound of mated gears. Tapered roller bearings are often used in locations to support gear shafts having a large diameter because they can be preloaded for high bearing rigidity, such as for a shaft on the differential gear side of a T/A.

Even though the tapered roller bearing is considered the best option for minimizing mated gear sounds, the bearing may lose preload and consequently permit gear noise if used in an aluminum transmission case. This is due to transmission case expansion, which is caused by heating of the transmission owing to the high linear expansion coefficient of aluminum.

Figs. 7 and 8 depict the equipment and conditions used for measuring the oil temperature of an actual T/A and the vibration of the T/A case, with the input shaft of the T/A supported with different types of bearings. Fig. 9 shows the measurements respectively. When the combination of tapered roller bearings was used, preload was lost and vibrations increased sharply at a certain temperature.

By contrast, the combination of a ball bearing and a cylindrical roller bearing, arranged such that the ball bearing is axially fixed while the cylindrical roller bearing is axially set free, has the advantage of freedom from the effect of case expansion at high temperatures.

There can also be a bearing noise problem in applications where tapered roller bearings are used for a short span, and the thermal expansion of the transmission case is not a significant problem. This is caused by an early loss of bearing preload on the market due to insufficient bearing running-in at the time of its preloading in an automotive assembly line. Developed in view of this automotive assembly process is the Quick-Assembly Tapered (QAT) roller bearing [4]. The QAT roller bearing requires a running-in time as short as one-fourth of that required by other tapered roller bearings until the assembly width is reduced to a design dimension. This bearing can reduce not only assembly time but can also stabilize preload.

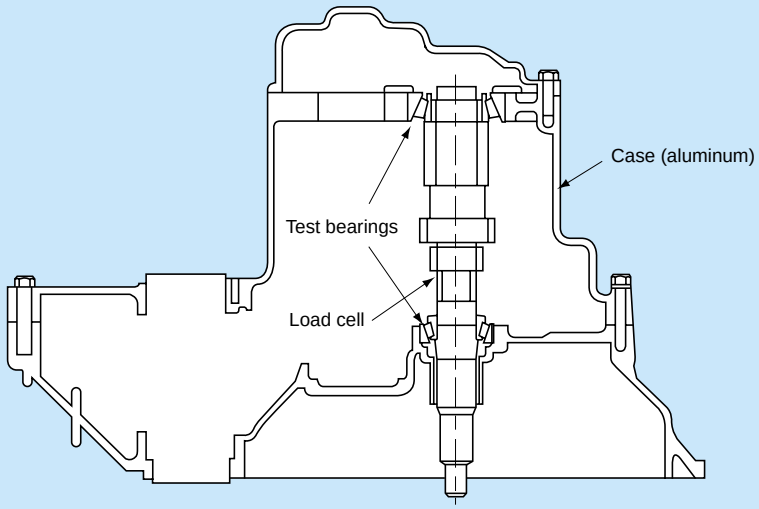

Fig. 10 Measurement of bearing preload

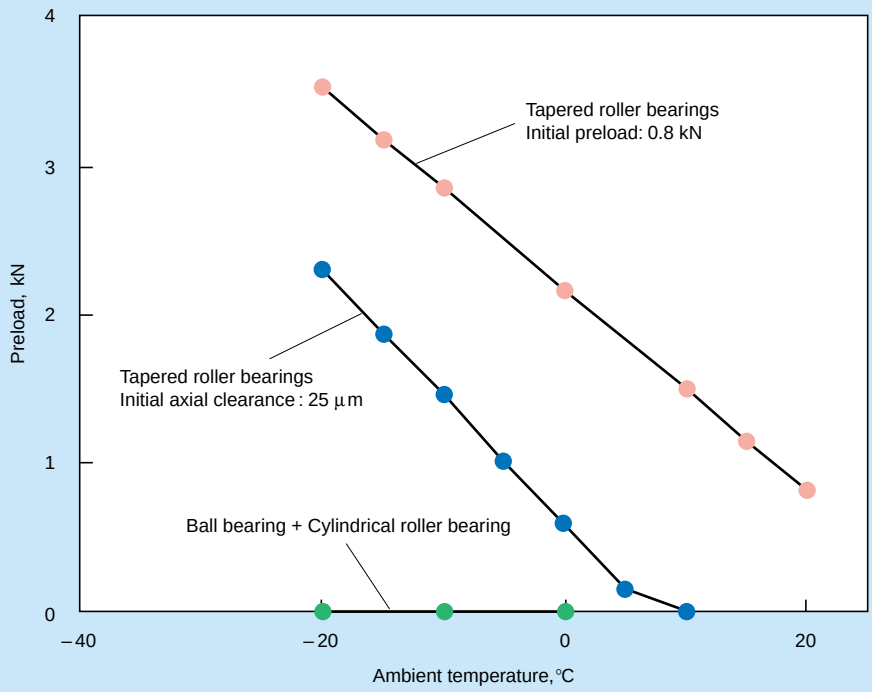

Fig. 11 Influence of ambient temperature on bearing preload

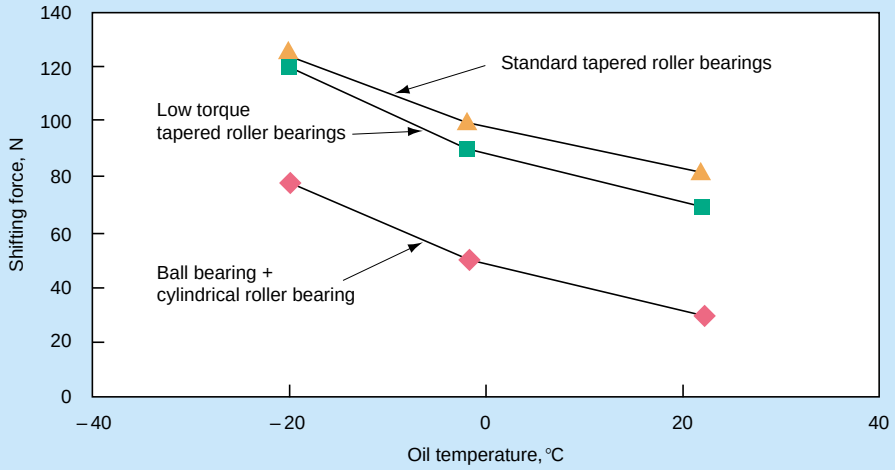

Fig. 12 Influence of oil temperature on shift-operating force

6. Shifting Operability of Manual Transmissions & Types of Bearings

Section 5 above, treated problems at high transmission temperatures when an aluminum transmission case was used. On the contrary, when the transmission temperature comes down, the transmission case may contract, and the preload of the tapered roller bearings in DF (face-to-face) arrangement may be increased, resulting in an increase in the rotating torque of the bearings and a subsequent increase in the gear shifting force at First gear from Neutral.

Figs 10 and 11 depict the measuring equipment and measurement results of bearing preload changes with temperatures of an actual full-size aluminum T/A case. Figure 12 shows the measurements of the gear shifting force that varied with temperature. When tapered roller bearings are used, preload increases and shifting force also increases as the temperature drops. By contrast, the combination of a ball bearing and a cylindrical roller bearing has the advantages of freedom from effects of T/A case contraction at low temperatures and small shifting force.

7. Conclusion

Ball bearings, cylindrical roller bearings, and tapered roller bearings are mainly used for automobile transmissions. These bearings have advantages and disadvantages for this particular application. On the part of the transmissions, they have their own aims and bearing usages depending on their designs. For future optimization of bearings to meet requirements of transmissions at higher levels, it is important to make greater approaches from the viewpoint of transmissions than ever before.

References

1) A. Tanaka, K. Furumura and T. Ohkuma, "Highly Extended Life of Transmission Bearings of 'Sealed-Clean' Concept," SAE Paper 830570 (1983).
T. Ohkuma, "Sealed Clean Ball Bearings for Transmissions," NSK Bearing Journal No. 641 (1981), 30-34*
2) T. Shiratani, Y. Murakami and K. Abe, "Fighting Debris: Increasing Life with HTF Bearings for Transmissions," SAE Paper 940728, (1994)
Y. Murakami, N. Mitamura and K. Furumura, "Super-TF, Hi-TF Bearings with Increased Life under Harsh Lubrication Environment," NSK Tech. J. No. 652 (1992), 9-16*
3) T. Momono and B. Noda, "Vibration and Noise of Rolling Bearings," NSK Tech. J. No. 661 (1996), 13-22*
4) "QAT Roller Bearing," NSK Tech. J. No. 657 (1994), 52-53*

*in Japanese

Takao Obara

Development of NSK S1 Series™ Ball Screws and Linear Guides

Hiroki Yamaguchi
Precision Machinery and Parts Division—Headquarters
Tsutomu Ohkubo
Corporate Research and Development Center

ABSTRACT

In recent years, along with achieving enhancement of machinery and equipment for manufacturing, users have expressed increasing concern about environmental issues. Ball screws and linear guides, which are the key components for the linear driving mechanisms of user's machinery and equipment, must offer smoother machine operation and less noise, reduce environmental impact in the manufacturing process, and ease working environments.To this end, we, at NSK Ltd., have developed and marketed "NSK S1 Series™" ball screws and linear guides that incorporate resin retaining pieces between the balls to avoid ball-to-ball contact.The new "NSK S1 Series™" has smoother operation and emits lower noise in a softer tone while maintaining compatibility with existing dimensions. In addition, reduction of load capacity and rigidity due to employment of the retaining piece are kept to a minimum, thereby retaining high durability.

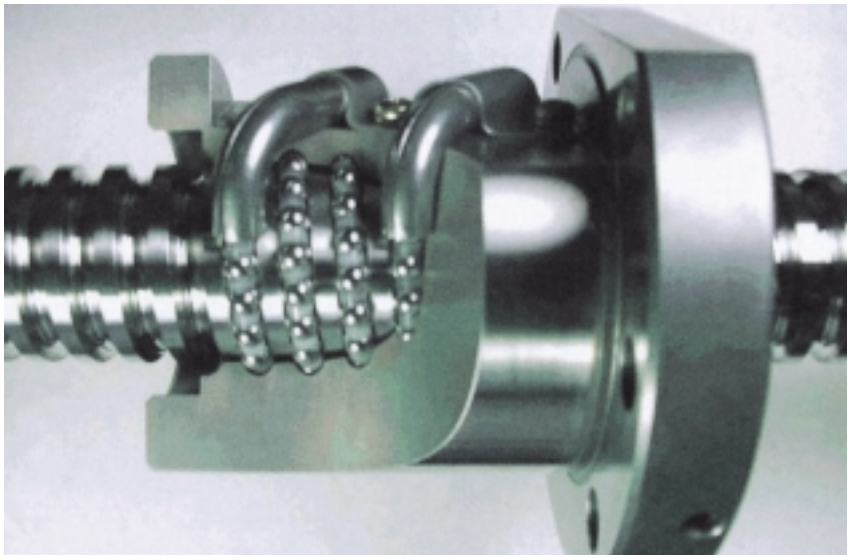

Photo 1 Construction of S1 Series ball screw

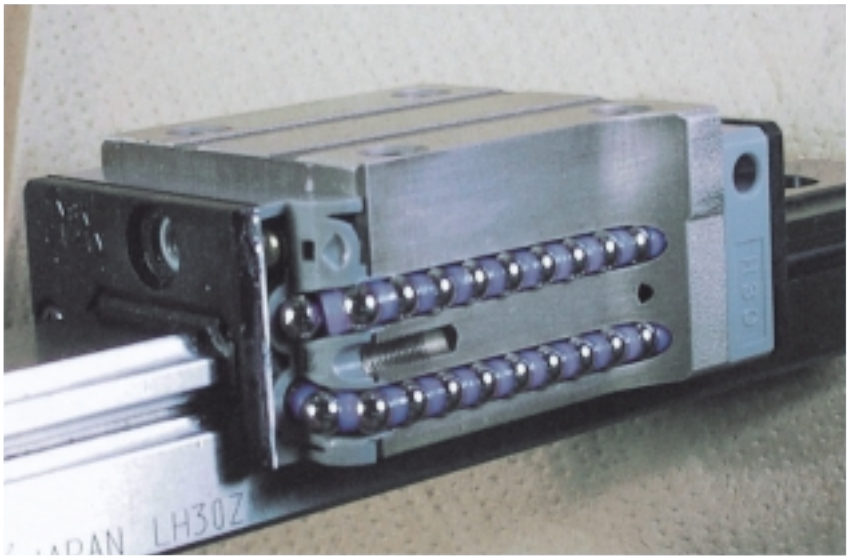

Photo 2 Construction of S1 Series linear guide

1. Introduction

In recent years, customers have expressed increasing concern regarding environmental issues, in addition to enhanced performance of various manufacturing systems. In line with this trend, ball screws and linear guides used in linear feed mechanisms must improve their operational characteristics with greater reductions of noise.

We at NSK have achieved smoother operability and greater noise reduction than conventional products by inserting a resin retaining piece between each steel ball that is in a ball screw and a linear guide, thus eliminating ball-to-ball contact. Our improved ball screws and linear guides are marketed under the brand name of NSK S1 Series™.

This paper describes the construction, development aim, and features of this series.

2. What is the NSK S1 Series™?

The ball screws and linear guides of the NSK S1 Series™ (hereafter abbreviated to S1 Series) have a resin retaining piece between each steel ball to prevent direct contact and skirmishes of balls in recirculation. This improves operational characteristics, reduces vibration and noise, and offers greater durability. Photos 1 and 2 provide cutaway models to look into the inside workings of the S1 Series ball screw and linear guide. In both photos, we can see the retaining pieces placed between each steel ball.

The S1 Series has several improvements that we will discuss later in greater detail. Although we have added retaining pieces, overall dimensions and shape remain the same as the previous series and conventional products. Therefore, the S1 Series is totally compatible with current equipment and can be used without making any changes.

The standard S1 Series includes a ball screw with return tubes for ball recirculation (return-tube type), a shaft diameter ranging from 16 to 50 mm, a lead of 5 to 32 mm, and a steel ball diameter of 3.175 mm to 6.35 mm.

Our linear guides, the conventional LH and LS Series, have offered high universality in the field of general industrial machinery. The original three numbers of the LH Series (LH20, 25, and 30), and the four numbers of the LS Series (LS15, 20, 25, and 30), have been renamed as the SH and SS Sub-Series of the S1 Series.

Other specifications and type numbers, which are still currently available and compatible, will be sequentially added to the standard S1 Series.

3. Aim of Development

The ball screws and linear guides consist of a mechanism in which steel balls are circulated infinitely to enable an infinite stroke theoretically. Accordingly, the route through which steel balls circulate consists of a load zone in which steel balls roll on the raceway groove under load, a no-load zone in which steel balls pass through, and a steel ball scoop section connecting these zones. Each zone has its own shape and curvature.

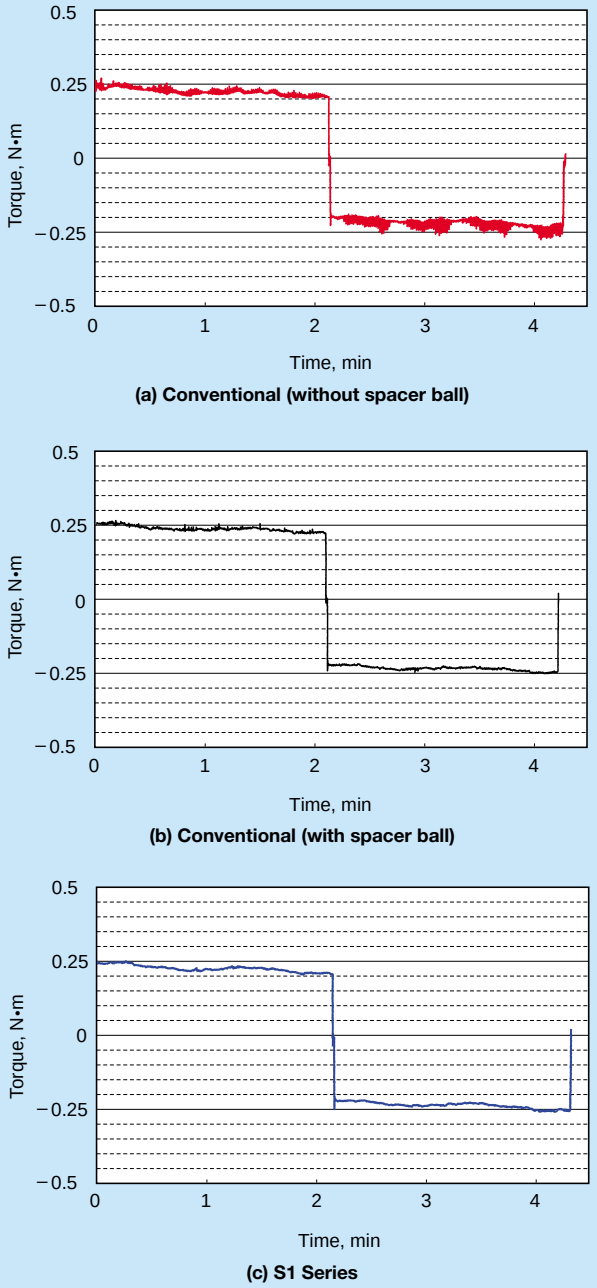

Fig. 1 Dynamic friction torque of ball screw under low speed

In a rolling bearing, which is similar to a ball screw and a linear guide as a rolling element, cages are generally used to avoid ball-to-ball contact. However, the complicated internal structures of a ball screw and a linear guide make insertion of a cage difficult. This may result in less-than-satisfactory effects on the operation, vibration, noise, and endurance characteristics of ball screws and linear guides.

To counteract such effects, a resin retaining piece has been inserted between each steel ball of the ball screws and linear guides (as opposed to a cage, as is the case for

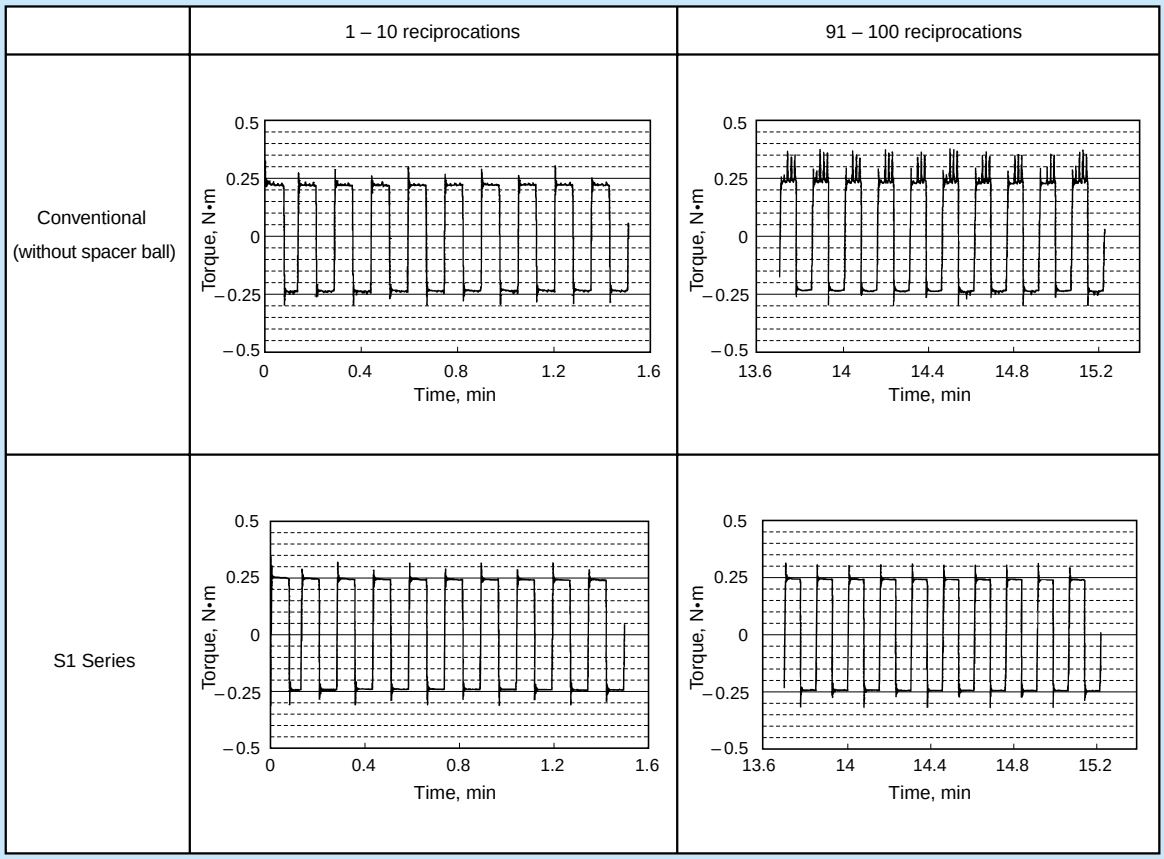

Fig. 2 Dynamic friction torque of ball screw in oscillation

rolling bearings), thus preventing direct contact of the steel balls. This is now a basic structure common to all of the S1 Series ball screws and linear guides.

The steel balls must circulate smoothly, together with the retaining pieces, along the entire route described above if the S1 Series are to demonstrate their features fully. Insertion of a retaining piece should never be the cause of deterioration in functions and durability. For this purpose, the retaining piece itself must also have sufficient durability. We decided, therefore, to employ specifications appropriate to each type of product and model number, concerning the material, dimensions and shape of the retaining pieces, design of the ball scoop zone, and clearance setting in the rolling direction of the steel ball in the route of the ball passage. We have evaluated and confirmed these functions and their durability.

The S1 Series incorporates these improvements while emphasizing the following points that have previously had a negative effect on the operation, vibration/noise qualities, and endurance of ball screws and linear guides:
(1) Prevention of direct contact and skirmishes of steel balls.
(2) Improvement of line-up straightness of steel balls in the passage hole (no load zone).
(3) Alleviation of interference and collision of steel balls with other parts in the ball scoop zone that connects the load and no-load zones.

As a result, the S1 Series have the superior features discussed in Section 4.

4. Features

As a result of making improvements as described above, the S1 Series are much smoother in operation, are quieter, and have better noise tone than conventional products even though outside dimensions remain unchanged. In spite of the insertion of retaining pieces, the decrease in load rating and stiffness has been kept to a small percentage, thus ensuring high endurance.

4.1 Operation characteristics

Adequate operability can be measured in the amount of friction fluctuation. There are two types of measured frictional forces in ball screws and linear guides, spike and jamming. Spike consists of short-cycle fluctuations of friction that occur during operation as shown in Fig. 1 (a) and Fig. 3 (a). Jamming consists of fluctuations of friction that increase in line with operation as shown in Fig. 3 (b).

These fluctuation components tend to appear under low-speed conditions or oscillation (reciprocal repetition with small strokes) and are undesirable because they may

adversely affect smooth operation of a table that is driven and guided by a ball screw and linear guides.

The S1 Series prevents skirmishes of steel balls, and thereby suppresses spike and jamming, and offers superior operability.

4.1.1 Ball screws

In comparison to ball bearings and linear guides, ball screws contain a larger number of steel balls within the recirculation circuit. Therefore, a higher risk of skirmishes among the steel balls exists. In addition, torque fluctuation due to spike and jamming may present substantial problems depending on the operating conditions. Conventionally, for fields requiring smooth operability, such as electric discharge machines, plotters, etc., spacer balls which were slightly smaller in diameter than the steel balls exposed to load, were inserted among the load carrying steel balls to alleviate the friction fluctuation. However, this method results in a decrease of the load rating and stiffness due to the decrease in the number of steel balls that can carry the load.

Fig. 1 shows measurements of friction torque for a ball screw with a shaft diameter of 25 mm and lead of 5 mm, was preloaded with oversized balls, and was operated under low speed (10 rpm) under oil lubricated conditions. In this figure, results are compared between the conventional ball screw (with and without spacer balls), and the S1 Series. The data shown is for one cycle of motion. The conventional ball screw with no spacer balls shows spike from the begining to the end while the S1 product shows improved operability to a level that exceeds or is equal to the case with spacer balls.

Fig. 2, as the result of a ball screw that has the same specifications as those of Fig. 1, shows a comparison of the dynamic torque characteristics during oscillation between a conventional ball screw (without spacer balls) and the S1 Series. The friction torque was measured after oscillation for 100 reciprocations under conditions of low speed (10 rpm), small strokes (3.75 mm), and oil lubrication. The figure shows data during one to ten reciprocations and 91 to 100 reciprocations. The conventional ball screw developed spike while repeating oscillations, but the S1 Series product maintained satisfactory operability till the end of 100 reciprocations.

4.1.2 Linear guides

One structural feature of the linear guide is that the number of steel balls in the no-load zone (passage holes) is larger than in the load zone that bears the load. It is, therefore, essential for smooth operability to ensure smooth circulation of steel balls while paying attention to steel ball line-up both inside and at the inlet of the passage holes.

The S1 Series incorporates design-related improvements from the above viewpoint in addition to insertion of the retaining piece.

Figures 3 (a) to (c) show comparisons of measured

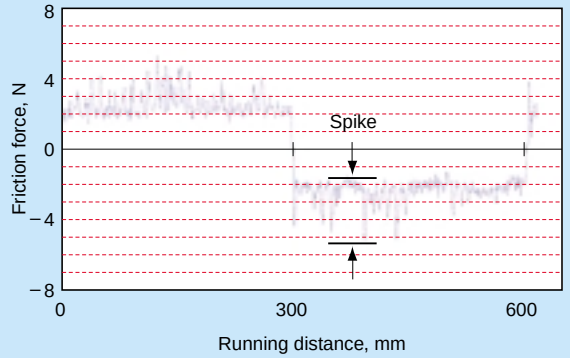

(a) Conventional (1)

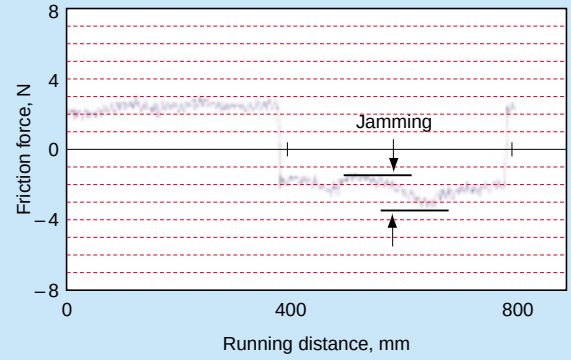

(a) Conventional (2)

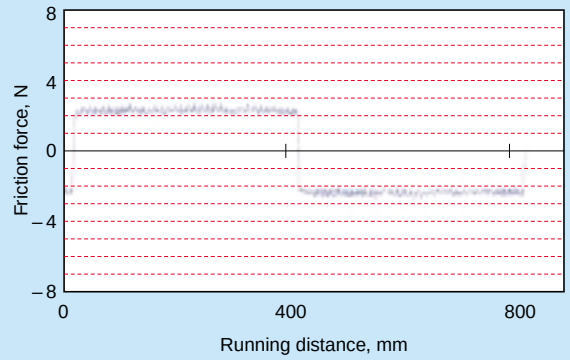

(c) S1 Series

Fig. 3 Dynamic friction force of linear guide

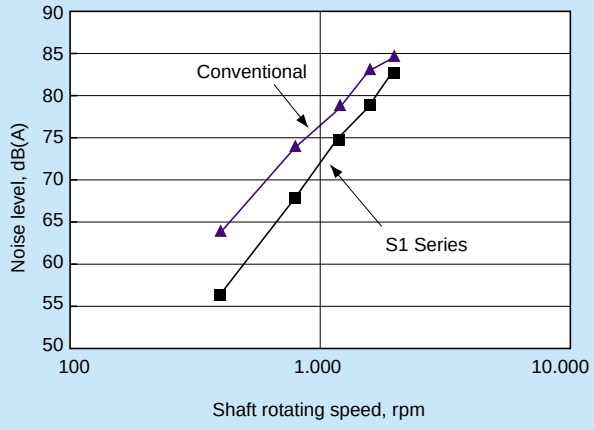

Fig. 4 Comparison of noise level of ball screw

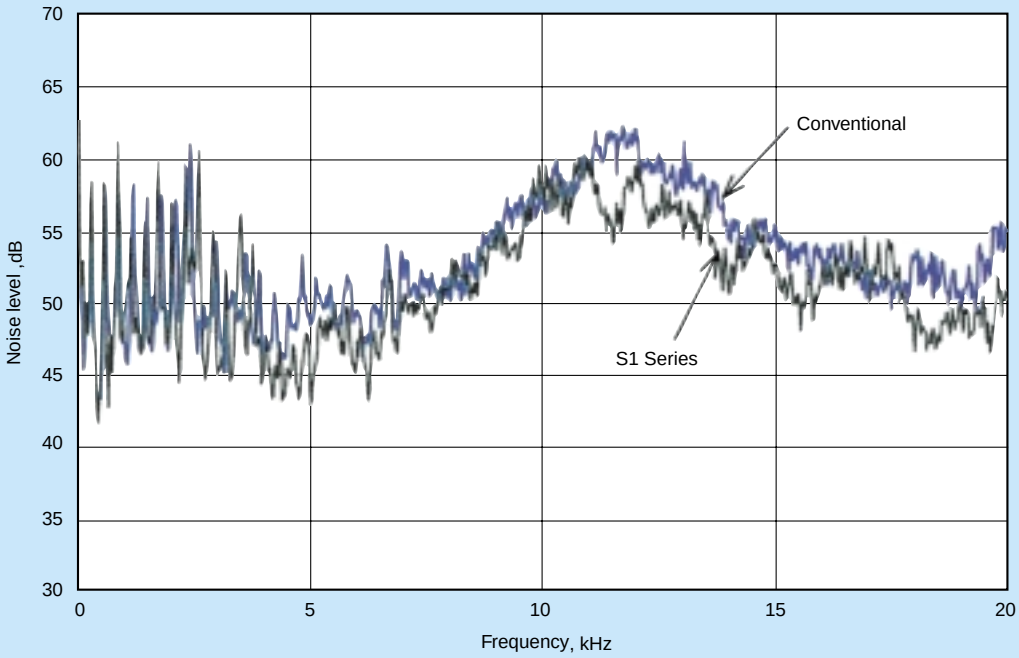

Fig. 5 Frequency analysis of noise of ball screw

dynamic friction force between the conventional NSK linear guide (LH30) and the S1 Series (SH30). For comparison, data was obtained for one cycle of motion under a "slight" preload (Z1), a feed rate of 1 m/min, and grease lubrication conditions.

Fig. 3 (a) shows noticeable excessive spike occurring in the conventional linear guide. (b) shows a case in which jamming occurs and spike is relatively small. However, (c) shows that the S1 Series have a smoother and more stable operability than that of conventional products.

4.2 Vibration and noise characteristics

With the increase in speed, vibration and noise from ball screws and linear guides also increase. There are two adverse effects, vibration itself and noise caused by vibration. Specifically, noise problems refer to noise levels and harsh tones.

Vibration and noise are caused by: metal-to-metal contact between the steel balls, rolling of steel balls in the raceway groove, and steel ball contact with the recirculation components or raceway groove in the scoop zone.

The S1 Series incorporates a retaining piece between each steel ball to ensure lower noise and better tone than that of conventional products. The retaining pieces help prevent, or alleviate in some cases, any metal-to-metal contact between the steel balls, and the collision of balls in the scoop zone.

4.2.1 Ball screws

Fig. 4 compares a conventional product and the S1 Series for measured noise levels of a ball screw with a shaft diameter of 40 mm, a lead of 10 mm, and preload with oversized balls. To measure the noise of a ball screw, a microphone was set 400 mm away from the shaft center. Figure 4 shows that the S1 Series has less noise especially in the low-speed range. The tone of a conventional product shows a rather harsh noise in the low-speed range, which is caused by direct contact of steel balls. As for the S1 Series, such noise is not heard since the retaining pieces do not allow steel balls to collide with each other.

Fig. 5 shows the results of frequency analysis for noise generated when a ball screw with a shaft diameter of 40 mm and a lead of 20 mm, was preloaded with oversized balls and driven at 2 000 rpm. The frequencies up to 20 kHz (limit of audible sound for humans) serve as the abscissa for comparison between the conventional product and the S1 Series.

Based on the results, we can see that there is little difference in the low-frequency range. This is due to the rolling of steel balls on the raceway groove, which is the predominate noise in the low-frequency range. In the high-frequency range, however, the S1 Series enjoy a lower noise level. The conventional product experiences direct contact between the steel balls, in addition to striking against the recirculation components and the raceway groove in the scoop zone. These account for most of the high-frequency noise components. The S1 Series have achieved reduction of noise levels and improvement of noise tone by suppressing these high-frequency noise components.

Vibration was measured by an acceleration pick-up (accelerometer) installed onto the outside diameter of the ball nut and subjected to frequency analysis, whose results also indicated the same trend.

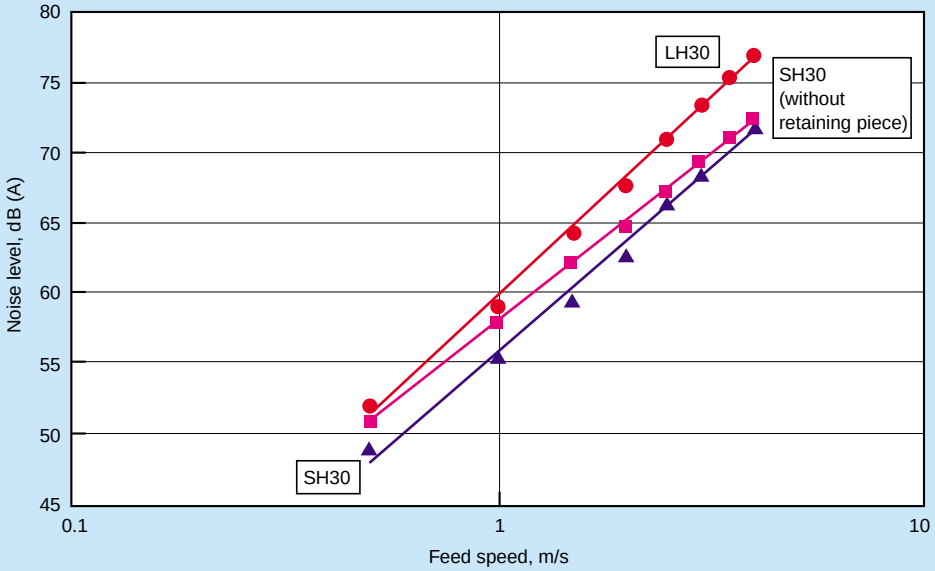

Fig. 6 Comparison of noise level (Model: LH30, SH30)

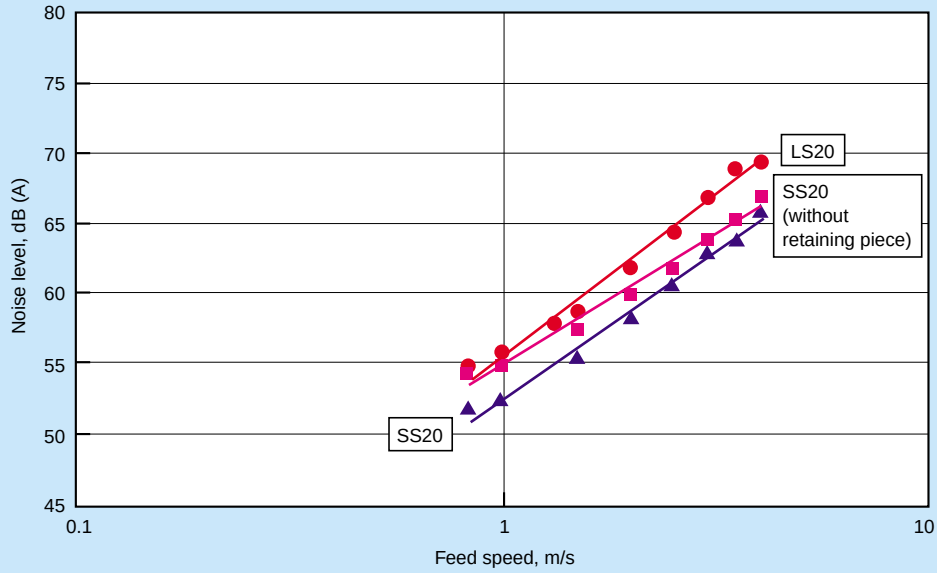

Fig. 7 Comparison of noise level (Model: LS20, SS20)

4.2.2 Linear guides

Fig. 6 shows the comparison results of noise levels between two linear guides of the same size: a conventional LH30 and an S1 Series SH30. Fig. 7 provides the same results for a conventional LS20 and an S1 Series SS20, which are also of the same size. For the linear guides, a microphone was positioned 500 mm above the rail. Figures 6 and 7 reflect the observations taken for the different types of linear guides and steel ball diameters. Furthermore, the S1 Series reveals lower noise levels at about 5 dB (A).

In both figures, a measurement for an S1 Series with no retaining pieces and with additional steel balls to fill empty space, which was made by taking out the retaining pieces, was also included in the sampling. This measurement was made in order to conduct separate evaluations of the effects that were obtained from inserting the retaining pieces and from the improvements that were made on the recirculation components to reduce collision between steel balls and the recirculation components or raceway groove in the scoop zone. Figures 6 and 7 reveal that the insertion of the retaining pieces is effective in relatively lower speeds, while the improvements on the recirculation components are rather effective as speed increases.

Judging from the sound frequency analysis of these linear guides, the S1 Series shows noticeable improvements, particularly in the high-frequency range,

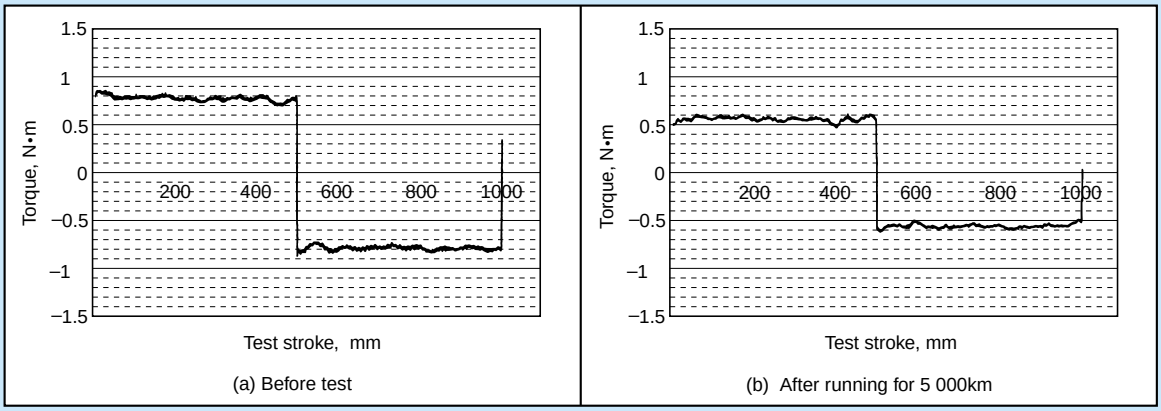

Fig. 8 Dynamic friction torque of ball screw before and after endurance test

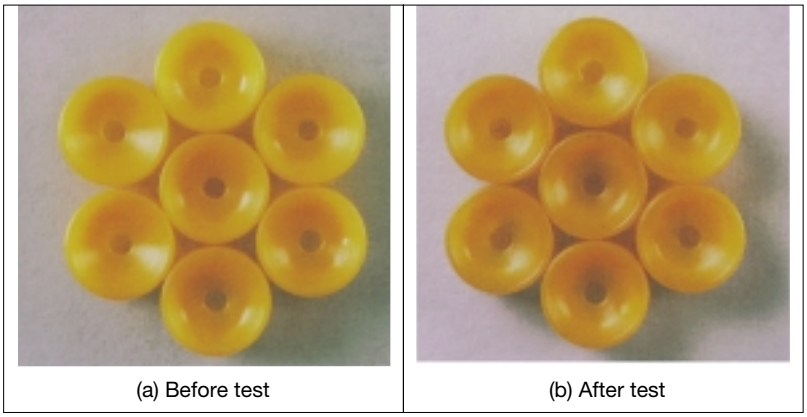

Photo 3 Retaining piece of linear guide

which leads to improvement in noise tone, as is also the case for ball screws.

4.3 Load rating and durability

Even though the S1 Series has a reduced number of steel balls that are exposed to load due to the insertion of retaining pieces, the reduction in the number of steel balls and the decrease in load rating and stiffness are kept to a bare minimum (a very small percentage) compared to that of conventional products. In addition, with the elimination of adverse effects caused by the skirmishes of steel balls, durability is enhanced and exceeds that of conventional products.

However, retaining pieces must not cause deterioration of durability of the ball screws and linear guides, including durability of the retaining piece itself. At NSK, we have conducted endurance tests under various operating conditions. This section discusses the representatives of variety of tests that we have conducted with the focus on the durability of the retaining piece and its effect on the durability of the products.

Table 1 Comparison of load rating and stiffness of ball screw

	Dynamic load rating (ratio) N	Static load rating (ratio) N	Stiffness (ratio) N/μm
S1 Series	13 400 (0.93)	28 900 (0.90)	395 (0.91)
Conventional (without spacer ball)	14 400 (1)	32 100 (1)	435 (1)
Conventional (with spacer ball)	9 070 (0.63)	16 100 (0.50)	235 (0.54)

Notes: Specifications: Shaft diameter 25 mm, lead 6 mm, 1.5 turns × 2 circuits
Stiffness indicates the value when preload is 5% of the dynamic load rating.

4.3.1 Ball screws

Test conditions consisted of an S1 Series ball screw with a shaft diameter of 40 mm and a lead of 10 mm, which was preloaded with oversized balls and operated continuously at 2 000 rpm for a distance of 5 000 km under grease lubrication. Fig. 8 shows the friction torque measurements that were taken before and after testing. Both measurements were taken at 10 rpm under grease lubrication. After running for 5 000 km, there was a slight drop in torque due to running-in of the raceway groove surface and grease. Even under low-speed conditions, satisfactory operability was maintained. No other particular abnormalities were observed. The check results

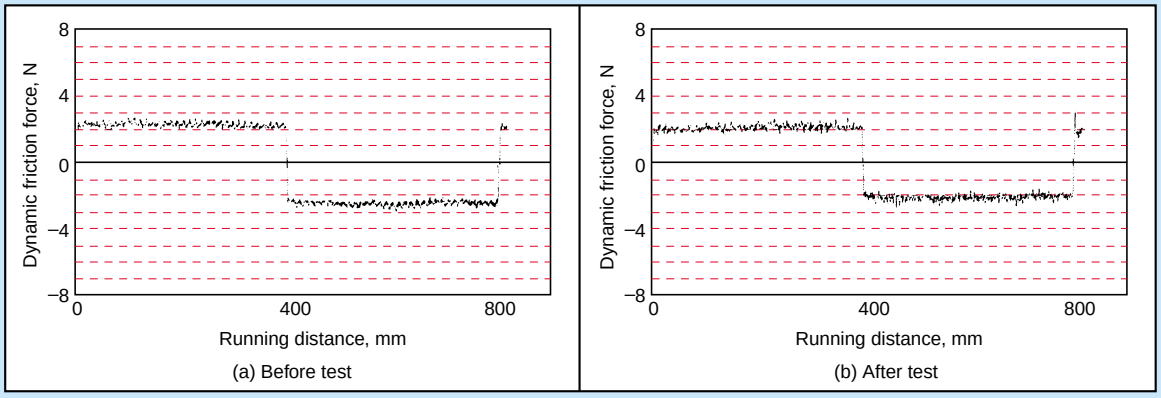

Fig. 9 Dynamic friction force of linear guide before and after endurance test

of retaining pieces were also the same as with the case in Photo 3, without any particular damage or deterioration. Even after the above investigation, operation was resumed and continued in excess of 9 000 km without any problems.

As previously described, ball screws with spacer balls for suppressing skirmishes of steel balls were used widely in fields where such operability was important. The use of spacer balls, however, causes a substantial reduction in the number of steel balls that are exposed to load, thus resulting in a decrease in load rating and stiffness. Table 1 shows the calculation and a comparison of the load rating and stiffness between conventional ball screws (with and without spacer balls) and the S1 Series with the same specifications. When compared with conventional products (no spacer ball), the dynamic load rating of the S1 Series decreases by about 7%, which is still a substantial increase when compared to cases with spacer balls. The S1 Series achieves greater operability and longer life through securing the load rating. In other words, the S1 Series is able to provide compact ball screws that have the same load rating as that of conventional products that use spacer balls.

4.3.2 Linear guides

Here we will discuss the test results of an S1 Series linear guide, the SH30. This linear guide was operated continuously at high speed (120 m/min) for 20 000 km. The ball slides were packed with grease and no additional greasing was applied during operation. A light load was added externally in addition to a “slight” preload (Z1). Fig. 9 shows the comparison of dynamic friction force measured under a feed speed of 1 m/min and oil-lubricated conditions for two cases; one prior to testing, and the other after running for 20 000 km. As we can see in the figure, the decrease in dynamic friction force after testing, compared to that from before testing, is small (10%), which indicates that satisfactory operability is maintained even after running for 20 000 km. In the raceway groove, no wear, except for initial running-in is observed, with sufficient stiffness maintained. We are sure that this linear guide could have been operated even more without problems.

Photo 3 shows the appearance of retaining pieces before and after testing. The photo shows no particular change due to continuous running. Furthermore, investigation results after testing show no particular deterioration, such as damage or wear.

5. Conclusions

In this paper, we have described the construction and features of the NSK S1 Series™ ball screws and linear guides. To cope with the increasing demand for advanced functions and diversifications of these products, NSK will continue to make efforts to achieve an ever-superior product, including a stronger commitment to the development and functional improvement of priority products, including the S1 Series™ products. We look forward to future reports of further achievements.

Hiroki Yamaguchi

Tsutomu Ohkubo

Bearings for Clean Environments

Bearings for clean environments, such as for semiconductor manufacturing systems, liquid crystal display (LCD) manufacturing systems, clean rooms, and hard disk drives (HDD) require lubricants with minimal splashing (out-particles) and gas discharge. As a result, bearings can continue to operate under an increased severity of high temperatures and high vacuum conditions. This is due to increased integration of devices, larger LCDs, and greater requirements for the efficient use of materials. At the same time, bearings must meet more stringent requirements for reduced out-particles and gas discharge.

One example comes from the semiconductor industry. The pattern width on a wafer is becoming thinner—0.35 μm (64 MB) to 0.25 μm (256 MB). Problems arise when extremely fine particles that are the size of 1/10 or less of wire width (0.025 μm in the case of 256 MB) and gases are absorbed onto the wafer.

NSK, using new technologies, has developed various bearings to respond to the stringent requirements of these clean environments (Photo 1).

1. Composition

Bearings for clean environments include bearings packed with clean grease and bearings coated with low out-particle special fluororesin (LDF).

The scope of application of these bearings is shown in Fig. 1.

Clean greases include LG2 (Li soap) and LGU (urea) for atmospheric use and LGA (fluorine) grease for vacuum use.

The LDF coated bearing is used where vacuum applications and high temperatures prohibit the use of grease.

Photo 1 Bearings for clean environments

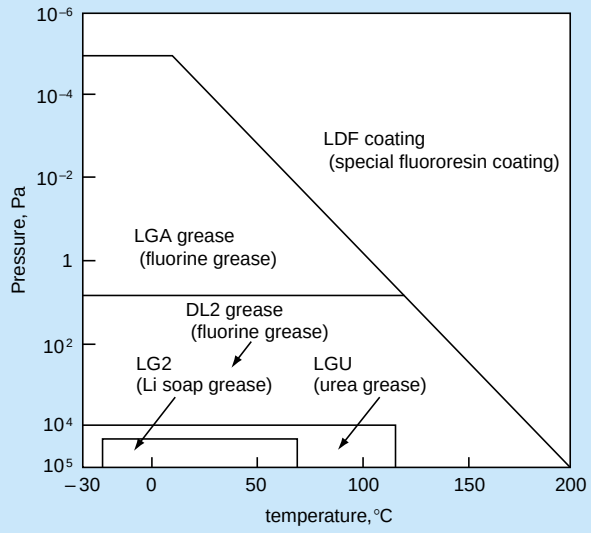

Fig. 1 Applicable environments for clean bearings

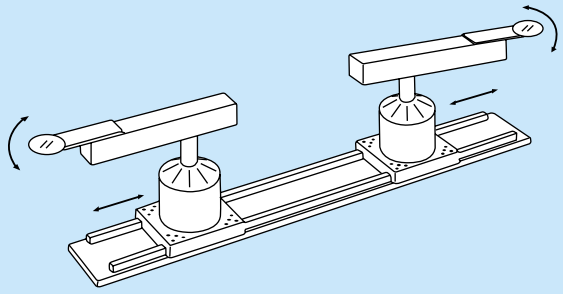

Fig. 2 Example of applications in clean environments (wafer handling robot)

Table 1 Characteristics of LG2 and LGU greases

Name	Thickener	Base oil	Kinematic viscosity of base oil mm²/s (40°C)	Consistency NLGI No.
LG2	Li soap	Synthetic hydrocarbon oil + mineral oil	30	3
LGU	Urea	Synthetic hydrocarbon oil	98	3

2. Features

2.1 Bearings packed with clean grease

Bearings packed with clean grease for atmospheric use (LG2 and LGU) are used in clean room drives, wafer handling robots (Fig. 2), and steppers. Additionally, bearings packed with clean grease (LGA) for vacuum use are incorporated into material handling robots, oxidation vapor deposition furnaces, and vacuum pumps.

Typical characteristics of LG2 and LGU greases are shown in Table 1. Features of LG2 and LGU greases are described below.

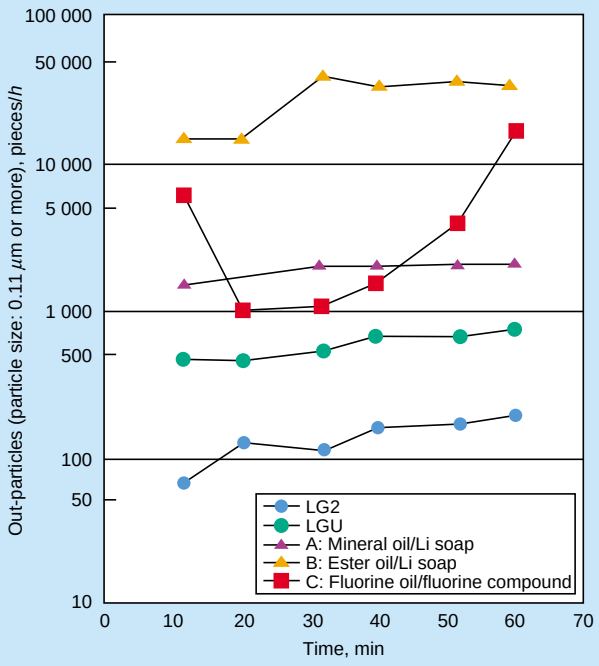

Fig. 3 Number of out-particles by bearings packed with clean grease

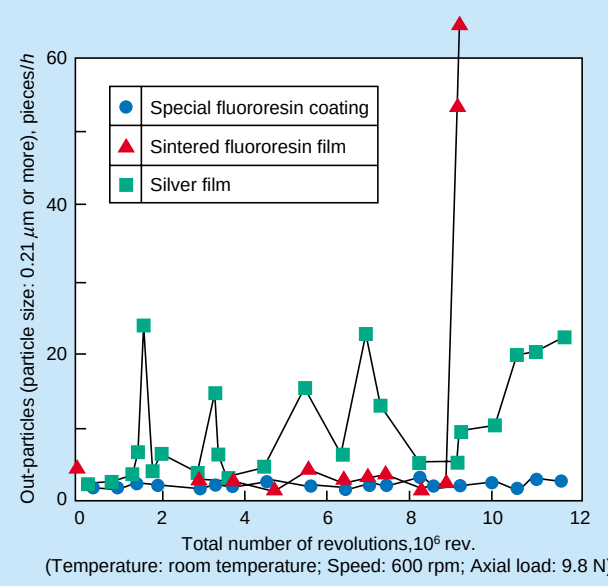

Fig. 4 Number of out-particles by LDF coated bearings (in vacuum)

(1) Extremely smaller out-particles compared to other greases available on the market (Fig. 3).
(2) Lower and more stable torque than that of fluorine grease for preventing out-particles.
(3) Sufficient durability.
(4) Superior corrosion preventive characteristics.
(5) LG2 grease can be used at a temperature not exceeding 70°C under normal conditions, while LGU grease is applicable to a higher temperature of 120°C.
(6) LGU grease contains no metals (Li, Na, Mg, etc.), sulfur, or chlorine.

LGA grease comprising wear-resistant additives, which is most suitable for fluorine grease, guarantees life to about five to ten times longer than fluorine greases available on the market for vacuum and atmospheric conditions. Out-particles are nearly equivalent to that of fluorine greases available on the market.

2.2 Bearings coated with low out-particle coating

Bearings used in CVD and sputtering systems operate under an increased severity of high temperatures and vacuum environments, where even fluorine grease that is highly resistant to evaporation presents a problem. In such fields, bearings coated with low out-particle special fluororesin (LDF) may be used. This type of bearing has a fluororesin film formed over bearing element surfaces using a special coating method free of any binder.

Features of LDF coated bearings are as follows:

(1) Extremely small out-particles and long life under atmospheric and vacuum environments (Fig. 4).
(2) Superior heat resistance with extremely small out-particles up to 200°C, even under high vacuum conditions.

LDF coated bearings are used in various CVD units, sputtering systems, and vacuum motors.

3. Summary

Our product line-up includes ball screws and linear guides for clean environments in addition to bearings, which will prove to be great contributions to various fields requiring clean environments. We will continue to further develop new products to meet increasingly sophisticated market needs.

CT Scan Bearings

Recent developments in medical technology have lead to more compact and affordable computed tomography (CT) scanners. Consequently, CT scanners are ever more present not only in large hospitals, but also in medium and small sized hospitals.

A CT scanner consists of an X-ray tube that rotates while the CT table, or examination table, moves at a given rate in the direction of the rotating axis. A bank of detectors opposite the X-ray tube takes the X-rays that pass through the patient's body and converts them into digital signals. Once the computer processes the data, an image of any selected area of the body can be obtained.

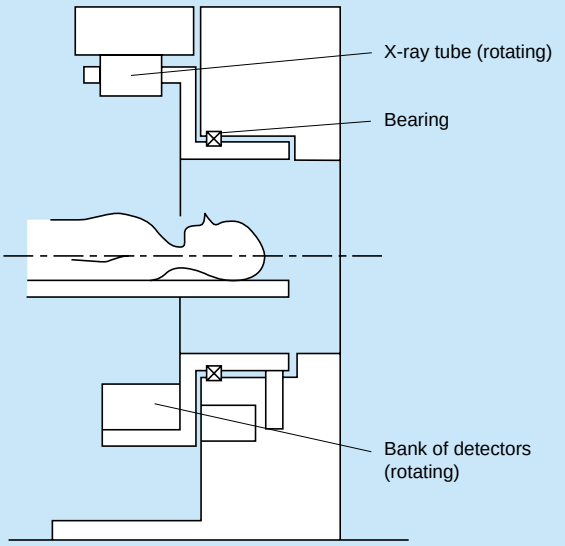

Fig. 1 Sectional view of a CT scanner

An extra-large, thin-wall bearing, with a bore diameter exceeding ϕ700 mm (Fig. 1), is used for the rotation support structure to which the X-ray tube and detectors are installed.

Since the bearing is used in close proximity to the patient's head, bearing noise has to be minimal. To alleviate the burden on the patient, the time required for rotating the X-ray tube around the patient's body should be decreased. At the same time, an accurate image must still be obtained.

NSK has developed a CT scanner bearing that meets requirements for quieter operation and higher speed. Major features of our newly developed bearing are introduced below.

1. Bearing Specifications

Four-point contact ball bearings and combined angular contact ball bearings are most commonly used for CT scanners. This is due to radial, axial, and moment loads, in addition to market demands for compactness and affordability. In response, we have developed high-speed, low noise bearings for both types of ball bearings (Fig. 2).

Major specifications of the newly developed bearings are described below.

(1) Optimum design of bearing internal specifications

Bearing specifications have been optimized in consideration of clearance, ball movement, and heat generation.

(2) Optimum design of cage

The cage is made from resin to reduce noise. In addition, cages are arranged along the circumference and connected to minimize noise generated from their mutual collision.

		Four-point contact ball bearing	Combined angular contact ball bearing
Sectional view of bearing		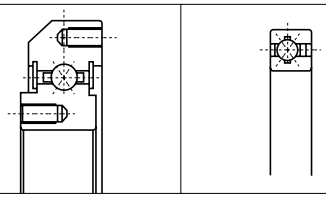	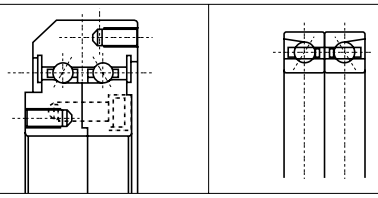
Bearing internal specification		Optimal bearing specifications taking clearance, ball movement, and heat generation into account	
Cage	Material	Nylon 66 (resin for noise reduction)	
	Shape	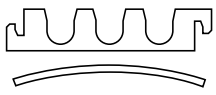	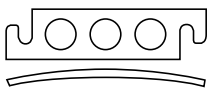
	Type	Separator connection type (separators arranged on the circumference)	

Fig. 2 Bearing specification

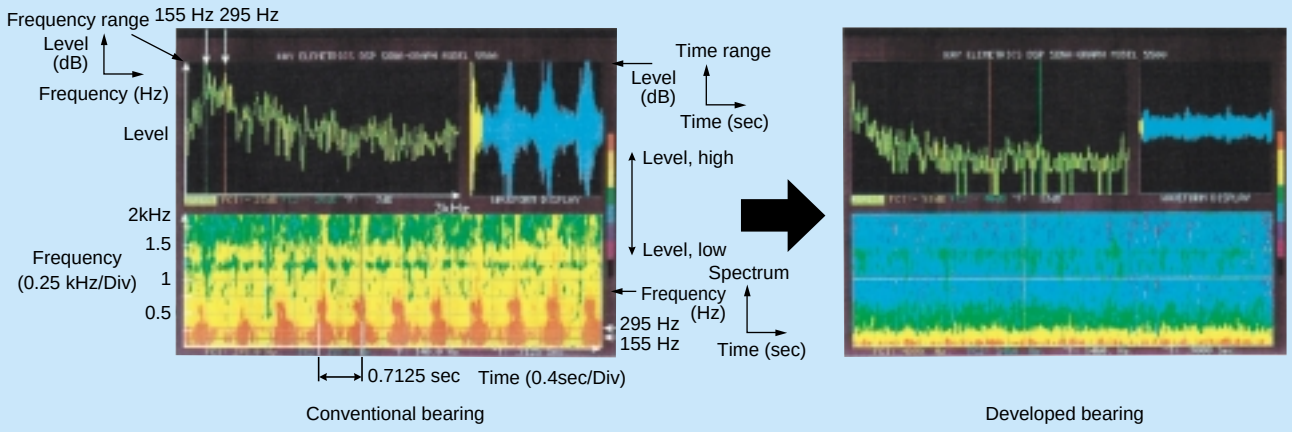

Fig. 3 Results of noise level analysis by real-time sound spectrum analyzing instrument

(3) Improvement of the heat treatment method

The heat treatment method has been improved to achieve even heat-treatment qualities.

2. Features

(1) Quieter operation

Fig. 3 shows the results of acoustic analysis of a four-point contact ball bearing using a real-time, audio spectrum analyzing instrument for both conventional and newly developed bearings. Our analysis shows that the newly developed bearing is much quieter than conventional bearings.

(2) Faster operation

Increasing the speed of four-point contact ball bearings is difficult due to heat that generates easily from spin slide and unstable behavior of the balls. Our new specification, however, shows a 30% increase in speed over conventional bearings.

3. Strengthened Quality Assurance

NSK has developed and introduced a dedicated bearing-sound inspection system (Photo 1), which further advances our quality assurance.

4. Conclusion

The NSK CT scanner bearing with reduced noise in the high-speed range achieves the goal of shortening scanning time as well as providing compactness. Furthermore, the thinner and larger diameter design of the bearing allows for a larger gantry.

NSK will continue to develop new products by fully exploiting our design, manufacturing, and quality assurance technologies.

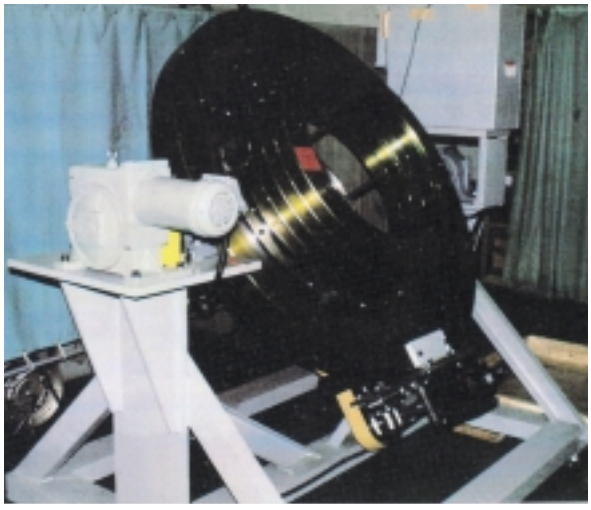

Photo 1 Noise tester

Column-Type Electric Power Steering with Tilt Mechanism

1. Introduction

The number of fuel-efficient cars, including compact and subcompact cars, is increasing in the face of global environmental problems. Manufacturers of compact vehicles throughout the world have become aware of the efficiency of Electric Power Steering (EPS) systems for their cars, which are more efficient than conventional hydraulic power steering systems. This article introduces NSK's development and full-scale production of a column-type EPS for compact cars (Photo 1).

The column-type EPS is currently installed on 1.0 to 1.4 L cars. Vehicles to be provided with this type of EPS include 1.7 L diesel vehicles. As a result, the motor rated current of 60 A (maximum) is achieved with an increase in assisted torque.

2. System Outline

Fig. 1 shows the system construction of a column-type EPS with tilt mechanism. The EPS system consists of a torque sensor that detects the steering operating force applied, an electronic control unit (ECU) that processes voltage signals, a motor that generates torque according to output from the ECU, and a reducer for reducing motor torque.

A tilt mechanism is also provided in consideration of marketability and to enable easy entry into and exit from.

3. Features

(1) Energy absorption mechanism

The column is mounted at an angle of 32 deg., separation load from the vehicle bracket is suppressed, and the bumper tube-type EA member is used. A shaft support bush is adopted to provide resistance to stick slip condition during shaft collapse.

(2) Tilt mechanism

This mechanism consists of a mid-tilt structure, in which the tilt pivot is positioned between the torque sensor and the steering wheel. Instead of a universal joint, the pivot uses a bell joint to increase the energy absorption capabilities. Tilt level clamping consists of a side clamp, which is similar to clamps used in the OPEL Astra and VW Polo.

(3) Noise reduction

Higher-class vehicles have harder suspension and chassis systems that are more rigid compared to compacts and subcompacts. Therefore, a larger kick-back torque is fed back to the steering column. In consideration of excess noise caused by driving surfaces, improvements have been made to damper materials and increased volume on the worm shaft.

(4) Motor

Torque of 43 N·m has been achieved through the use of a high-torque, high-speed motors with a maximum current of 60A.

(5) ECU

A twin-circuit base construction and other layout

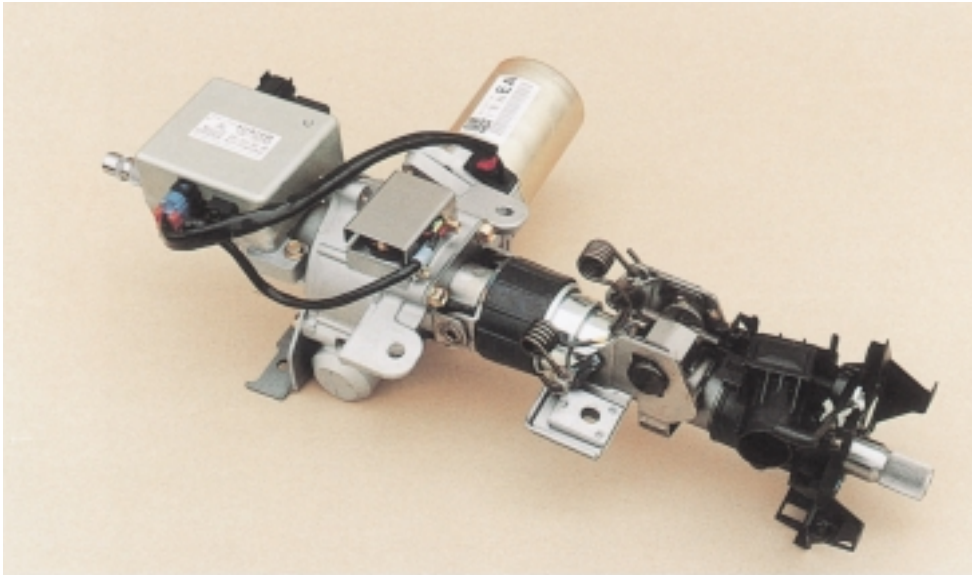

Photo 1 Column-type Electric Power Steering with tilt mechanism

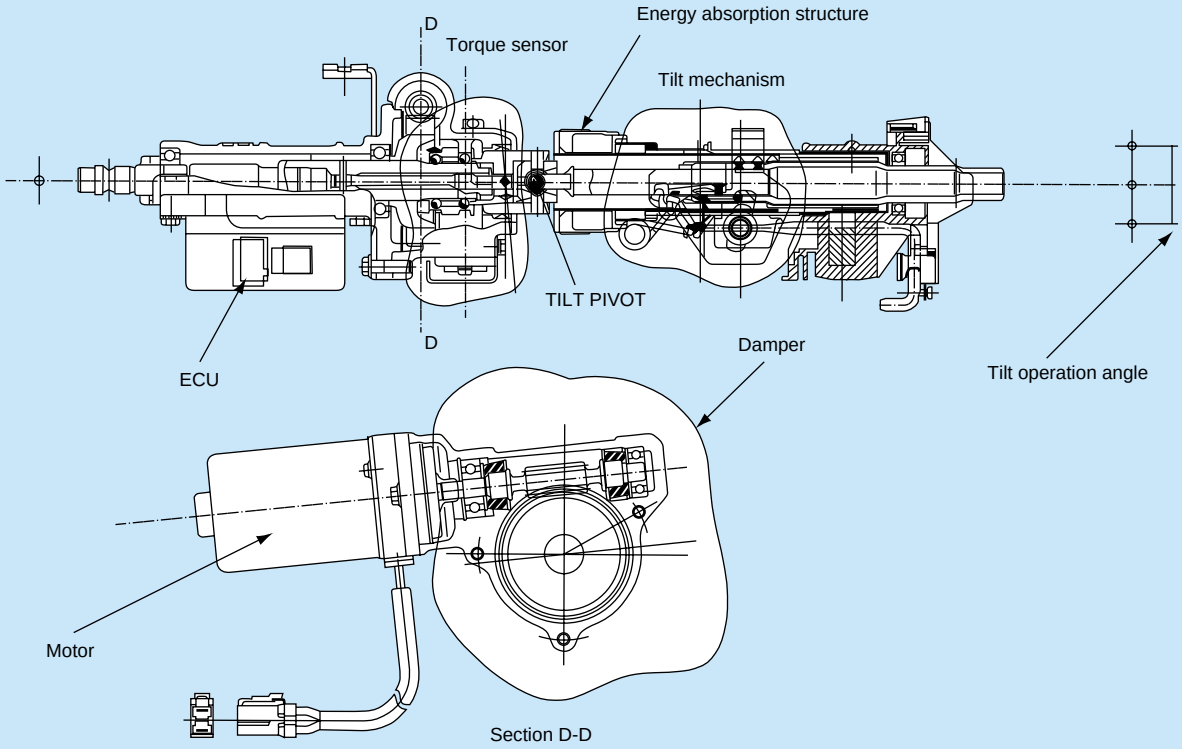

Fig. 1 Construction of a column-type EPS

considerations contribute to the achievement of a compact construction, enabling integration with the column structure. An improved AD converter helps achieve smoother handling.

4. EPS Specifications

	Newly developed product
1) Assembly	
a) Torque assist	43 N•m
b) Control range	Over the entire range
c) Tilt range	+/– 25 mm
2) Torque sensor	
Type	Potentiometer
Rated voltage	DC5V
3) Reduction gears	
Gears	Worm gear
Worm screw	Two threads
Gear ratio	15:1
4) Motor	
Type	DC brush motor
Voltage supply	12V
Maximum current	60 A
Rated torque	3.19 N•m
Rated speed	1 150 rpm

5. Conclusion

With proper development and marketing, the 60A EPS system shows great potential for 1.6 L compact cars. The mid-tilt structure ensures a superior layout, such as an increase in the energy absorbing collapse stroke that has been an issue to be solved with the column-type EPS.

Low Inertia Series of Nut Rotatable Ball Screws

In 1992, NSK developed ball screws with rotatable nuts for practical use in the field. These products continue to enjoy a favorable reputation throughout various industries. Recently, users from industries that include electronic parts mounting machines, punching presses, laser machines, woodworking machines, robots, and transport systems, have demanded increased feeding speed and longer stroke. To meet the needs of the market, NSK has developed a new series of ball screws that ensure increased feeding speed through reduction of inertia. Photo 1 shows the new ball screws with low inertia rotatable nuts.

1. Construction

A nut rotatable ball screw is a ball screw unit comprised of an integrated ball nut with a support bearing whose inner raceways are directly formed on the periphery of the ball nut. An example of mounting and the internal structure is shown in Fig. 1.

2. Features

(1) The ball recirculation method has been changed from an internal design (end cap), as is found with conventional products, to an external recirculation design (return tube). Furthermore, ball nut thickness has been reduced. Therefore, the inertia of a rotating section has been reduced by 21% compared to conventional products. Table 1 shows the inertia comparison.

(2) A conventional molded end cap design involves many difficulties beyond the standard design due to a substantial cost increase. Our new series uses a return tube design, which helps increase the number of designs available and makes it much easier to offer compatible combinations with special shaft diameters and leads.

(3) The optional vibration damper enables use of the product in a range exceeding critical speed limits that may pose a problem during increased feeding speed with a long stroke. There are no changes in the overall dimensions of the ball screw if the vibration damper is used.

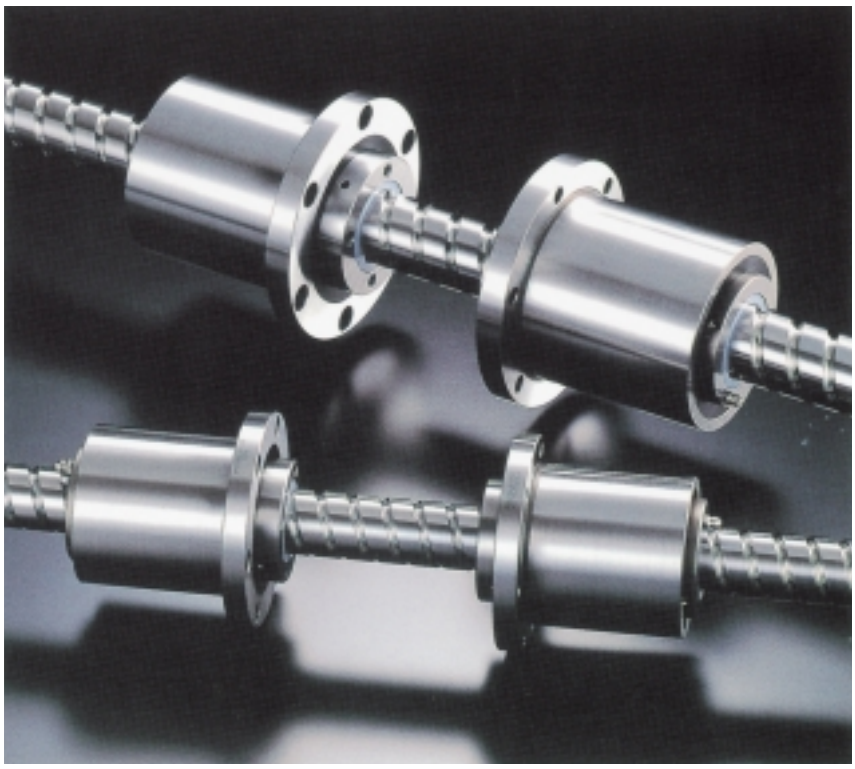

Photo 1 Nut rotatable ball screws; Low inertia series

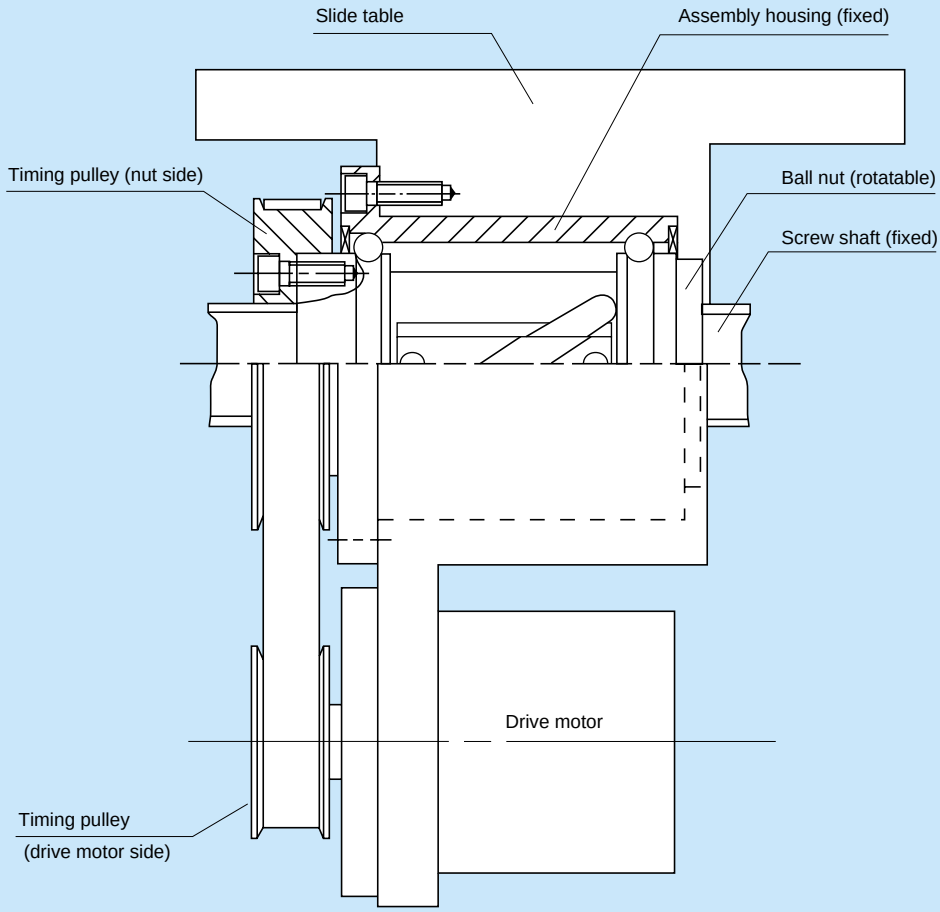

Fig. 1 Internal construction and assembly

Table 1 Comparison of nut inertia

Shaft dia. × lead (mm)	Conventional series* (kg · cm²)	Low inertia series (kg · cm²)	Reduction ratio
$\phi 32 \times 32$	7.6	6.2	18% decrease
$\phi 40 \times 40$	24.2	19.2	21% decrease
$\phi 50 \times 50$	55.2	48.7	12% decrease

* Values for conventional series include the mounting collar.

(4) The support bearing has an outer ring that is comprised of double-row preloaded angular contact ball bearings. Preload is maintained constantly for high axial and moment stiffness.
(5) Apart from above, there are conventional advantages. For example, multiple nuts can be driven on one axis respectively. The user does not have to make any design or assembly adjustments to the support bearing.

3. Permissible Rotational Speed

Rotational speed restrictions are based on the $d_m n$ value in addition to critical speed limits.

(1) Rotational speed restriction based on the $d_m n$ value
Standard specification: $d_m n \leqq 70\,000$
Enhanced specifications for higher speed: $d_m n \leqq 100\,000$
Where,
d_m: ball pitch circle diameter (mm)
n: Rotational speed (min^{-1})

(2) Critical speed limitations with vibration damper
Increased feeding speed with a long stroke may often not be possible because of critical speed limitations due to resonance of the screw shaft. However, by using the optional vibration damper, you can safely exceed critical speed limitations.
For further details, see Motion and Control (NSK Technical Journal) No.8.

4. Types

This series consists of ten types with different combinations of shaft diameters (32 mm, 40 mm, and 50 mm) and leads (20 mm to 50 mm). Table 2 gives the boundary dimensions of this series.

Table 2 Dimensions

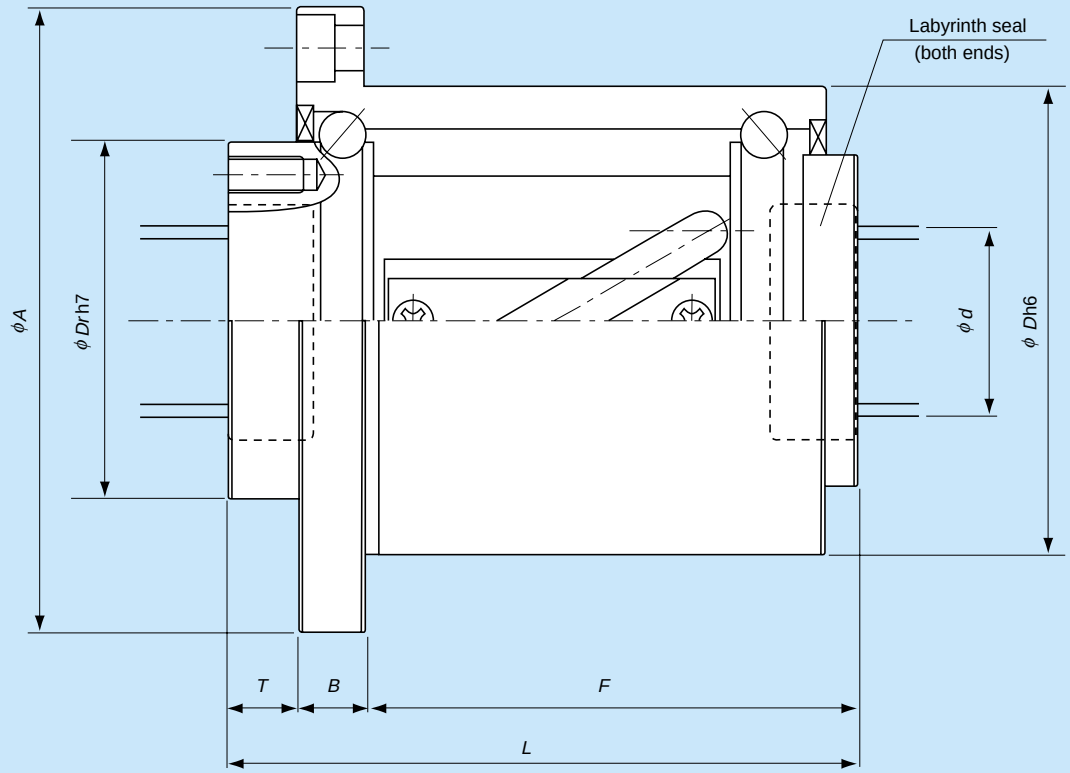

Model No.	Shaft dia. *d*	Lead	Ball pitch circle dia. d_m	Effective turns of balls × Circuits	Basic load rating Dynamic *Ca* (N)	Basic load rating Static C_0a (N)	Moment of inertia *J* (kg·cm²)	Ball nut mass *W* (kg)	Ball nut dimensions *D*	*A*	*Dr*	*T*	*B*	*F*	*L*
NDT 3220-2.5	32	20	33.25	2.5 × 1	17 900	41 800	6.2	2.9	78	105	60	12	12	83	107
NDT 3225-2.5		25	33.25	2.5 × 1	17 900	41 800	6.7	3.2	78	105	60	12	12	96	120
NDT 3232-1.5		32	33.25	1.5 × 1	11 500	24 800	6.2	2.9	78	105	60	12	12	83	107
NDT 3232-3				1.5 × 2	18 900	44 600									
NDT 4025-2.5	40	25	41.75	2.5 × 1	28 500	70 000	19.3	6.0	100	133	76	15	15	106	136
NDT 4032-1.5		32	41.75	1.5 × 1	18 400	41 200	18.0	5.5	100	133	76	15	15	92	122
NDT 4032-3				1.5 × 2	30 100	74 100									
NDT 4040-1.5		40	41.75	1.5 × 1	18 400	41 200	19.2	6.0	100	133	76	15	15	106	136
NDT 4040-3				1.5 × 2	30 100	74 100									
NDT 5025-2.5	50	25	52.25	2.5 × 1	42 700	109 000	45.7	8.5	120	156	96	15	18	107	140
NDT 5032-2.5		32	52.25	2.5 × 1	42 700	109 000	48.9	9.4	120	156	96	15	18	125	158
NDT 5040-1.5		40	52.25	1.5 × 1	27 500	66 500	45.5	8.5	120	156	96	15	18	107	140
NDT 5040-3				1.5 × 2	44 900	120 000									
NDT 5050-1.5		50	52.25	1.5 × 1	27 500	66 500	48.7	9.4	120	156	96	15	18	125	158
NDT 5050-3				1.5 × 2	44 900	120 000									

Note: For detailed shapes and dimensions, refer to NSK Catalog No. E3155.

5. Conclusion

NSK has made this series available for practical use in the field as a long-stroke ball screw with increased feeding speed. We will continue our development of products to meet market needs.

High Load Capacity Mini LH Series of NSK Linear Guides

The LH Series of NSK linear guides, designed to provide high load capacity and self-aligning capability, are a practical and popular choice for manufacturers of various robots, transport systems, and semiconductor manufacturing systems.

The current trend of downscaling in the semiconductor and liquid crystal display (LCD) manufacturing equipment has resulted in a growing demand for smaller linear guides.

NSK's miniature LH Series of high load capacity linear guides (Photo 1) has been developed to satisfy such a demand.

In this article we describe some of the features of this series.

1. Features

(1) High load capacity and rigidity in the vertical direction.
(2) High impact load resistance.
(3) High self-aligning performance (rolling direction) ensures a high capacity to absorb mounting error.
(4) Easy to handle.
LH15, 12, and 10 are easier to handle since a retainer is used to keep the balls from falling out when the ball slide is removed from the rail.
(5) The NSK K1™ lubrication unit can be mounted to provide effective lubrication and to ensure long-term maintenance-free performance.
(6) Stainless steel is used to ensure high corrosion-resistance. Fluoride low-temperature chrome plating is available for even greater corrosion protection.
(7) Interchangeable series are available.
The rails and ball slides of model number LH15 are produced and stored separately, and then matched at random as needed. Maintaining a standard stock of rails and ball slides reduces delivery time.

2. Specifications

Table 1 shows accuracy grade and specification standards. Table 2 shows the classification of preload.

Standard dimensions for each type are shown in Tables 3 and 4.

3. Applications

Applications include semiconductor manufacturing systems, LCD manufacturing systems, medical equipment, optical stages, microscope X-Y stages, optical fiber transport systems, small robots, computer peripheral equipment, pneumatic equipment, measuring instruments, and inspection systems.

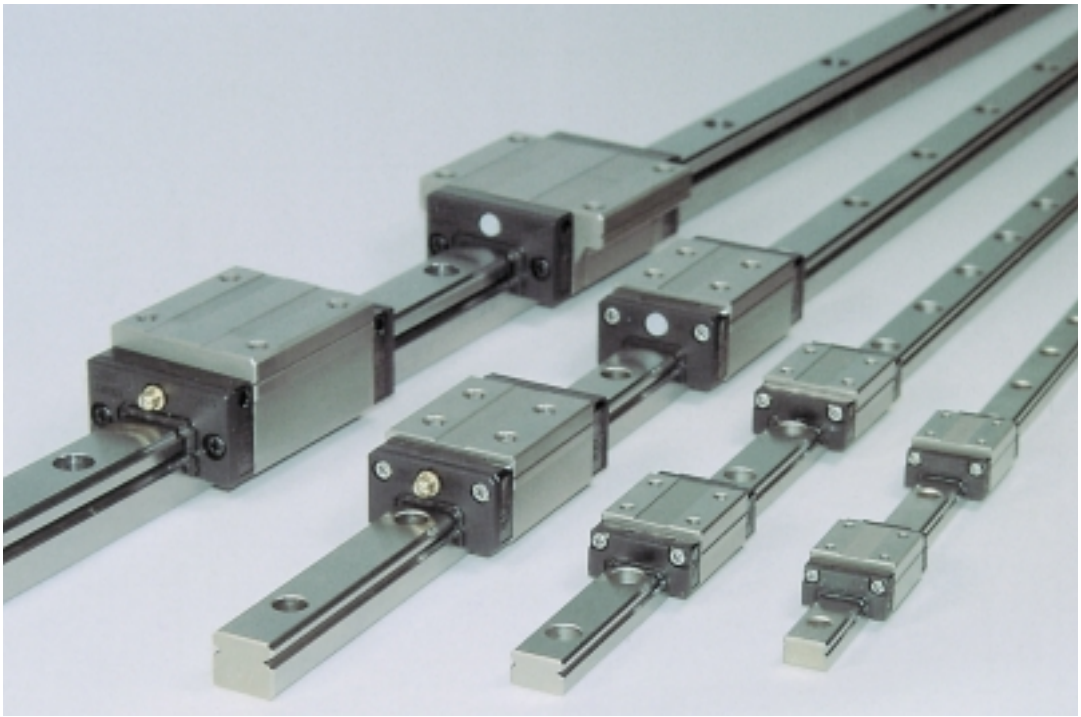

Photo 1 High load capacity miniature LH Series of NSK linear guides

Table 1 Classification of accuracy grades

Model No.	Preloaded assembly (non-interchangeable)					Interchangeable assembly
	Ultra-precision P3	Super precision P4	High precision P5	Precision P6	Normal grade PN	Normal grade PC
LH 08,10,12		○	○	○	○	
LH 15	○	○	○	○	○	○

Table 2 Classification of preload

Model No.	Preloaded assembly (non-interchangeable)			Interchangeable assembly	
	Medium preload Z3	Slight preload Z1	Fine clearance Z0	Slight preload ZZ	Fine clearance ZT
LH 08,10,12		○	○		
LH 15	○	○	○	○	○

Table 3 Standard dimensions (LH08, 10, 12, 15AN, 15BN)

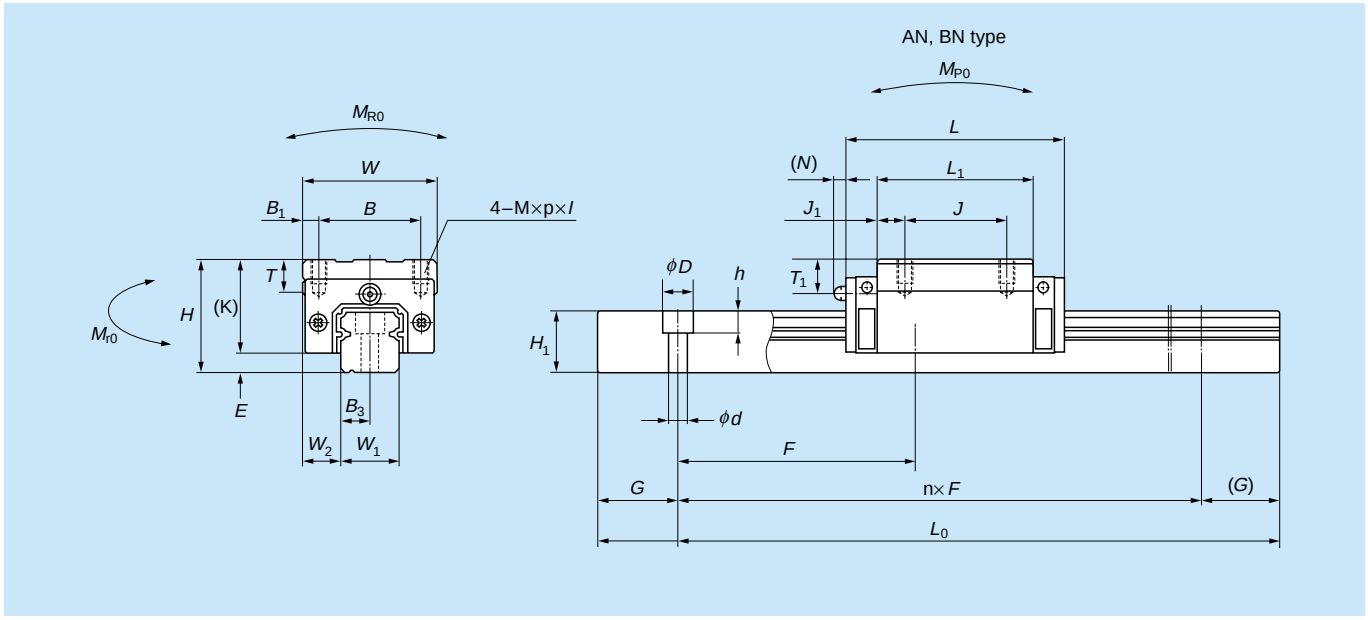

Unit: mm

Model No.	Assembly			Ball slide												
	Height			Width	Length	Mounting tap hole								Grease fitting		
	H	E	W_2	W	L	B	J	M × Pitch × l	B_1	L_1	J_1	K	T	Mounting hole	T_1	N
LH08AN	11	2.1	4	16	24	10	10	M2 × 0. 4 × 2.5	3	15	2.5	8.9	—	—	—	—
LH10AN	13	2.4	5	20	31	13	12	M2.6 × 0.45 × 3	3.5	20.2	4.1	10.6	6	—	—	—
LH12AN	20	3.2	7.5	27	45	15	15	M4 × 0.7 × 5	6	31	8	16.8	6	ϕ3	5	4
LH15AN	28	4.6	9.5	34	55	26	26	M4 × 0.7 × 6	4	39	6.5	23.4	8	ϕ3	8.5	3.3
LH15BN					74					58	16					

Model No.	Rail							Basic load rating					Ball dia.
	Width	Height	Pitch	Mounting bolt hole		G	Max length $L_{0\,max}$	Dynamic	Static	Static moment (N·m)			
	W_1	H_1	F	d × D × h	B_3	(recommended)	( ) is SUS	C (N)	C_0 (N)	M_{RO}	M_{PO}	M_{YO}	Dw
LH08AN	8	5.5	20	2.4 × 4.2 × 2.3	4	7.5	(375)	980	2 260	7	4	4	1.2
LH10AN	10	6.5	25	3.5 × 6 × 3.5	5	10	(600)	1 860	3 920	16	10	10	1.5875
LH12AN	12	10.5	40	3.5 × 6 × 4.5	6	15	(800)	4 310	9 020	42	34	32	2.3812
LH15AN	15	15	60	4.5 × 7.5 × 5.3	7.5	20	2 000	8 300	16 200	98	78	78	3.175
LH15BN							(1 800)	11 200	25 000	147	177	177	

Table 4 Standard dimensions (LH15EL, GL, FL, HL)

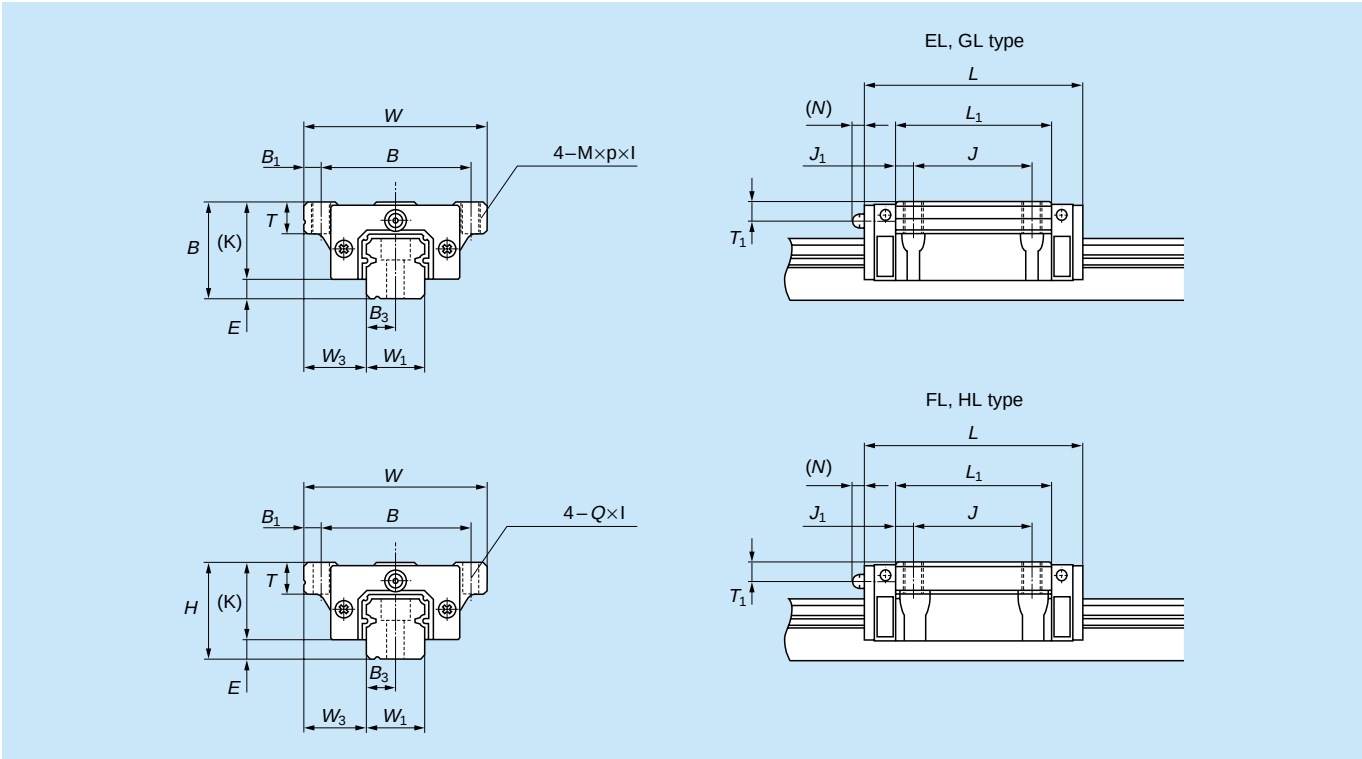

Unit: mm

Model No.	Assembly			Ball slide												
	Height			Width	Length	Mounting tap hole								Grease fitting		
	H	*E*	W_2	*W*	*L*	*B*	*J*	M × Pitch × *l* *Q* × *i*	B_1	L_1	J_1	*K*	*T*	Mounting hole	T_1	*N*
LH15EL	24	4.6	16	47	55	38	30	M5 × 0. 8 × 8	4.5	39	4.5	19.4	8	ϕ3	4.5	3.3
LH15GL					74					58	14					
LH15FL	24	4.6	16	47	55	38	30	4.5 × 7	4.5	39	4.5	19.4	8	ϕ3	4.5	3.3
LH15HL					74					58	14					

Model No.	Rail							Basic load rating					Ball dia.
	Width	Height	Pitch	Mounting bolt hole		*G*	Max length $L_{0\,max}$ ( ) is SUS	Dynamic	Static	Static moment (N•m)			
	W_1	H_1	*F*	*d* × *D* × *h*	B_3	(recommended)		*C* (N)	C_0 (N)	M_{RO}	M_{PO}	M_{YO}	*Dw*
LH15EL	15	15	60	4.5 × 7.5 × 5.3	7.5	20	2 000	8 300	16 200	98	78	78	3.175
LH15GL							(1 800)	11 200	25 000	147	177	177	
LH15FL	15	15	60	4.5 × 7.5 × 5.3	7.5	20	2 000	8 300	16 200	98	78	78	3.175
LH15HL							(1 800)	11 200	25 000	147	177	177	

Worldwide Sales Offices and Manufacturing Plants

NSK LTD.–HEADQUARTERS, TOKYO, JAPAN www.nsk.com
AMERICAS & EUROPE DEPARTMENT: Nissei Bldg., 6-3, Ohsaki 1-chome, Shinagawa-ku, Tokyo 141-8560, Japan
P: 03-3779-7120 F: 03-3779-7433 T: 2224280 NSK BRG J C: 81
ASIA MARKETING & SALES DEPARTMENT: Nissei Bldg., 6-3, Ohsaki 1-chome, Shinagawa-ku, Tokyo 141-8560, Japan
P: 03-3779-7121 F: 03-3779-7433 T: 2224280 NSK BRG J C: 81

Africa

South Africa:

NSK SOUTH AFRICA (PTY) LTD.
JOHANNESBURG 25 Galaxy Avenue, Linbro Business Park, Sandton, 2146, Gauteng, South Africa
P: (011) 458 3600 F: (011) 458 3608 C: 27

Asia and Oceania

Australia:

NSK AUSTRALIA PTY. LTD. www.nskaustralia.com.au
MELBOURNE 11 Dalmore Drive, Scoresby, Victoria 3179, Australia
P: (03) 9764-8302 F: (03) 9764-8304 C: 61
SYDNEY Unit 1, Riverside Centre, 24-28 River Road West, Parramatta, N.S.W. 2150, Australia
P: 02-9893-8322 F: 02-9893-8406 C: 61
BRISBANE 91 Wellington Road, East Brisbane, Queensland 4169, Australia
P: 07-3393-1388 F: 07-3393-1236 C: 61
ADELAIDE 64 Greenhill Road, Wayville, South Australia 5034, Australia
P: 08-8373-4811 F: 08-8373-1053 C: 61
PERTH Unit 4, 36 Port Kembla Drive, Bibra Lake, Western Australia 6163, Australia
P: 089-434-1311 F: 089-434-1318 C: 61

China:

NSK HONG KONG LTD.
HONG KONG Room 512, Wing On Plaza, Tsim Sha Tsui East, Kowloon, Hong Kong
P: 2739-9933 F: 2739-9323 C: 852

KUNSHAN NSK CO., LTD.
KUNSHAN 258 South Huang Pu Jiang Rd Kunshan E&T Development Zone Jiang Su 215335, China
P: 0520-7305654 F: 0520-7305689 C: 86

GUIZHOU HS NSK BEARINGS CO., LTD.
ANSHUN Dongjiao, Anshun, Guizhou, 561000, China
P: 0853-3521505 F: 0853-3522722 C: 86

NSK (SHANGHAI) TRADING CO., LTD.
SHANGHAI Room 826, No. 1Ji Long Road, Wai Gao Qiao Free Trade Zone, Shanghai, China
P: 021-62099051 F: 021-62099053 C: 86

NSK REPRESENTATIVE OFFICES
BEIJING Room 515, Beijing Fortune Bldg., 5 Dong san Huan Bei Lu, Chao Yang District, Beijing, 100004, China
P: 010-6590-8161 F: 010-6590-8166 C: 86
SHANGHAI Room 1005, Shanghai International Trade Center 2200 Yan An Road (w.), Shanghai, 200336, China
P: 21-6209-9051 F: 21-6209-9053 C: 86
GUANGZHOU Room 2701-02, Guangzhou International Electronics Tower 403, Huan Shi Rd East, Guangzhou, 510095, China
P: 020-8732-0583 F: 020-8732-0574 C: 86
ANSHUN Dongjiao, Anshun, Guizhou, 561000, China
P: 0853-3522522 F: 0853-3522552 C: 86

India:

RANE NASTECH LTD.
CHENNAI 14, Rajagopalan Salai, Vallancherry Guduvancherry, Pin-603 202, India
P: 04114-65313, 65314, 65365, 66002 F: 04114-66001 C: 91

NSK REPRESENTATIVE OFFICE
CHENNAI 2A, First Street, Cenotaph Road, Chennai, 600 018, India
P: 044-4334732 F: 044-4334733 C: 91

Indonesia:

P.T. NSK BEARINGS MANUFACTURING INDONESIA
JAKARTA PLANT Blok M-4, Kawasan Berikat, MM2100 Industrial Town Cibitung, Bekasi 17520, Jawa Barat, Indonesia
P: 021-898-0155 F: 021-898-0156, 021-898-0183 C: 62

Korea:

NSK KOREA CO., LTD.
SEOUL 9F (West Wing) Posco Center 892, Deachi 4 Dong Kangnam-Ku, Seoul, Korea
P: 02-3287-0300 F: 02-3287-0345, 0445 C: 82
CHANGWON 60, Songsan-Dong, Changwon, Kyungsangnam-Do, Korea
PLANT P: 0551-287-6001 F: 0551-285-9982 C: 82

Malaysia:

NSK BEARINGS (MALAYSIA) SDN. BHD.
KUALA LUMPUR 1st Floor, Kompleks Kemajuan, No.2, Jalan 19/1B, 46300 Petaling Jaya, Selangor Darul Ehsan, Malaysia
P: 03-7958-4396 F: 03-7958-4412 C: 60
PRAI 10, Lengkok Kikik 1, Taman Inderawasih, 13600 Prai, Penang, Malaysia
P: 04-399-1763 F: 04-399-1830 C: 60
JOHOR BAHRU Ground Floor, No. 27, Jalan Bakawali 50, Taman Johor Jaya, 81100 Johor Bahru, Johor, Malaysia
P: 07-354-6290 F: 07-354-6291 C: 60
KOTA KINABALU Lot 10, Lrg. Kurma 4, Likas Ind. Centre, 5 ½Miles, Jalan Tuaran, 88450 Inanam Sabah, Malaysia
P: 088-421-260 F: 088-421-261 C: 60

NSK MICRO PRECISION (M) SDN. BHD.
MALAYSIA PLANT No.43 Jalan Taming Dua,Taman Taming Jaya, 43300 Balakong, Selangor Darul Ehsan, Malaysia
P: 03-961-6288 F: 03-961-6488 C: 60

New Zealand:

NSK NEW ZEALAND LTD. www.nsk-rhp.co.nz
AUCKLAND 3 Te Apunga Place Mt. Wellington, Auckland, New Zealand
P: (09) 276-4992 F: (09) 276-4082 C: 64

Philippines:

NSK REPRESENTATIVE OFFICE
MANILA Unit 910 PS Bank Tower Sen. Gil Puyat Avenue Corner Tindalo Street, Makati City 1200, Metro Manila, Philippines
P: 02-759-6246 F: 02-759-6249 C: 63

Singapore:

NSK INTERNATIONAL (SINGAPORE) PTE LTD.
SINGAPORE 48 Toh Guan Road #04-02 Singapore 608837
P: (65) 273 0357 F: (65) 275 8937 C: 65

NSK SINGAPORE (PTE) LTD.
SINGAPORE 48 Toh Guan Road #02-03 Singapore 608837
P: (65) 278 1711 F: (65) 273 0253 T: RS24058 C: 65

Taiwan:

TAIWAN NSK PRECISION CO., LTD.
TAIPEI 9th Fl., 34, Chung Shan N. Rd., Sec. 3, Taipei, Taiwan R.O.C.
P: 02-2591-0656 F: 02-2597-3101 C: 886
TAICHUNG 107-6, SEC, 3, Wenxin Rd., Taichung, Taiwan R.O.C.
P: 04-2311-7978 F: 04-2311-2627 C: 886

Thailand:

NSK BEARINGS (THAILAND) CO., LTD.
BANGKOK 25th Floor RS Tower, 121/76-77 Rachadaphisek Road, Dindaeng, Bangkok 10320, Thailand
P: 02-6412150~58 F: 02-6412161 C: 66

NSK SAFETY TECHNOLOGY (THAILAND) CO., LTD.
CHONBURI 700/415 Moo 7 Amata Nakorn Industrial Estate T. Don-Hua-Roh A. Muang, Chonburi 20000, Thailand
P: (038) 214-317-8 F: (038) 214-316 C: 66

SIAM NASTECH CO., LTD.
CHACHOENGSAO 90 Moo 9, Wellgrow Industrial Estate, Km. 36 Bangna-Trad Road, Bangwao, Bangpakong, Chachoengsao 24180, Thailand
P: (038) 522-343~350 F: 038-522-351 C: 66

Europe

NSK EUROPE LTD. (EUROPEAN HEADQUARTERS) www.nsk-rhp.co.uk
MAIDENHEAD, UK Belmont Place, Belmont Road, Maidenhead, Berkshire SL6 6TB U.K.
P: 01628-509800 F: 01628-509808 C: 44
RUDDINGTON, UK Mere Way, Ruddington, Nottinghamshire, NG11 6JZ U.K.
P: 0115-936-6464 F: 0115-936-6400 C: 44

France:

NSK FRANCE S.A.
PARIS Quartier de l'Europe, 2 Rue Georges Guynemer, 78283 Guyancourt Cedex, France
P: 01 30 57 39 39 F: 01 30 57 00 01 C: 33

Germany:

NSK DEUTSCHLAND GMBH
DÜSSELDORF Harkortstr. 15, 40880 Ratingen, Germany
P: 02102-481-0 F: 02102-481-2290 C: 49
STUTTGART Sielminger Str. 65, 70771 Leinfelden-Echterdingen, Germany
P: 0711-79082-0 F: 0711-79082-289 C: 49
LEIPZIG Zschortauer Str. 76, 04129 Leipzig, Germany
P: 0341-5631241 F: 0341-5631243 C: 49

NSK STEERING SYSTEMS EUROPE LTD.
STUTTGART Sielminger Strasse 65 D-70771 Leinfelden-Echterdingen, Germany
P: 0771-79082-277 F: 0771-79082-289 C: 49

NEUWEG FERTIGUNG GMBH
CORPORATE Ehinger Strasse 5, D-89593 Munderkingen, Germany
OFFICE/PLANT P: 07393-540 F: 07393-3732 C: 49

Italy:

NSK ITALIA S.P.A.
MILANO Via Garibaldi, 215 20024 Garbagnate Milanese (Milano), Italia
P: 02-995-191 F: 02-99025778, 02-99028373 C: 39

Poland:

NSK EUROPE LTD. WARSAW LIAISON OFFICE
WARSAW LIAISON OFFICE Przedstawicielstowo w Warszawie, ul. Migdalowa 4 lok. 73, 02-796 Warsaw, Poland
P: 48-22-645-1525, 1526 F: 48-22-645-1529 C: 48

NSK ISKRA S.A.
CORPORATE Ul. Jagiellońska 109, 25-734 Kielce, Poland
OFFICE/PLANT P: 48-41-366-6111 F: 48-41-345-4599 C: 48

Spain:

NSK SPAIN S.A.
BARCELONA Calle de la Hidráulica, 5, P.I. "La Ferrería" 08110 Montcada i Reixac (Barcelona), Spain
P: 93-575-4041 F: 93-575-0520 C: 34

Switzerland:

WAELZLAGER INDUSTRIEWERKE BULLE AG (W.I.B.)
CORPORATE Rue Champ-Barby 25, Ch-1630 Bulle, Switzerland
OFFICE/PLANT P: 026-9191100 F: 026-9191120 C: 41

Turkey:

NSK BEARINGS MIDDLE EAST TRADING CO., LTD.
ISTANBUL Eski Uskudar Cad. Cayir Yolu Sok. Nora Center Kat 1, 81120 Icerenkoy, Istanbul, Turkey
P: 90-216-574-5350 F: 90-216-574-6901 C: 90

United Kingdom:

NSK BEARINGS EUROPE LTD.
OFFICE/MAIN PLANT: 3 Brindley Road, South West Industrial Estate, Peterlee, Co. Durham, SR8 2JD U.K.
P: 0191-586-6111 F: 0191-586-3482 C: 44
FORGE PLANT: Davey Drive, North West Industrial Estate, Peterlee, Co. Durham, SR8 2PW U.K.
P: 0191-518-0777 F: 0191-518-0303 C: 44
NEWARK PLANT: Northern Road, Newark, Nottinghamshire, NG24 2JF U.K.
P: 01636-605123 F: 01636-605000 C: 44
BLACKBURN PLANT: Roman Road Industrial Estate, Blackburn, Lancashire, BB1 2LZ U.K.
P: 01254-661921 F: 01254-679502 C: 44
AEROSPACE PLANT/SALES: Oldends Lane, Stonehouse, Gloucestershire, GL10 3RH U.K.
P: 01453-822333 F: 01453-825945 C: 44

NSK EUROPEAN TECHNOLOGY CO., LTD.
RUDDINGTON Mere Way, Ruddington, Nottinghamshire, NG11 6JZ U.K.
P: 0115-940-5409 F: 0115-940-5419 C: 44

NSK UK LTD.
RUDDINGTON Mere Way, Ruddington, Nottinghamshire, NG11 6JZ U.K.
P: 0115-936-6600 F: 0115-936-6702 C: 44

NSK STEERING SYSTEMS EUROPE LTD.
CORPORATE Silverstone Drive, Rowiey's Green, Coventry, CV6 6PA U.K.
OFFICE/PLANT P: 024-76-588588 F: 024-76-588599 C: 44
PETERLEE COLUMN PLANT: 1 Palmer Road, South West Industrial Estate, Peterlee, Co. Durham, SR8 2JJ U.K.
P: 0191-518-6800 F: 0191-518-6808 C: 44
PETERLEE EPAS PLANT: 7 Doxford Drive, South West Industrial Estate, Peterlee, Co. Durham, SR8 2RL U.K.
P: 0191-518-6400 F: 0191-518-6421 C: 44

North and South America

NSK AMERICAS, INC. (AMERICAN HEADQUARTERS)
ANN ARBOR, USA 3861 Research Park Drive, Box 1507, Ann Arbor, Michigan 48106-1507, U.S.A.
P: 734-761-9500 F: 734-761-9511 C: 1

Argentina:

NSK ARGENTINA SRL
Calle San Lorenzo, 4292-Munro-Buenos Aires-Argentina
P: 011-4762-6556 F: 011-4762-6466 C: 54

Brazil:

NSK BRASIL LTDA. www.nsk-ltd.com.br
SÃO PAULO Rua Treze de Maio, 1633-14° Andar-Bela Vista São Paulo-SP, Brazil 01327-905
P: 011-3269-4700 F: 011-3269-4720 C: 55
SUZANO PLANT Av. Vereador João Batista Fitipaldi, 66-Vila Maluf Suzano-SP, Brazil 08685-000
P: 011-4741-4090 F: 011-4748-2355 C: 55
BELO HORIZONTE Rua Ceará, 1431-4° Andar-Sala 405-Funcionários Belo Horizonte-MG, Brazil 30150-311
P: 031-3274-2477 F: 031-3273-4408 C: 55
JOINVILLE Rua Mário Lobo, 61-11° Andar-Sala 1112-Centro Joinville-SC, Brazil 89201-330
P: 047-422-5445/433-3627 F: 047-422-2817 C: 55
PORTO ALEGRE Av. Cristovão Colombo, 1694-Sala 202-Floresta Porto Alegre-RS, Brazil 90560-001
P: 051-3222-1324/3346-7851 F: 051-3222-2599 C: 55
RECIFE Av. Conselheiro Aguiar, 2738-6° Andar-Conj. 604-Boa Viagem Recife-PE, Brazil 51020-020
P: 081-3326-3781 F: 081-3326-5047 C: 55

Canada:

NSK CANADA INC.
HEAD OFFICE 5585 McAdam Road, Mississauga, Ontario L4Z 1N4, Canada
P: 905-890-0740 F: 905-890-0434 C: 1
MONTREAL 2150-32E Avenue, Lachine, Quebec H8T 3H7, Canada
P: 514-633-1220 F: 514-633-8164 C: 1
TORONTO 5585 McAdam Road, Mississauga, Ontario L4Z 1N4, Canada
P: 905-890-0561 F: 905-890-1938 C: 1
EDMONTON 9267-41st Avenue, Edmonton, Alberta T6E 6R5, Canada
P: 604-294-1151 F: 604-294-1407 C: 1
VANCOUVER 3353 Wayburne Drive, Burnaby, British Columbia V5G 4L4, Canada
P: 604-294-1151 F: 604-294-1407 C: 1

Mexico:

NSK RODAMIENTOS MEXICANA, S.A. DE C.V.
MEXICO CITY Minas Palacio No.42-6, Col. San Antonio Zomeyucan Naucalpan de Juarez, C.P. 53750 Estado de Mexico, Mexico
P: 5-301-2741, 5-301-3115, 5-301-4762 F: 5-301-2244, 5-301-2865 C: 52

United States of America:

NSK CORPORATION www.nsk-corp.com
[CORPORATE OFFICE, Aftermarket Business Unit, OEM Business Unit]
ANN ARBOR 3861 Research Park Drive, Box 1507, Ann Arbor, Michigan 48106-1507, U.S.A.
P: 734-761-9500 F: 734-761-9511, 734-668-7888 C: 1
[BRANCHES and DISTRIBUTION CENTERS]
LOS ANGELES 13921 Bettencourt Street, Cerritos, California 90703, U.S.A.
P: 562-926-2975 F: 562-926-3553 C: 1
INDIANAPOLIS 1581 S. Perry Road, Plainfield, Indiana 46168, U.S.A.
P: 317-837-8879 F: 317-837-7207 C: 1
ATLANTA 5575 Gwaltney Drive, Atlanta, Georgia 30336, U.S.A.
P: 404-349-2888 F: 404-349-1209 C: 1
[PLANTS]
ANN ARBOR 5400 South State Road, Box 990, Ann Arbor, Michigan 48108, U.S.A.
P: 734-996-4400 F: 734-996-4707 C: 1
CLARINDA 1100 N First Street, Clarinda, Iowa 51632, U.S.A.
P: 712-542-5121 F: 712-542-4905 C: 1
FRANKLIN 3400 Bearing Drive, Franklin, Indiana 46131, U.S.A.
P: 317-738-5000 F: 317-738-4310 C: 1
LIBERTY 1112 East Kitchel Road, Liberty, Indiana 47353, U.S.A.
P: (765) 458-5000 F: (765) 458-7832 C: 1

NSK AMERICAN TECHNICAL CENTER
ANN ARBOR 3917 Research Park Drive, Ann Arbor, Michigan 48108, U.S.A.
P: 734-668-0877 F: 734-668-0852 C: 1

NSK PRECISION AMERICA, INC.
CHICAGO 250 Covington Drive, Bloomingdale, Illinois 60108, U.S.A.
P: 630-924-8000 F: 630-924-8197 C: 1
SAN JOSE 1900 McCarthy Boulevard, Suite 107, Milpitas, California 95035, U.S.A.
P: 408-944-9400 F: 408-944-9405 C: 1

NASTECH
CORPORATE 110 Shields Drive Route 2, Box 0030, Bennington, Vermont 05201-8309, U.S.A.
OFFICE/PLANT P: 802-442-5448 F: 802-442-2253 C: 1
SALES OFFICE 2851 Boardwalk Drive, Ann Arbor, Michigan 48104, U.S.A.
P: 734-669-8272 F: 734-669-8102 C: 1

NSK LATIN AMERICA, INC. www.latinamerica.nsk.com
MIAMI 2500 NW 107 Avenue, Suite 300, Miami, Florida, 33172, U.S.A.
P: (305) 477-0605 F: (305) 477-0377 C: 1

P: Phone F: Fax T: Telex C: Country Code

Printed in Japan

Motion & Control

No.11 October 2001

Published by NSK Ltd.